NASA-159801

DEVELOPMENT OF IMPROVED HIGH PRESSURE TURBINE OUTER GAS PATH SEAL COMPONENTS

By

L. T. Shiembob

UNITED TECHNOLOGIES CORPORATION
Pratt & Whitney Aircraft Group
Commercial Products Division

Prepared for

National Aeronautics and Space Administration

NASA Lewis Research Center
Contract NAS3-20590

1. Report No.	2. Government Accession No.	3. Recipient's Catalog No.
NASA-CR-159801		

4. Title and Subtitle	5. Report Date
Development of Improved High Pressure Turbine Outer Gas Path Seal Component	January 1980
	6. Performing Organization Code
7. Author(s)	8. Performing Organization Report No.
Lawrence T. Shiembob	PWA-5568
	10. Work Unit No.
9. Performing Organization Name and Address	11. Contract or Grant No.
United Technologies Corporation Pratt & Whitney Aircraft Group - CPD East Hartford, Connecticut 06108	NAS3-20590
	13. Type of Report and Period Covered
12. Sponsoring Agency Name and Address	Cont. Rpt. 12/76-10/79
National Aeronautics and Space Administration Washington, D.C. 20546	14. Sponsoring Agency Code

15. Supplementary Notes

Project Manager, Dr. Robert C. Bill
U.S. Army Propulsion Lab, Lewis Research Center
Cleveland, Ohio 44135

16. Abstract

A plasma sprayed graded layered ceramic/metallic (ZrO_2/CoCrAlY) seal was evaluated for JT9D turbine application by rig and engine tests. Abradability and erosion testing on engine hardware correlated well with previous work on subscale parts. Four cyclic thermal shock rig tests were conducted during the program. Three completed 1000 simulated engine thermal cycle tests and the fourth completed 500 cycles without severe cracking or spalling.

Three ceramic seals were installed in a JT9D experimental engine to evaluate the effect of the engine thermal environment on the seals. All three seals completed the test successfully without severe cracking or spalling. The three seals did have slight laminar cracks at the 85/15-40/60 ZrO_2/CoCrAlY interface.

The second engine test evaluated the rub capabilities of the seal. Six ceramic seals were installed in the engine with fourteen abrasive tip blades. Three of the six seals rubbed to a depth of 24 mils. Eight of the fourteen abrasive tip blades showed evidence of wear. Three of the eight blades wore a maximum of five mils.

Engine rub test results demonstrated the potential of reducing turbine clearances and thereby improving engine performance by use of sprayed ceramic seals.

17. Key Words (Suggested by Author(s))	18. Distribution Statement
o Seal, Abradable o Seal, Turbine o Seal, Blade Tip o Seal, Gas Path	

19. Security Classif. (of this report)	20. Security Classif. (of this page)	21. No. of Pages	22. Price*
Unclassified	Unclassified		

* For sale by the National Technical Information Service, Springfield, Virginia 22161

NASA-C-168 (Rev. 10-75)

PRECEDING PAGE BLANK NOT FILMED

17. Key Words (Continued)

- o Material Properties, Sprayed Ceramic
- o Engine Test, Ceramic Seal
- o Seal, Ceramic
- o Seal, High Temperature
- o Zirconia
- o Abradability

- . Erosion
- o Elastic Modulus
- o Thermal Conductivity
- o Thermal Expansion
- o Thermal Shock

- o Thermal Stress
- o Rupture Modulus
- o Ultimate Strength
- o Residual Stress
- o Prestress
- o Properties, Materials

- o Properties, Physical
- o Properties, Mechanical

- o Engine Test - Sprayed Ceramic Seal

FOREWORD

Work performed under this program was supported by the NASA-ECI (Engine Component Improvement) program.

The demonstration of the feasibility of sprayed ceramics for gas turbine sealing described in this report was made possible by the cooperative effort of individuals who contributed their talents to this program. Without them this achievement would not have been possible and their assistance is hereby acknowledged with thanks.

- Oscar Stewart for assistance in program planning as well as the direction of the analysis and testing during most of the program.
- David Cloud for continuing this effort, helping to make the engine rub test a success and assisting in the preparation of this report.
- Jim Hyland for engine test analysis and Andrew Boursy for test rig operation.

Additional thanks is extended to Dr. Robert C. Bill of the U. S. Army R&T Laboratory at Lewis Research Center who served as NASA Project Manager. His technical expertise and advice helped to make the program flow smoothly and maximized the efficiency of our effort.

Table of Contents

1.0 SUMMARY

A sprayed graded ceramic/metallic (ZrO_2/CoCrAlY) seal segment shown in Figure 1 was designed with the goal of minimizing thermal stresses in JT9D turbine application. The design is interchangeable with current Bill of Material 1st stage seals in sets. The spray process was refined to provide for scale-up of the fabrication process from sub scale parts to engine size hardware. Abradability and erosion rig test results correlated well with previous experience with similar but subscale hardware. Four cyclic thermal shock rig tests, simulating the JT9D-70 1st turbine seal thermal cycle, were completed on sprayed ceramic engine segments during the course of design effort. Three segments completed 1000 cycles without spalling. The fourth completed 500 cycles with only minor spalling. Thermal stress analysis, based on measured physical properties was used in the design.

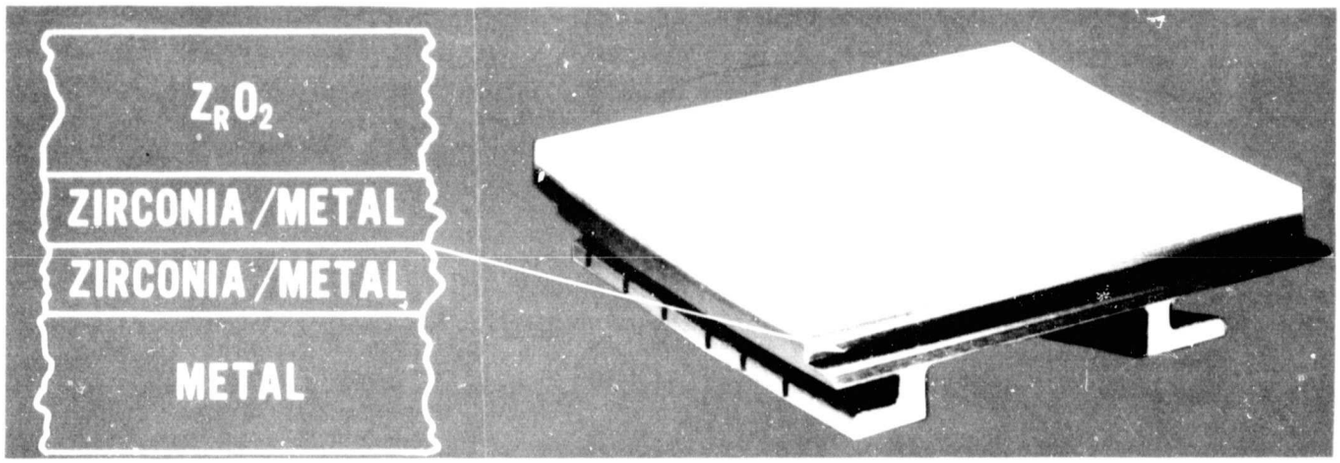

Figure 1 JT9D Sprayed Ceramic Turbine Seal

The sprayed ceramic seal system was evaluated in two engine tests of a Pratt & Whitney Aircraft Group Commercial Products Division JT9D engine shown in Figure 2.

The first engine test was conducted to evaluate the effect of the engine environment on the plasma sprayed seal system. Three ceramic seals were tested in the engine, two with a 0.152 cm (0.060 in.) thick ZrO_2 layer and the other with a 0.229 cm (0.090 in.) thick layer. The accumulated engine test time was 16.9 hours of operation. All three seals successfully completed the test without severe cracking or spalling of the ceramic. Post test visual inspection revealed tight laminar cracks in the corners at the 85/15-40/60 ZrO_2/CoCrAlY layer interface.

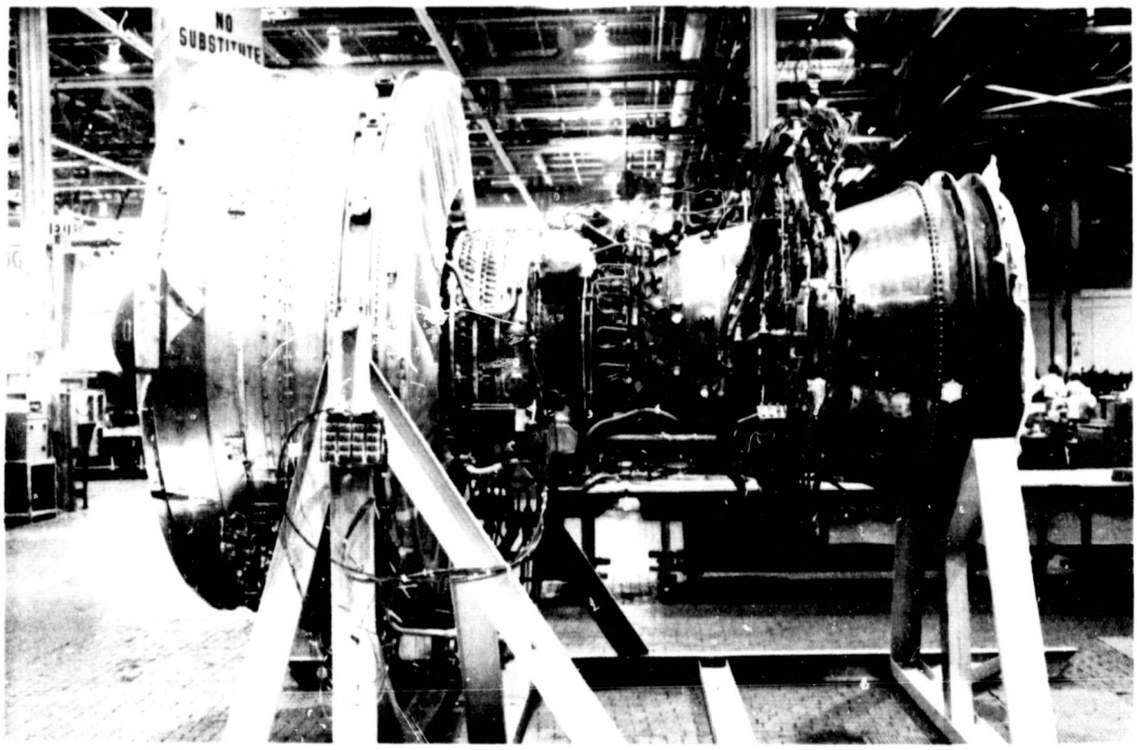

Figure 2 *JT9D Experimental Engine Used to Evaluate Sprayed Ceramic Turbine Seals*

The second engine test evaluated the abradability characteristics of the sprayed ceramic seal in conjunction with abrasive tip blades. Six ceramic seal segments and fourteen abrasive tip blades were installed and tested for 8.4 hours. Three seals were rubbed by the abrasive tip blades producing clean rub grooves up to 0.061 cm (0.024 in.) deep with minimal material transfer as shown in Figure 3. Eight blades participated in the rub, only three with measurable wear up to 0.013 cm (0.005 in.). Tight laminar cracks, similar to the first engine test, also resulted from this test.

The successful demonstration of the abradability of the sprayed ceramic seal system substantiated the potential of reducing operating clearances and thereby improved engine performance. Although the cracks did not result in spalling or adversely affect the rub performance of the system, their presence does indicate the need to improve the thermal stability of the seal system.

NAS3-20590 Ceramic Seals Run in X583-15 Locations 6-11 (NASA)
September 21, 1979

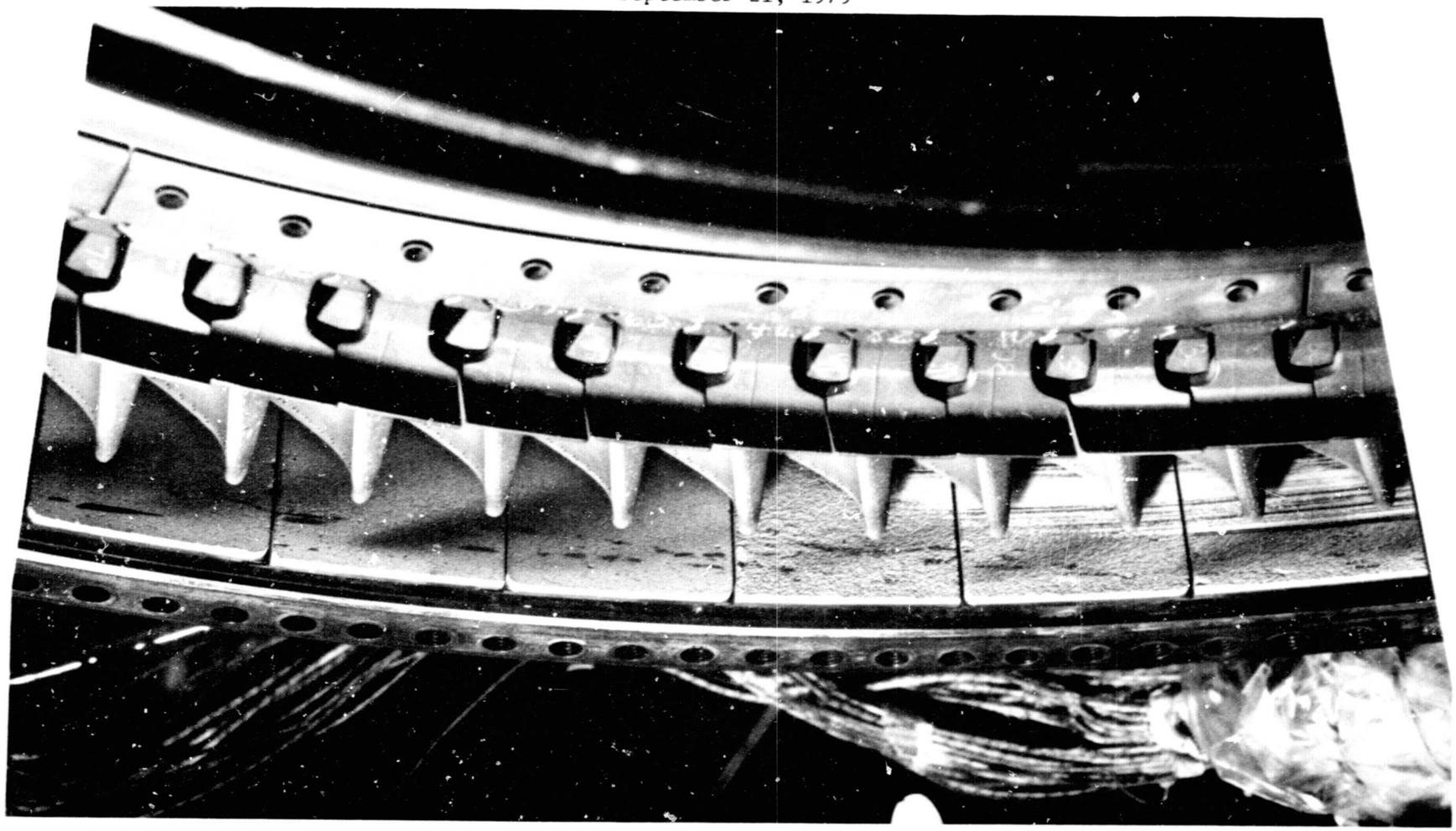

Seals are numbered left to right

Figure 3 *Sprayed Ceramic Seals Tested in a JT9D Engine Showing Rub Grooves*

2.0 INTRODUCTION

Improved gas path sealing is an effective method of insuring engine performance and/or reducing fuel consumption. A sprayed layered ZrO2/CoCrAlY seal system has demonstrated potential for 1589°K (2400°F) turbine blade tip seal application in subscale rig testing in NASA CR-135183 and NASA CR-159669. Used in conjunction with abrasive blade tip treatment this sprayed ZrO_2/CoCrAlY system is expected to reduce rotor wear during eccentric blade/seal interaction, thereby allowing operating clearances to be reduced. Additionally, the 1589°K (2400°F) operating surface temperature capability and thermal resistance of the system is greater than that of current metallic seal systems. As a result, use of the sprayed zirconia system will reduce the requirement for turbine seal cooling and will reduce metal substrate temperatures and stresses. Less sophisticated metals, therefore, may be used in future designs and configurations may be altered to provide lower leakage designs.

The purpose of this program was to demonstrate the feasibility of a full scale sprayed layered ZrO_2/CoCrAlY seal system, developed on subscale parts in NASA CR-135183 and NASA CR-159669, for use in the JT9D turbine by engine test evaluation.

The first phase of the program utilized information generated under the previous NASA contracts to define a sprayed ceramic configuration which, with the metallic substrate to which it would be applied would be interchangeable with current JT9D bill of material seal segments. Fabrication processes were reviewed and evaluated to accommodate the JT9D size segments which is larger than previous subscale parts. The initial design was evaluated by rig tests identifying abradability, erosion resistance and cyclic thermal shock capability. The sprayed ceramic seal design was modified to improve thermal shock resistance and subsequent rig and engine tests demonstrated the potential of the sprayed ceramic system to 1) accommodate the thermal environment of the JT9D turbine and 2) provide sufficient abradability in conjunction with abrasive blade tip treatment to permit reduction of operating clearances and thereby provide an engine performance benefit.

3.0 TECHNICAL PROGRAM

This program is based on the results of NASA CR-135183 and earlier contracts on subscale parts which indicated that a sprayed ceramic seal could be designed and fabricated to operate in an engine environ- ment. The purpose of this program was to design, fabricate and demon- strate, by engine test, the feasibility of utilizing a sprayed ceramic seal concept in the high turbine of the JT9D. Utilizing previously developed data, an initial seal design was generated. Spray fabrication procedures were investigated in order to scale-up the process to engine size hardware. Parts were fabricated, property measurements taken and rig tests conducted to evaluate abradability, erosion and cyclic thermal shock resistance. Rig test results were reviewed and correlated with an updated analysis utilizing the latest property measurements. Methods to improve the design were evaluated, design improvements incorporated, parts fabricated and rig and engine tests conducted. Results of engine tests were evaluated to determine the effectiveness of the design.

3.1 Initial Design

The initial JT9D sprayed ceramic seal design is a scale-up of the configuration generated under previous NASA contracts. Previous effort involved specimens with a 12.7 cm (5 in.) radius of curvature, approximately 1.83 cm (0.72 in.) wide and 7.11 cm (2.8 in.) long. Material properties generated under these earlier programs were used to define a sprayed seal configuration which, based on a thermal stress to strength ratio, had potential to be developed, to survive the engine environment. The seal segment was designed to be interchangeable with the current JT9D Bill-of-Material seal.

Subsequent scaling up of the spray process to engine size hardware having a 50.2 cm (19.8 in.) radius of curvature, 6.1 cm (2.4 in.) wide and 6.9 cm (2.7 in.) long was completed successfully. Parts were fabricated and rig tests of abradability and erosion resistance indicated the sprayed ceramic seal had potential for engine application. Cyclic thermal shock testing, however, resulted in laminar cracks at the interface between the intermediate layers indicating the need for design improvements.

3.1.1 Requirements

The sprayed ceramic seals developed under this contract are for use in the 1st stage of the JT9D high turbine. A 1589°K (2400°F) seal surface temperature was selected for design. To facilitate engine tests provisions were made to permit interchangeability in small groups with current bill-of-material seals and be compatible with the current high turbine case.

The following additional preliminary design goals were established:

1. The surface to be sprayed would be free of steps and other sharp discontinuities.

2. The seal would have the same nominal operating clearance as the B/M seal.

3. Geometric features would be designed to minimize thermal stresses.

4. Abradability and erosion resistance capability similar to that demonstrated on subscale parts during previous contracts would be maintained.

3.1.2 Analysis

The preliminary design effort was directed toward application of the sprayed ceramic system geometry evaluated in NASA CR-135183 to a modified JT9D metallic seal substrate. The ceramic system configuration consisted of three layers, a top layer of Yttria (20 percent) stablized ZrO_2 (Metco 202NS) 0.229 cm (0.090 in.) thick, an intermediate layer sprayed with a powder mixture of 85 percent Yttria stabilized ZrO_2 and 15 percent CoCrALY (62 % Co, 23 % Cr, 14% Al and traces), 0.076 cm (0.030 in.) thick, another intermediate layer of 40 percent Yttria stabilized ZrO_2 and 60 percent CoCrALY, 0.076 cm (0.030 in.) thick, and a bond coat of NiCrAl (Metric 443) approximately 0.013 cm (0.005 in.) thick. The metallic substrate of cobalt based Mar-M-509 material was designed to accommodate this 0.394 cm (0.155 in.) thick graded ceramic structure and be compatible with engine seal attachment and blade/seal clearance dimensions and to be interchangeable with current JT9D Bill-of-Material segments. Analysis was conducted to refine the geometric features of the design and particular consideration was given to thermal stresses expected during engine operation. Thermal and stress analysis programs previously developed by the Commercial Products Division of the Pratt & Whitney Aircraft Group were utilized in this effort.

3.1.2.1 Description of Analytical Programs

The analytical design system used in this program consists of three analytical computer programs. The first provides a two dimensional finite element nodal breakup of the design. Both axial and circumferential seal breakups were generated. The temperature distribution through the seal was calculated using a second program which performs a finite difference heat transfer analysis for transient and steady state temperature distribution based on engine operating cycle boundary conditions. The required input for the heat transfer program consists of 1) the finite element breakup, 2) appropriate thermal boundary conditions and 3) thermal conductivity and specific heat as a function of temperature for each of the three layers of the ceramic seal system and the substrate.

Temperature distribution through the seal was calculated in both the axial and circumferential directions at four engine operation points, idle, acceleration from idle to sea level take off, sea level take off, and deceleration from sea level take off to idle. The output from the finite difference heat transfer analysis was then used to calculate the stress distribution through the seal by means of a third analytical program which conducted a two-dimensional stress analysis.

3.1.2.2 Properties

Physical and thermal properties of each of the constituent layers of the sprayed ceramic seal were required in order to conduct the analysis. The finite difference heat transfer analysis required values for thermal conductivity, density, and specific heat. The stress program, in addition to the output from the thermal program required values for the modulus of elasticity and the coefficient of thermal expansion. Material properties used in the selection and evaluation of the initial design were presented in NASA Report CR-135183.

Because residual stresses are generated during the spray process they were included in the analysis. The analytical programs required that the residual stresses be incorporated by using a modeling method developed at P&WA Group which uses an associated Stress Free Temperature (SFT) distribution. The SFT is the temperature distribution at which the part is stress free and is used to calculate stresses by means of the difference between the operating temperature and the SFT. The SFT distribution used in the initial analysis of the seal segment design was taken from NASA CR-135387 and is shown in Figure 4.

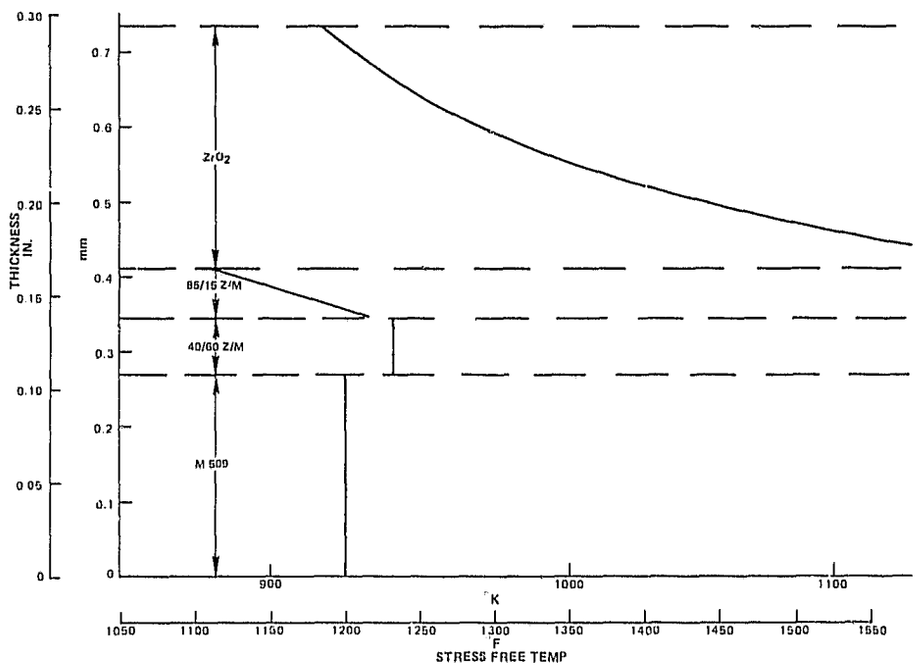

Figure 4 *Stress Free Temperature Distribution Used in the Initial Analysis of a JT9D Ceramic Seal Segment*

3.1.2.3 Results of Analysis

Two substrate designs shown in Figure 5 in comparison with the current Bill-of-Material were considered and analyzed. Each involved the same ceramic system configuration, the only difference was in the design of the substrate attachment rails. Design A represented an attempt to make the stiffness in the circumferential and axial planes similar. Design B represented a configuration as close as possible to the current Bill of-Material. In addition, Design B with its much reduced rail cavity was expected to be less costly in terms of machining requirements. Both configurations were analyzed using properties from the previous contracts. Results of preliminary analysis reported in NASA CR-135387 indicated some benefit in application of compressive residual stresses by means of heating of the substrate during the spray process. For this reason, both designs were analyzed using the residual stress of parts fabricated with a 930°K (1200°F) substrate temperature, as measured in NASA CR-135387, and shown in Figure 4.

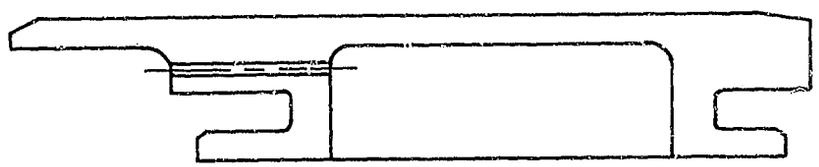

JT9D-70 B/M SEAL

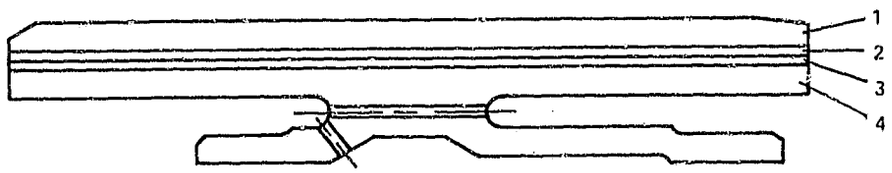

SEAL DESIGN A

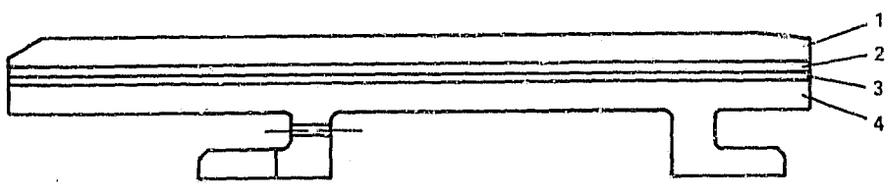

SEAL DESIGN B

1 Z_rO_2

2 85/15 Z_rO_2/C_oC_rAlY

3 40/60 Z_rO_2/C_oC_rAlY

4 MAR-M-509

Figure 5 JT9D Sprayed Ceramic First Turbine Seal Designs in Comparison With Bill-Of-Material Seal

Analysis identified the thermal stress distribution throughout both seal configurations at four JT9D engine operating conditions. Idle, 6 seconds into acceleration to sea level take off, sea level take off, and 12 seconds into deceleration to idle were chosen as conditions representative of minimum and maximum steady state points and the most severe transients during acceleration and deceleration. The stress map was surveyed and locations and magnitudes of maximum principal stress in each of the layers for each of the operating conditions were identified. Earlier analysis had shown that compressive stresses generated during engine operation would be well within the compressive strength of the material and that critical stresses were tensile. For this reason the results presented in Figure 6 and 7 show only the ratio of maximum principal (tensile) stress to strength ratio for the axial and circumferential plane for each configuration. A stress to strength ratio greater than one indicates that stresses exceed the strength of the material and, therefore, crack initiation would be expected. It should be noted that the stress to strength ratios are generally the same in the axial plane and that Design B shows a definite advantage with respect to lower stresses in the circumferential plane.

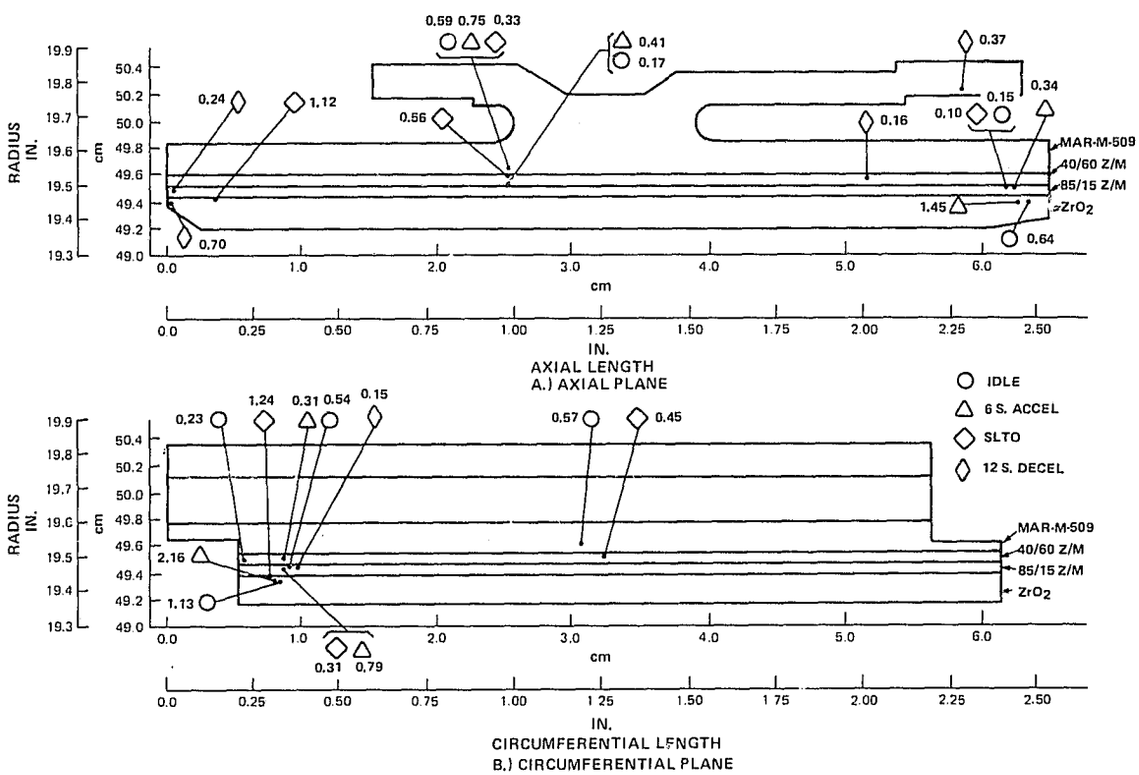

Figure 6 *Stress/Strength Ratios For Seal Design A in Circumferential and Axial Planes*

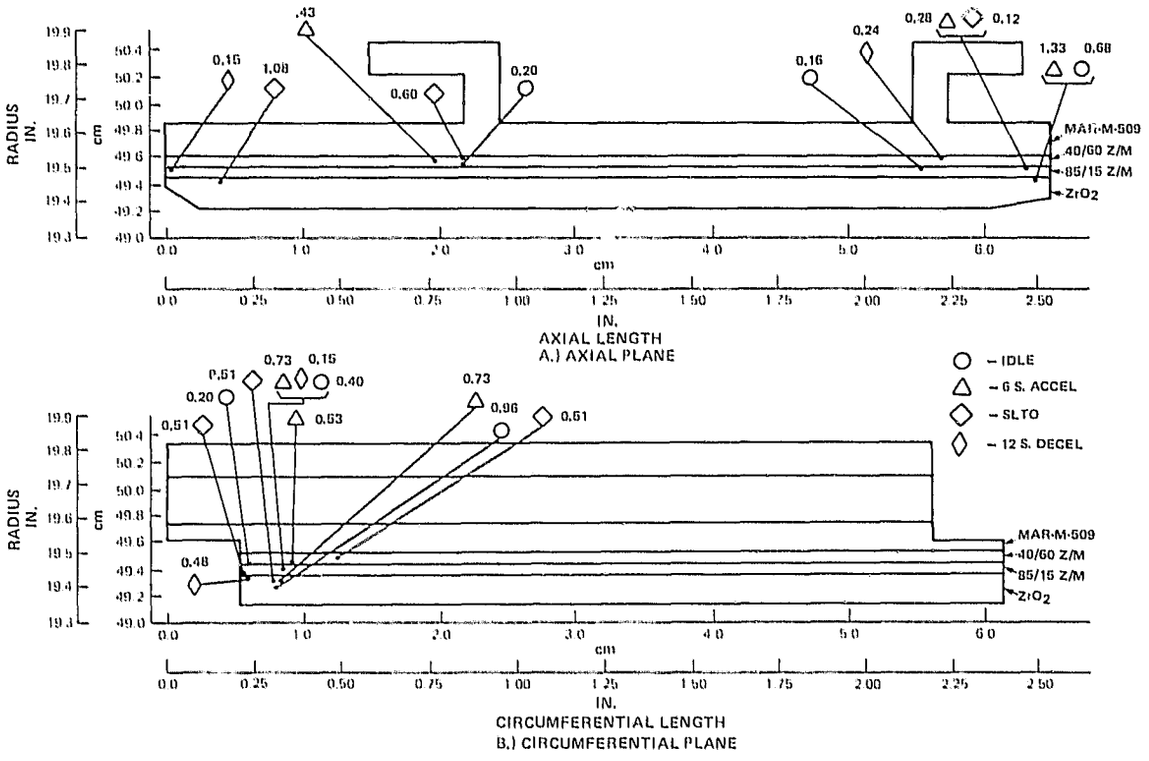

Figure 7 Stress/Strength Ratios For Seal Design B in Circumferential and Axial Planes

In view of the closer similarity with the current Bill-of-Material seal, the substrate machining advantage and the benefit in terms of lower thermal stresses, Design B was selected for evaluation.

The maximum principal stress during operation of Design B was estimated to exceed the strength of the material at the ZrO_2 interface at the edge of the segment with a ratio of 1.33. However, because of the uncertainty of the accuracy of the property data and the fact that analysis indicated that geometry changes would not reduce stresses below the estimated strength, it was decided to fabricate and test that configuration.

3.1.3 Fabrication

All parts, those used for material property measurements, residual stress measurements and rig and engine tests were sprayed using Metco plasma spray equipment. Material specimens utilized flat plate low alloy steel with a bond coat and the individual layer sprayed material. All other parts were of the complete system, bond coat plus 3 layers. The cyclic thermal shock rig specimens, residual stress specimens and engine parts were sprayed on engine seal substrates rather than flat plates.

A fixture similiar to that shown in Figure 8 was used to spray all parts. Flat plates used for material property measurements and engine segment substrates used for rig and engine tests were wired to the inner diameter of the fixture. The diameter of the fixture is 25.4 cm (10 in.). During spraying the fixture was rotated at approximately 375 RPM and the spray gun traveled at a rate of 50 cm/min (20 in./min) axially back and forth during the spray process to form the structure.

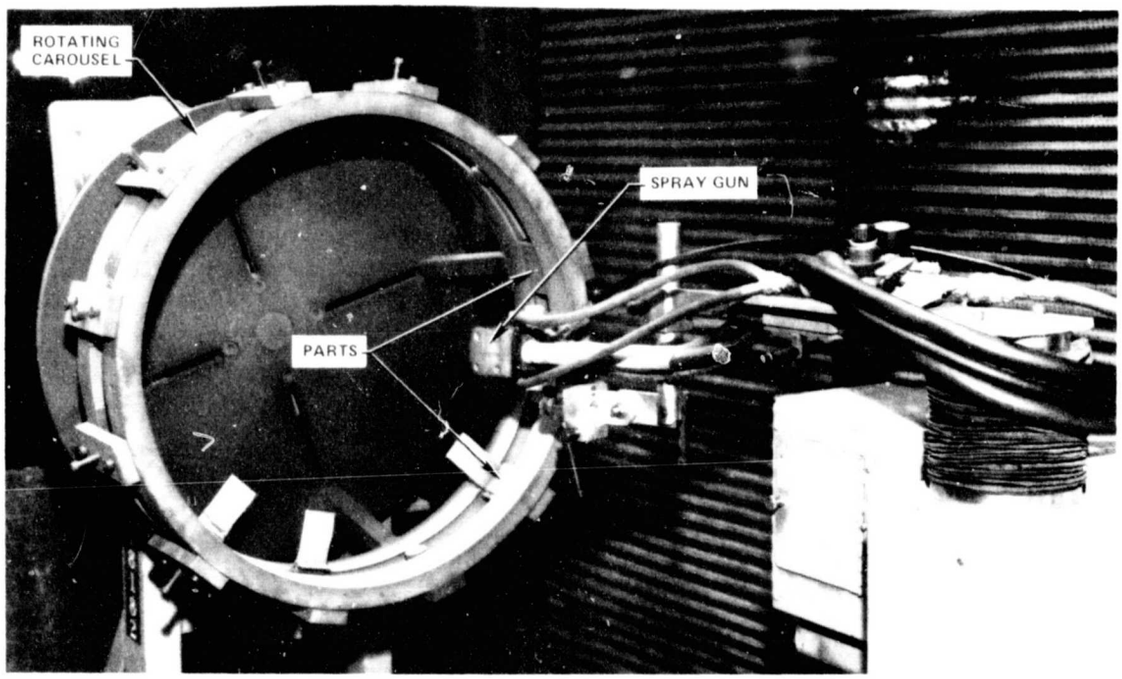

Figure 8 Fixture Used to Spray Parts

3.1.3.1 Results of Scale Up

Two initial trials were conducted to determine if scaling up to engine size hardware would require modifications to the spray process. An evaluation of the deposited structure, microstructure, hardness, and deposition rates was conducted. This evaluation indicated the advisability of tightening controls on powder preparation and to minimize gaps between parts to reduce turbulence during spraying. The tightened controls included drying of powder prior to spraying and incorporation of a completely separate powder feed system for the ZrO_2 powder.

A third set of parts was fabricated after incorporation of the improved procedures. Metallographic examination showed that the structure of each of the layers to be essentially identical with those of subscale parts fabricated under previous contracts. Average hardness was also comparable, approximately 5 points lower than subscale parts on Superficial Rockwell 45Y hardness. These results, therefore, indicated that scale-up of the spray process would be accommodated by incorporating the procedure modification noted above.

3.1.4 Evaluation of the Initial Design

A JT9D sprayed ceramic turbine seal was designed with the goal of minimizing thermal stresses during engine operation utilizing material properties generated under previous contracts with subscale parts. Fabrication procedures were refined to fabricate full scale engine parts with basically the same hardness and structure. An evaluation of the sprayed ceramic seal design fabricated with the scale-up refinements was conducted by rig testing. Seal performance capability was evaluated by abradability and erosion testing. The capability of the seal segment to survive in the thermal environment of the engine was evaluated by cyclic thermal shock rig testing simulating the engine environment.

A thermal stress analysis was conducted to estimate the stresses generated during cyclic thermal shock rig testing to correlate analytical results with crack initiation.

3.1.4.1 Abradability

Abradability rig tests were conducted under simulated engine conditions of seal surface temperature, blade tip speed, and incursion rate.

All abradability tests were performed with P&WA's high temperature abradability test rig shown in Figure 9 which evaluated the rub characteristics of the sprayed ceramic seal system at engine conditions of rotor speed, seal temperature, and incursion rate. Twelve simulated turbine blade tips were mounted in the periphery of a disk driven at the required speed by a compressed air turbine. The seal segment specimen was mounted in a fixture at the end of a horizontal post attached to a moving carriage assembly. The carriage assembly moved the specimen radially into the rotor assembly at the required incursion rate. The seal specimen was heated from both surfaces by an oxygen-jet fuel burner directed at the front surface of the seal and an electric hot air heater directed at the rear surface of the seal. Gas flow, fuel flow, and current flow were varied to control the seal surface temperature.

Seal surface temperature was monitored by optical pyrometers. Carriage travel was monitored by a linear differential transformer. All data was recorded continuously on a strip chart.

Blade tip and seal wear was determined through pre and post-test measurements. Relative abradability between different incursion rates and different blade tips was assessed on the basis of the Volume Wear Ratio (VWR); the seal wear volume divided by the blade tip volume. The higher the Volume Wear Ratio, the better the abradability of the seal system.

Four abradability tests were conducted on the initial design. The test conditions and results are summarized in Table 1.

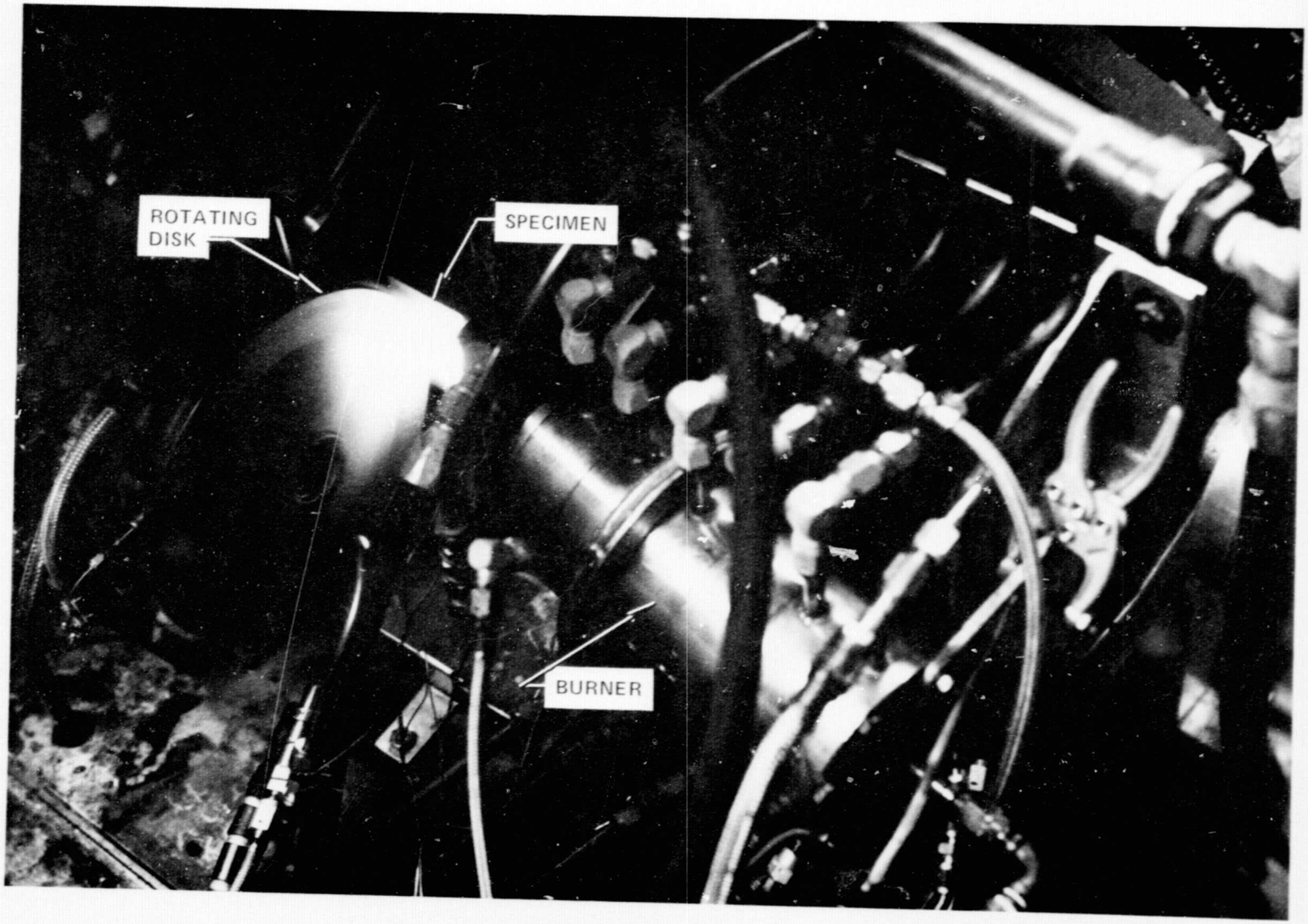

Figure 9 *High Temperature Abradability Rig*

TABLE 1

RESULTS OF ABRADABILITY TESTS OF INITIAL DESIGN

Test No.	1	2	3	4
Test Conditions:				
Seal Temp, ^{o}K (^{o}F)	1589 (2400)	1589 (2400)	1589 (2400)	1589 (2400)
Blade Tip Speed, m/sec(ft/sec)	304.8 (1000)	304.8 (1000)	304.8 (1000)	304.8 (1000)
Incursion Rate, mm/sec(in/sec)	0.0254 (0.001)	0.0254 (0.001)	0.00254 (0.0001)	0.254 (0.010)
Incursion Depth, mm(in)	0.508 (0.020)	0.508 (0.020)	0.508 (0.020)	0.508 (0.020)
Blade Tip Material	B-1900	Al_2O_3 Coated SiC grids in Metal Matrix	B-1900	B-1900
No. Blades	12	6	12	12
Test Results:				
Seal Wear Depth, (0.015)(1) mm (in.), max.	0.508 (0.020)	0.381 (0.015)	0.127 (0.005)	0.381
Blade Tip Wear, (0.0141)(2) mm (in.), avg.	0.046 (0.0018)	0.169 (0.0066)	0.335 (0.0131)	0.361
VWR = Seal Vol./Tip Vol	4.878	5.917	0.096	0.091

(1)Groove in center of rub area approximately 1/3 width of rub. Heavy blade transfer on both sides.

(2)Negligible blade tip wear in center of blade. Very heavy wear on both sides.

The first test was conducted at 1589°K (2400°F) surface temperature with a rotor speed of 304.8 m/sec (1000 ft/sec) with twelve B-1900 blades at an incursion rate of 0.0254 mm/sec (0.001 in/sec). The blades grooved the seals to a maximum depth of 0.508 mm (0.020 in.) with an average blade tip wear of 0.046 mm (0.0018 in.). This gave a VWR of 4.88. The value is similar to results of testing of subscale parts on previous contracts.

Results presented in Table 1 indicate a strong sensitivity of abradability to incursion rate, (tests 1, 3 & 4), with minimum blade tip wear (maximum VWR) occurring in the vicinity of 0.0254 mm/sec (0.001 in/sec) incursion rate. Slower and faster incursion rates (tests 3 and 4) resulted in blade wear approximately eight times greater than at 0.0254 mm/sec. (0.001 in/sec).

The use of six abrasive tip blades, test No. 2, resulted in a 20 percent increase in VWR at the 0.0254 mm/sec (0.001 in/sec) incursion rate.

Figure 10 illustrates the results of the abradability tests. The spalling of the ceramic seal used for the first three tests shown is attributed to the rapid thermal transients generated during heat-up and to cool down from test conditions.

Blade and seal wear resulting from test number 4 shown in Figure 10 was very irregular. Seal wear was heavy in the center and very slight at the edges. Blade wear pattern corresponded to the seal wear profile. Post test inspection failed to produce a reason for the irregular wear.

3.1.4.2 Erosion

Erosion resistance was evaluated in the hot particulate erosion rig shown in Figure 11. This rig enables the erosion resistance of the sprayed system to be evaluated at various impingement angles and temperatures. The specimens were positioned at a distance of 3.81 cm (1.5 in) at the various impingement angles relative to the end of the combustor exit nozzle by a compound vise. The specimen was heated by impinging JP-5 fuel and air combustion products on the ZrO_2 surface of the specimen through a 1.905 cm (0.75 in.) diameter exit nozzle. The temperature of the specimen and the exit gas velocity was controlled by varying fuel and air flows.

After stabilization of the specimen surface temperature and gas velocity, particulate flow was initiated. The 80 grit Al_2O_3 particulate was gravity fed into a tube connected into the combustor exit nozzle approximately 5.08 cm (2.0 in.) upstream of the nozzle end. The particulate was picked up and accelerated to the specimen surface by the hot gas stream. The flow rate of the particulate was controlled by a precalibrated orifice placed in the storage hopper discharge line. The particulate flow rate was checked by monitoring the weight of the particulate used and the duration of the particulate flow during the test.

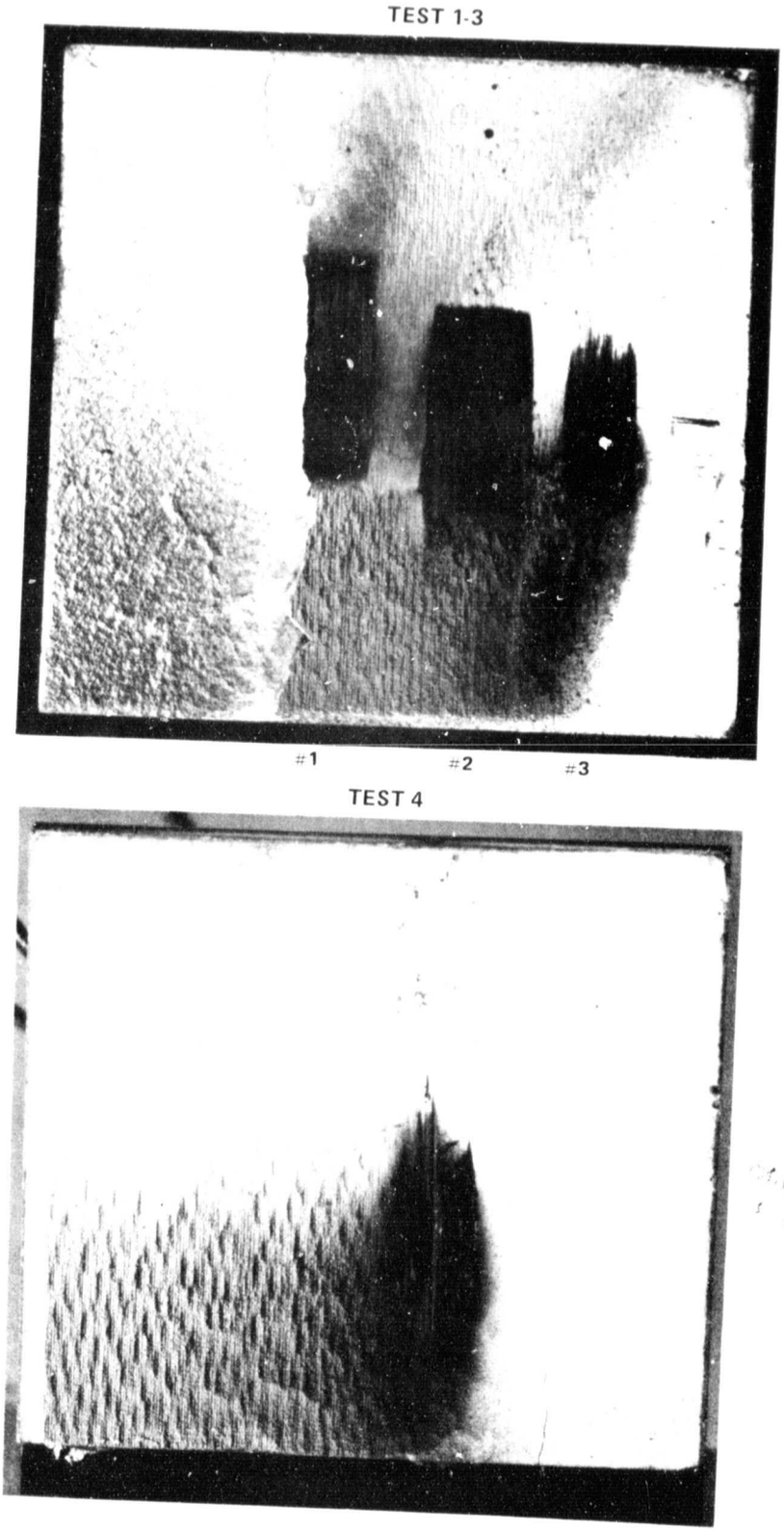

Figure 10 *Abradability Tests Results - Post Test Condition*

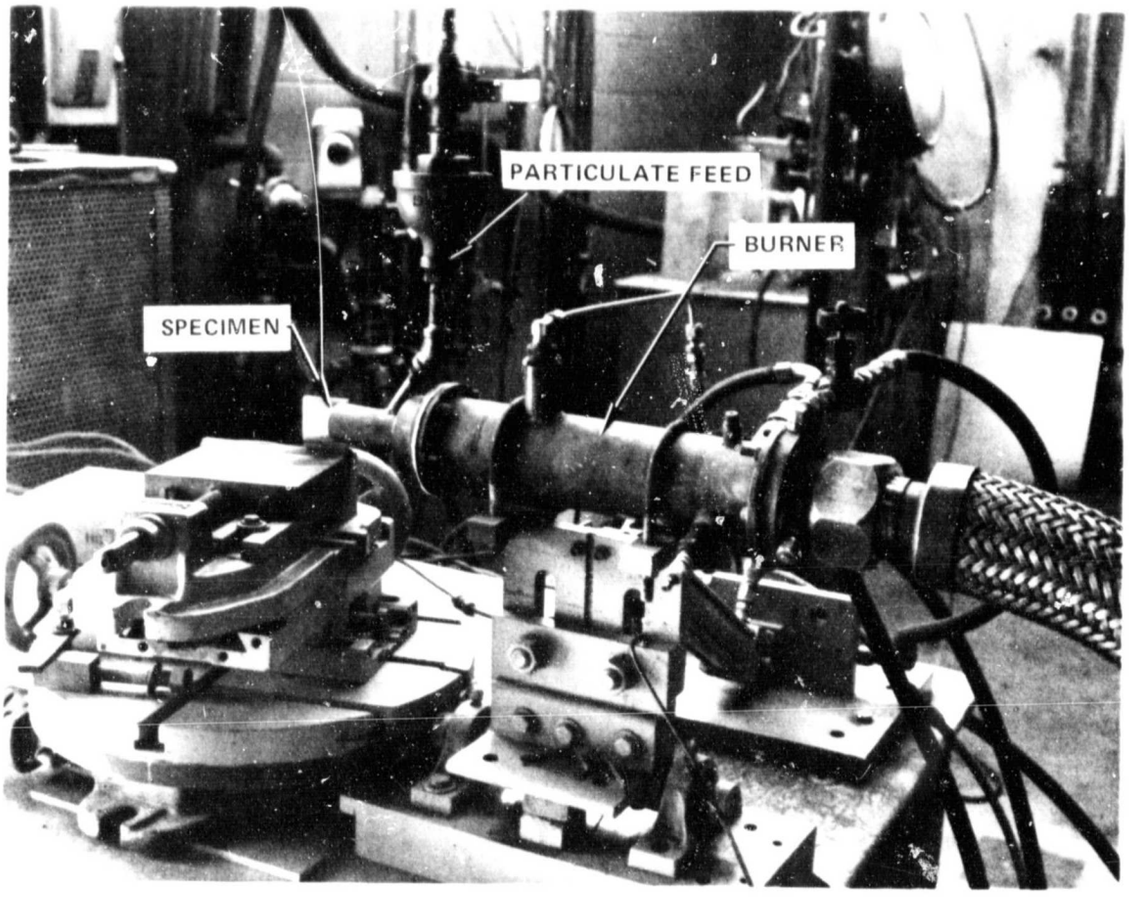

Figure 11 Hot Particulate Erosion Rig

Specimen temperature was measured optically on the ZrO_2 surface. Erosion wear was determined by measuring the weight loss of the specimen at five minute intervals.

The erosion specimen consisted of the composite seal system sprayed on a flat Hastelloy-X plate 0.483 x 0.508 cm (1.9 x 2.0 in.). A cap screw was welded to the center of the flat Hastelloy-X plate for mounting in the test fixture. Three erosion resistance tests were conducted at a ZrO_2 surface temperature of 1589°K (2400°F) and particulate impingement angle of 0.262, 0.786, and 1.572 radians (15°, 45°, and 90°). Gas velocity during testing was 0.35 Mach number and a particulate flow of 9.07 gm/min was used.

Weight loss measurements at 5 minute intervals for each of the tests are shown in Figure 12. The tests exhibited a strong sensitivity to impingement angle, as the impingement angle increased the rate of erosion also increased. Erosion rates were calculated and are also shown in Figure 12.

Post test results of each of the three tested parts are pictured in Figure 13.

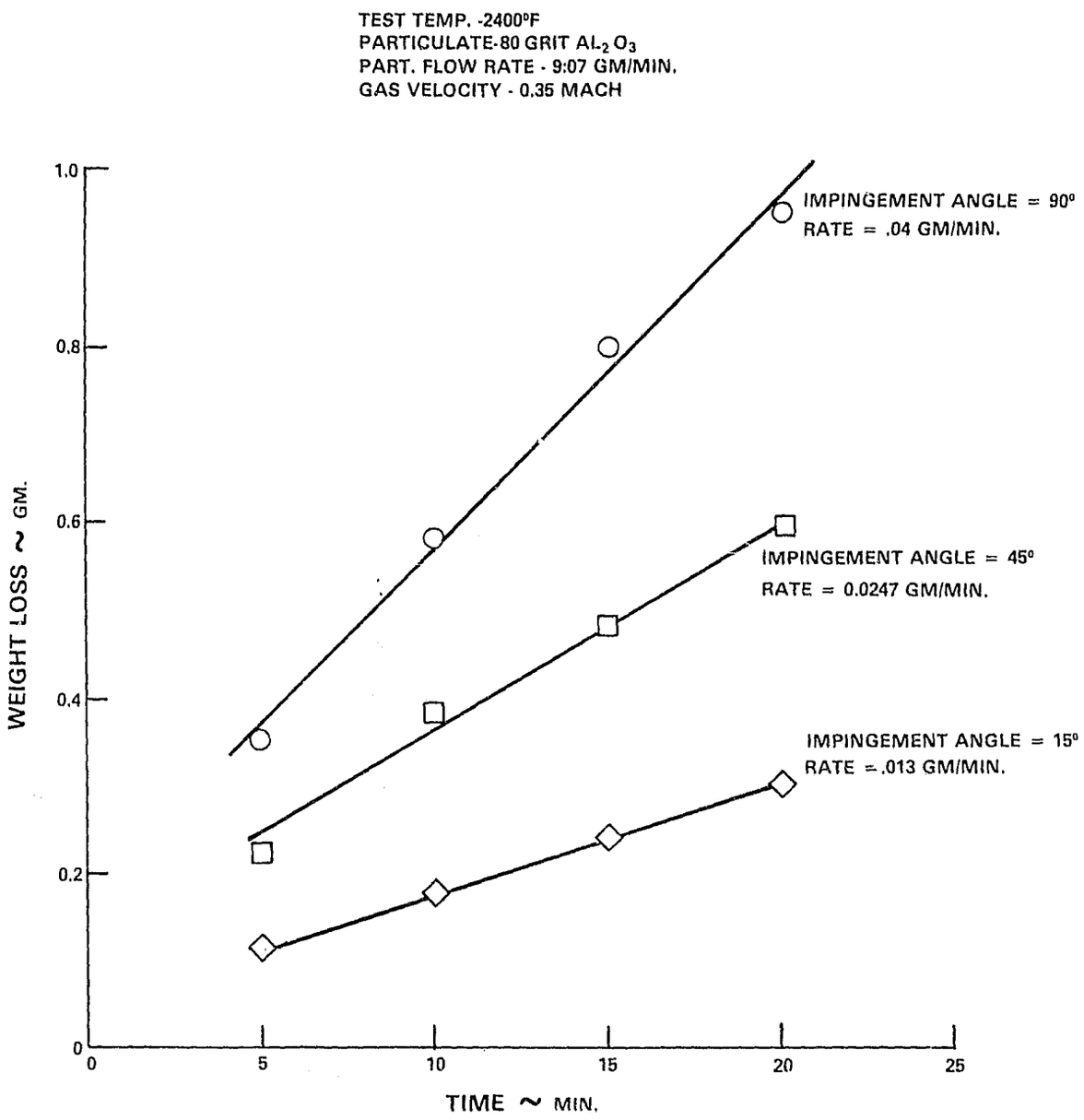

Figure 12 Results of Erosion Test of Initial Design

Impingment Angle = 15° (.262 radians)

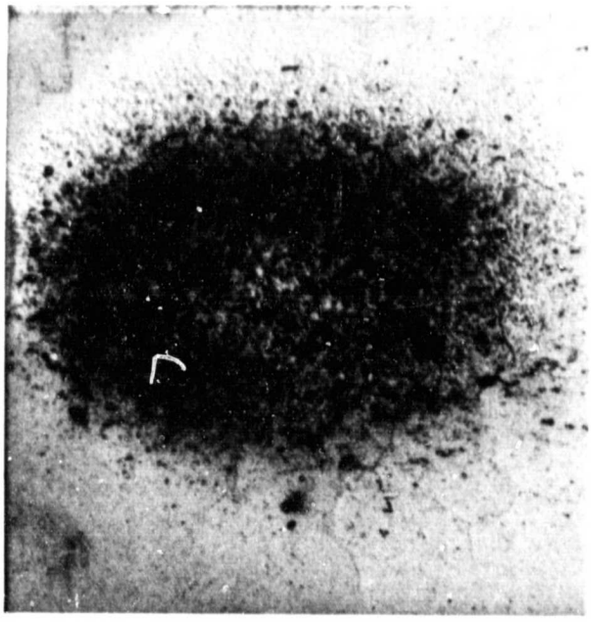

Impingment Angle = 45° (.785 radians)

Impingment Angle = 90° (1.57 radians)

Figure 13 Erosion Test Results-Post Test Condition

3.1.4.3 Thermal Shock Test Results

The durability of the sprayed ZrO_2/CoCrAlY seal system in an engine application depends greatly on its capability to successfully survive the initial and subsequent thermal cycles corresponding to the engine operational conditions. The graded, layered system was designed specifically to compensate for the large difference in thermal expansion between the metal substrate and ceramic.

Cyclic thermal shock characteristics were evaluated by rig tests which subjected the seal specimens to a thermal cycle simulating the gas turbine engine cycle from idle to sea level take off and back to idle.

The specimen was mounted in the cyclic thermal shock test rig, shown in Figure 14, by a fire brick holding fixture held by a water cooled copper fixture. A combination of oxygen-propane torches and cooling air jets were used to achieve the desired thermal cycles on the ZrO_2 and metal substrate surfaces. The torches were mechanically moved toward or away from the specimen at controlled rates to provide the required thermal cycle. Fixed cooling air jets were turned on or off or the flow was changed at predetermined intervals to meet the cycle requirements. The ZrO_2 and metal substrate surface temperatures were monitored continuously with an optical pyrometer and thermocouples, respectively, and recorded on a strip chart.

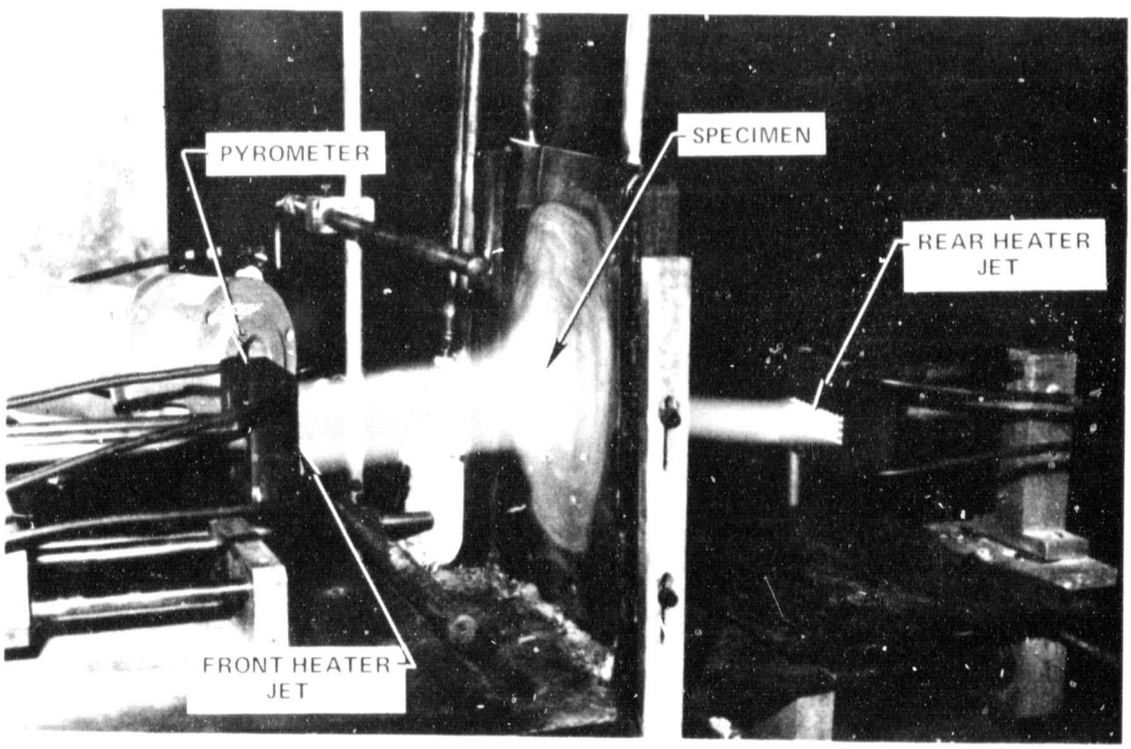

Figure 14 *Cyclic Thermal Shock Rig Operating at a Simulated Sea Level Take-Off Condition*

Two full-scale JT9D engine seal segments were tested. The segments were machined to remove edge pyramiding, form segment-to-segment lap joint seal configurations and provide the required final radius on the ZrO_2 surface. Pre-test inspection revealed tight laminar cracks, up to 0.75 inch long in the circumferential direction along the leading and/or trailing edges of all full scale segments. Cracks were generally located along or near the ZrO_2-85/15 ZrO_2/CoCrAlY or 85/15 ZrO_2/CoCrAlY - 40/60 ZrO_2/CoCrAlY interfaces and were at the corners. Axial depth appeared generally less than 0.152 cm (0.060 in.). Machining the leading and trailing edges of the thermal shock specimens back 0.152-0.203cm (0.060-0.080 in.) removed the cracks. Both parts successfully completed 1000 simulated engine thermal cycles without spalling.

The typical rig test thermal cycle, measured in the central area of the seal, is shown in Figure 15. An engine cycle is shown for comparison and illustrates the closeness of simulation. Analysis indicated that maximum principal stresses will occur during the accel portion of the test cycle and that the stresses would exceed material strengths in both the ZrO_2 and 85/15 ZrO_2/CoCrAlY layers. This analysis was substantiated by rig test results, reported in NASA CR-135183 which indicated thermal stress cracking initiated at some point within the first 15 cycles.

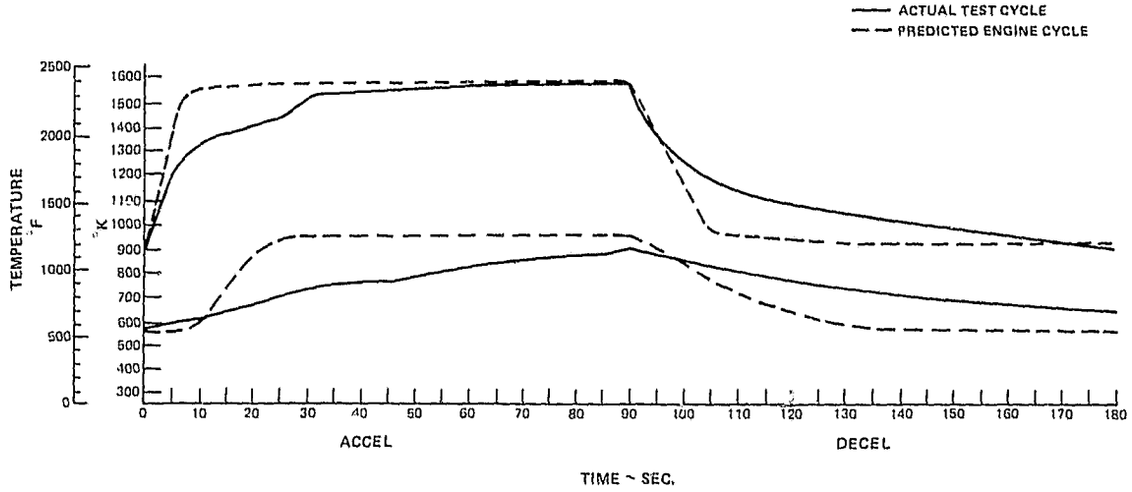

Figure 15 Cycle Thermal Shock Test Cycle

To better define when or where thermal cracks were initiating, the seal segments were subjected to an initial acceleration transient. Care was taken during cool-down to avoid thermal conditions which would generate stresses that would exceed the strength of the seal.

The parts were inspected after the initial acceleration transient and periodically thereafter to determine the point of crack initiation and progression.

The first part developed laminar cracks at the 85/15-40/60 ZrO_2/CoCrAlY layers interface and the ZrO_2 - 85/15 ZrO_2/CoCrAlY layers interface across the axial ends after the initial acceleration transient. Radial (mud flat) cracks initiated during the first complete idle sea level take off test cycle. Laminar cracks propagated approximately 1.27 cm (0.5 in.) in the circumferential direction within the first 200 cycles and remained apparently stable afterwards.

Part of the delaminated area at the male shiplap joint end of the first specimen spalled during inspection handling after approximately 200 cycles. Since the spalled area only represented approximately 10 percent of the total surface area, testing was continued to a total of 1000 cycles. No further deterioration of the specimen was observed. The only apparent effect of the spalled area was an increase in the substrate temperature of approximately 269°K (25°F). The nature of the crack progression is illustrated in Figure 16.

The second part also completed 1000 cycles. Crack initiation and progression and location of the cracks was essentially the same as the first test except that spalling did not result -- the part remained intact for the complete 1000 cycles.

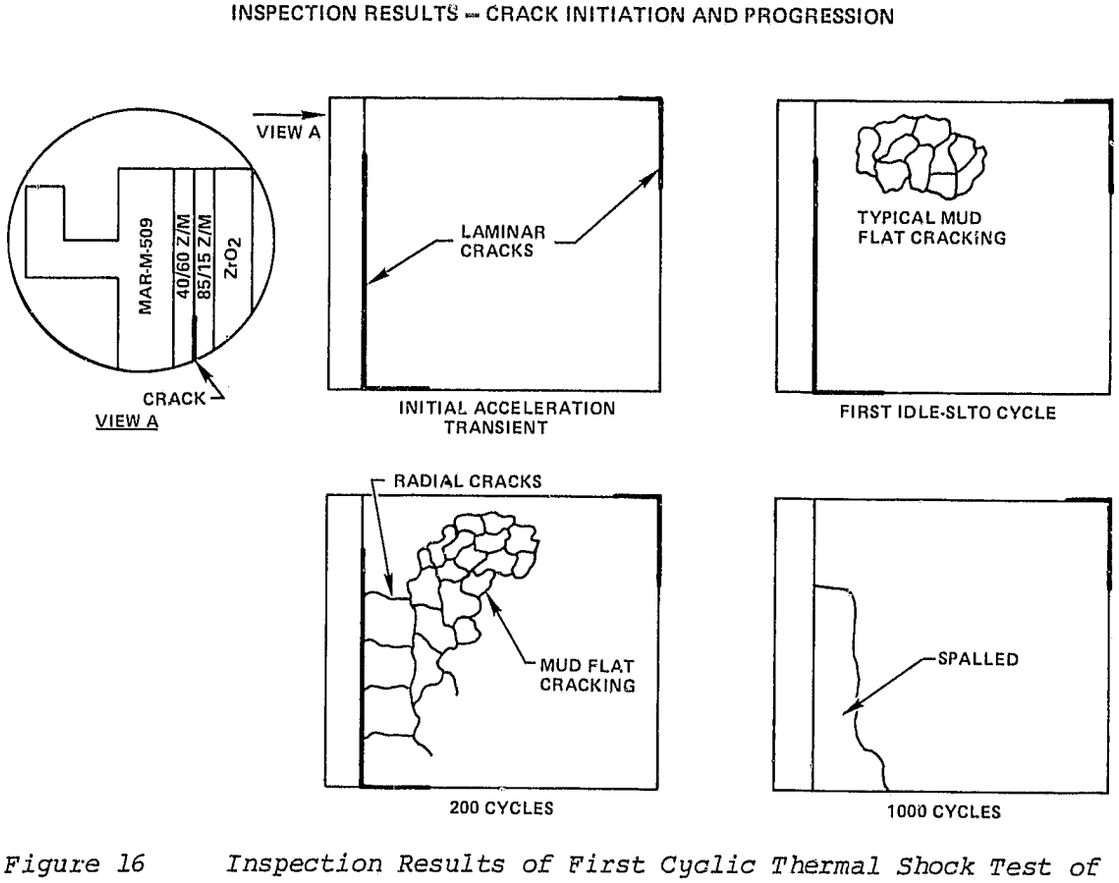

Figure 16 *Inspection Results of First Cyclic Thermal Shock Test of Initial Design*

Crack initiation and progression during testing for the second test is shown in Figure 17. A comparison of these figures, Figure 16 and 17, illustrates the repeatability of the effects of the cyclic thermal shock testing. Post test appearance of the parts is shown in Figure 18.

Two important results of the cyclic thermal shock test are prominent. First, one sprayed ceramic engine seal successfully completed 1000 simulated engine cycles without spalling. Second, spalling did not precipitate further deterioration indicating that any damage to the ceramic would not result in progressive failure of the seal or directly result in the initiation of failure of any other engine component.

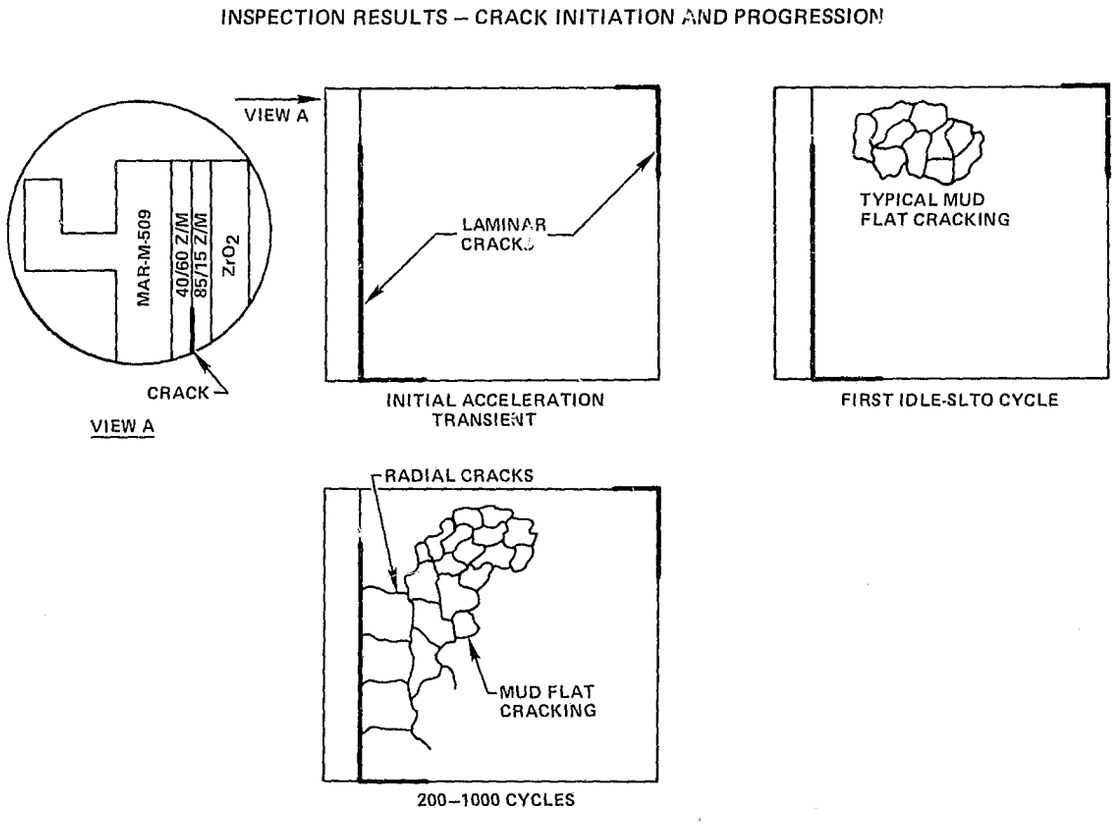

Figure 17 *Inspection Results of Second Cyclic Thermal Shock Test of Initial Design*

1st Test

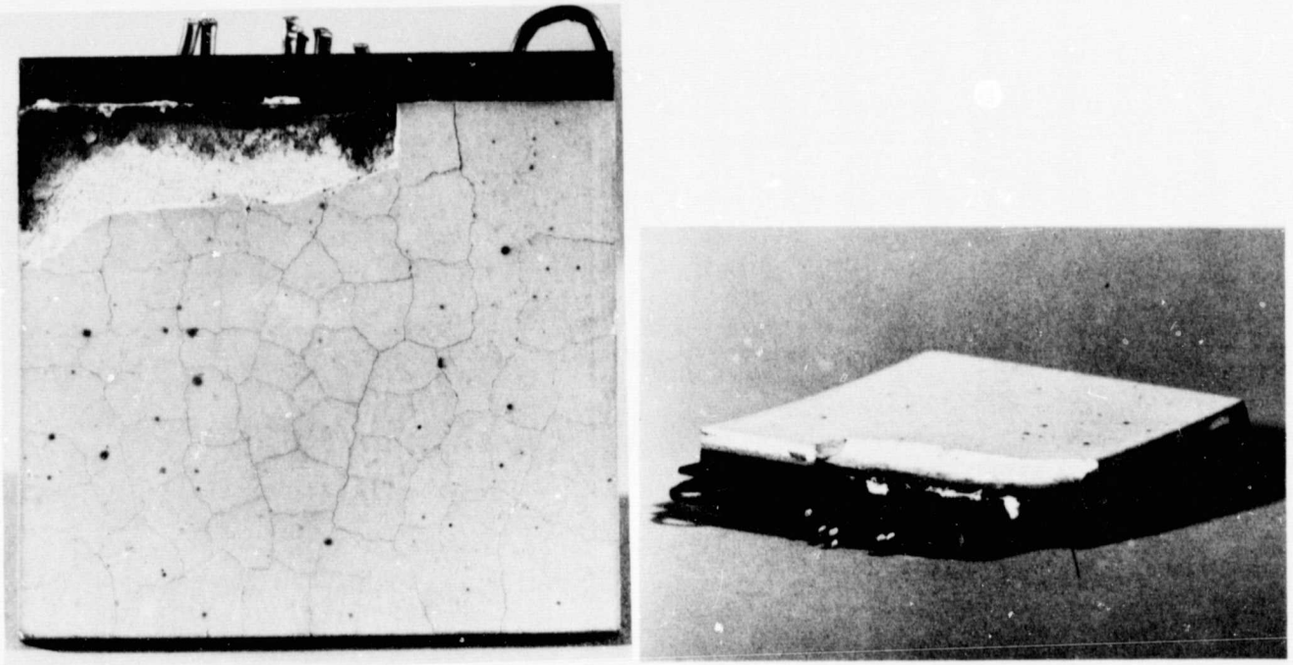

2nd Test

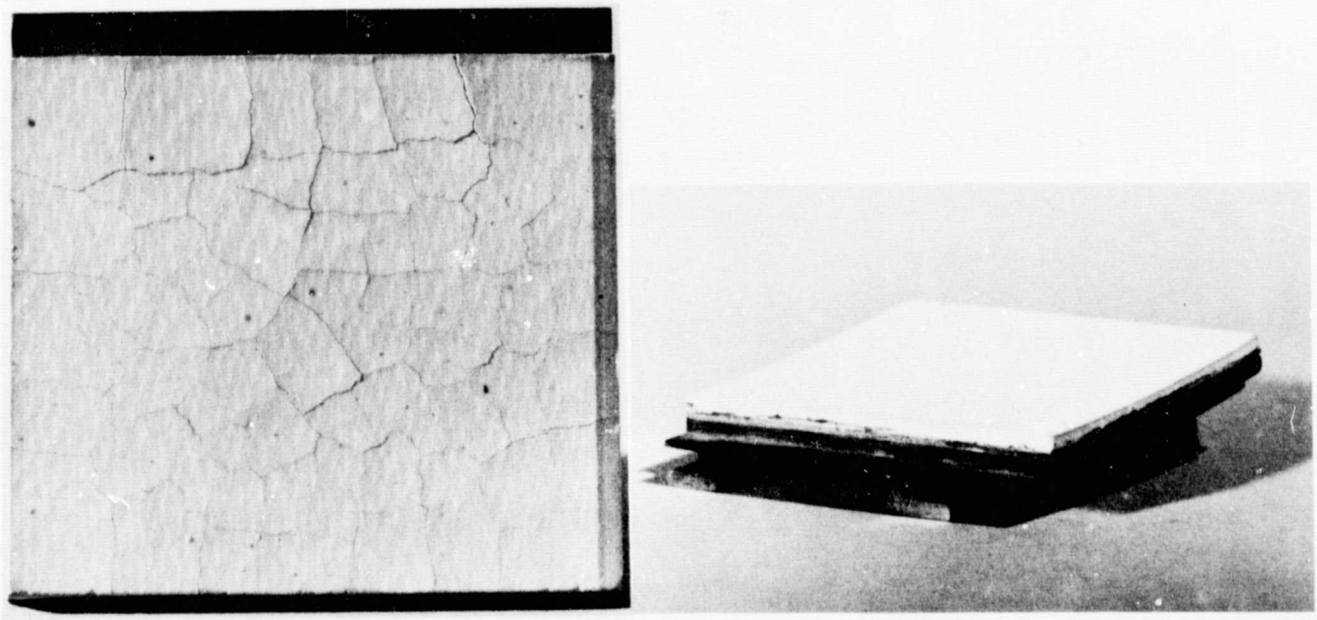

Figure 18 Cyclic Thermal Shock Results of Initial Design - Post Test Condition

3.1.4.4 Analysis

The rig test evaluation of the scaled-up engine size parts indicated that the abradability and erosion resistance of the sprayed ceramic seal system was comparable to that of subscale parts which had demonstrated potential for turbine sealing. Cyclic thermal shock testing exceeded the duration of previous tests by reaching 1000 cycles without spalling. Cyclic thermal shock testing, however, did produce both radial and laminar cracks. Post test inspection indicated significantly less severe laminar cracks in the axial plane in comparison with the circumferential plane. This is considered to be attributable to the fact that the stiffness is much less in the axial plane.

An analysis was conducted utilizing measured material properties and test conditions generated in the cyclic thermal shock rig. The purpose of the analysis was to evaluate the accuracy of the analysis in predicting crack initiation and form the base for evaluating future design improvements to reduce thermal stresses during engine operation.

3.1.4.4.1 Material Properties

Material properties of each of the sprayed ceramic seal system layers including modulii of elasticity and rupture, strain-to-failure, thermal expansivity, as well as the shear strength at the ZrO_2-85/15 ZrO_2/CoCrAlY interface were measured. Material specimens were sprayed on mild steel substrates. The substrates were subsequently removed by machining prior to property measurement.

All property data reported in this section with the exception of residual stress were measured on parts fabricated utilizing supplementary heating of the substrate to 930°K (1200°F) during spraying. Early analytical data from the program described in NASA CR-135387 indicated that spraying parts with substrates heated at 930°K (1200°F) would have potential for reducing thermal stresses during engine operation. As properties were being measured, experimental data in NASA CR-135387 revealed that parts fabricated with supplemental heating had considerably less cyclic thermal shock capability than analytically predicted. As a result, parts fabricated for rig testing of the initial design and the parts used to measure residual stress were fabricated without supplementary heating. Properties presented below, with the exception of residual stresses were therefore not used in the cyclic thermal shock analysis of the initial design. Earlier property measurements reported in NASA CR-135183 were used.

Modulus of Elasticity and Rupture and Strain to Failure

Modulus of Elasticity and Rupture and Strain to failure were determined at room temperature and at an elevated temperature approximately equal to the estimated maximum temperature each of the layers would be exposed to during engine operation. Measurements were taken using the four point bend method. A strain gage, placed at mid span and center of each specimen was used to measure strain at room temperature. Test measurements of cross-head deflection were used to determine specimen strain

at temperatures above strain gage capability of 589°K (600°F). Test specimens measured 3.048 x 0.953 x 0.254 cm (1.20 x 0.375 x 0.100 in.) and were prepared such that the length of the specimen was in the circumferential direction. Property characteristics were determined at 294° and 1589°K (70° and 2400°F) for the Y_2O_3 stabilized ZrO_2, 294° and 1255°K (70° and 1800°F) for the 85/15 ZrO_2/CoCrAlY and 294° and 1144°K (70° and 1600°F) for the 40/60 ZrO_2/CoCrAlY layer. Measurements are presented in Table 2. Data substantiated the trend of increasing strength and modulus with increasing percentage of metal that had been seen in measurements taken under previous contracts. Also, the modulus and strength of the ceramic layer were lower at elevated temperature then at room temperature, while the modulus and strength of the metal bearing layers were higher at elevated temperature.

TABLE 2

FOUR-POINT BEND TEST DATA

Material %	Temp °K (°F)	Modulus of Rupture $10^3 N/cm^2$ (ksi)	Modulus of Elasticity $10^3 N/cm^2$ (10^6psi)	Strain To Failure %
Y_2O_3	RT	2.71 (3.93)	3.03 (4.40)	0.157
Stabilized	RT	2.55 (3.70)	3.08 (4.47)	0.131
ZrO_2	RT	3.41 (4.94)	2.50 (3.63)	0.238
Avg.		2.89 (4.19)	2.88 (4.17)	0.175
	1589 (2400)	1.70 (2.47)	0.87 (1.26)	0.477
	1589 (2400)	1.75 (2.54)	0.56 (0.81)	0.577
	1589 (2400)	1.71 (2.48)	0.51 (0.74)	0.444
Avg.		1.72 (2.50)	0.65 (0.94)	0.493
85/15	RT	- - -	- - -	- - -
ZrO_2/CoCrAlY	RT	3.65 (5.30)	3.97 (5.75)	0.119
	RT	4.17 (6.05)	4.52 (6.56)	0.146
Avg.		3.92 (5.68)	4.25 (6.16)	0.133
	1255 (1800)	5.01 (7.27)	3.30 (4.78)	0.152
	1255 (1800)	5.65 (8.19)	3.01 (4.37)	0.187
	1255 (1800)	5.81 (8.43)	2.80 (4.06)	0.208
Avg.		5.49 (7.96)	3.03 (4.40)	0.182
40/60	RT	13.7 (19.9)	7.64 (11.1)	0.270
ZrO_2/CoCrAlY	RT	13.4 (19.5)	7.51 (10.9)	0.226
	RT	9.30 (13.5)	7.58 (11.0)	0.140
Avg.		11.91 (17.3)	7.58 (11.0)	0.212
	1144 (1600)	13.57 (19.7)	2.41 (3.50)	0.739
	1144 (1600)	12.33 (17.9)	2.49 (3.62)	0.599
	1144 (1600)	13.57 (19.7)	2.49 (3.61)	0.658
Avg.		13.15 (19.1)	2.47 (3.58)	0.651

Thermal Expansion

The thermal expansivity of each of the three sprayed ceramic system layers was measured in the circumferential direction. Specimens were 2.540 x 0.508 x 0.254 cm (1.0 x 0.2 x 0.1 in.).

After being accurately measured in the 2.54 cm (1.0 in.) direction the specimens were instrumented with a Netzch Electronic Automatic Recording Dilatometer. The system was placed in the center zone of a closed chamber which was evacuated and then back-filled with helium. The specimens were then programmed for temperature rise and equilibrium at approximately 100°K (180°F) intervals from 293°K (68°F) to 1144°K (1600°F), 1255°K (1800°F) and 1589°K (2400°F) for the 40/60 and 85/15 ZrO_2/CoCrAlY layers and the ZrO_2 layers respectively. An equivalent program for temperature decrease was also implemented. The rate of temperature increase and decrease was approximately 5°K/min (9°F/min).

The ZrO_2 material demonstrated a noticeable shrinkage at approximately 1422°K (2100°F) during the first thermal cycle as shown in Figure 19. Total shrinkage of 0.4 percent was measured. Subsequent cycles did not exhibit this shrinkage and were very repeatable. Figure 19 also shows cycle 3 data which is typical of subsequent cycles.

Both the 85/15 and 40/60 materials demonstrated much more repeatable dimensional change during heating and cooling and from cycle to cycle. Some tendency for elongation was observed, however. Data is presented in Figures 20 and 21. Generally, the data is in close agreement with that developed under previous contracts on parts sprayed without supplementary heating of the substrates indicating 1) good repeatability of the data and 2) the insensitivity of the property to spraying on a heated substrate.

Weight, volume and dimensional changes were measured for each of these materials as a result of exposure to high temperature in air. Weight and volume measurements are shown in Figure 22. Dimensional changes are plotted on Figure 23. The dimensions of the ZrO_2 decreased while both of the ZrO_2/CoCrAlY intermediate layers increased with exposure to temperature. This relative dimensional change in each of the layers as a result of exposure to the thermal environment of the engine over a period of time may influence the thermal stability of the sprayed ceramic seal system. In particular, this dimensional change may be a factor in the magnitude of the stresses generated at the ZrO_2 and 85/15 ZrO_2/CoCrAlY interface. Volume and dimensional decrease of the ZrO_2 sprayed onto 930°K (1200°F) substrates under this contract was less than previous data for parts sprayed on substrates without supplemental heating.

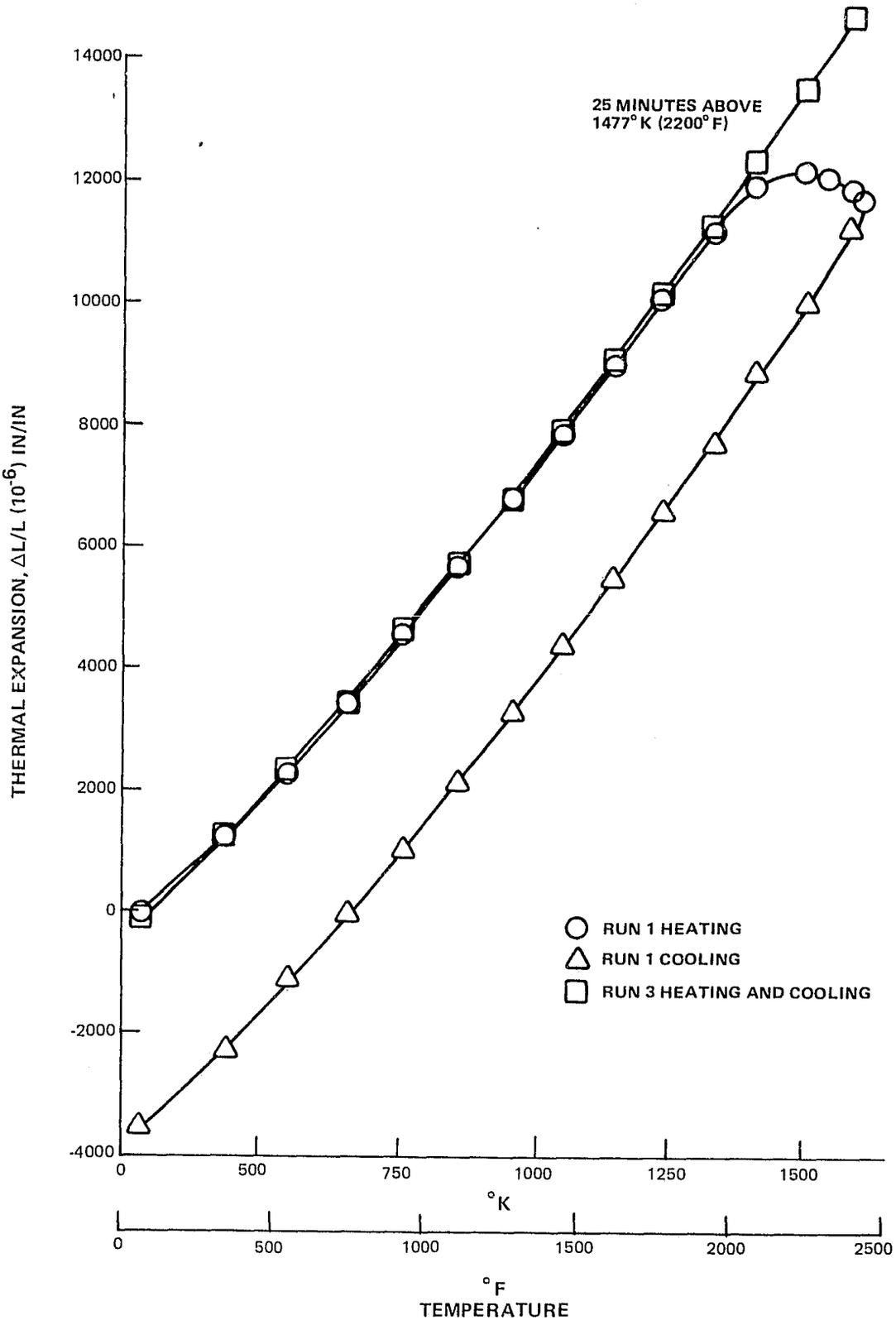

Figure 19 Thermal Expansivity Of ZrO_2

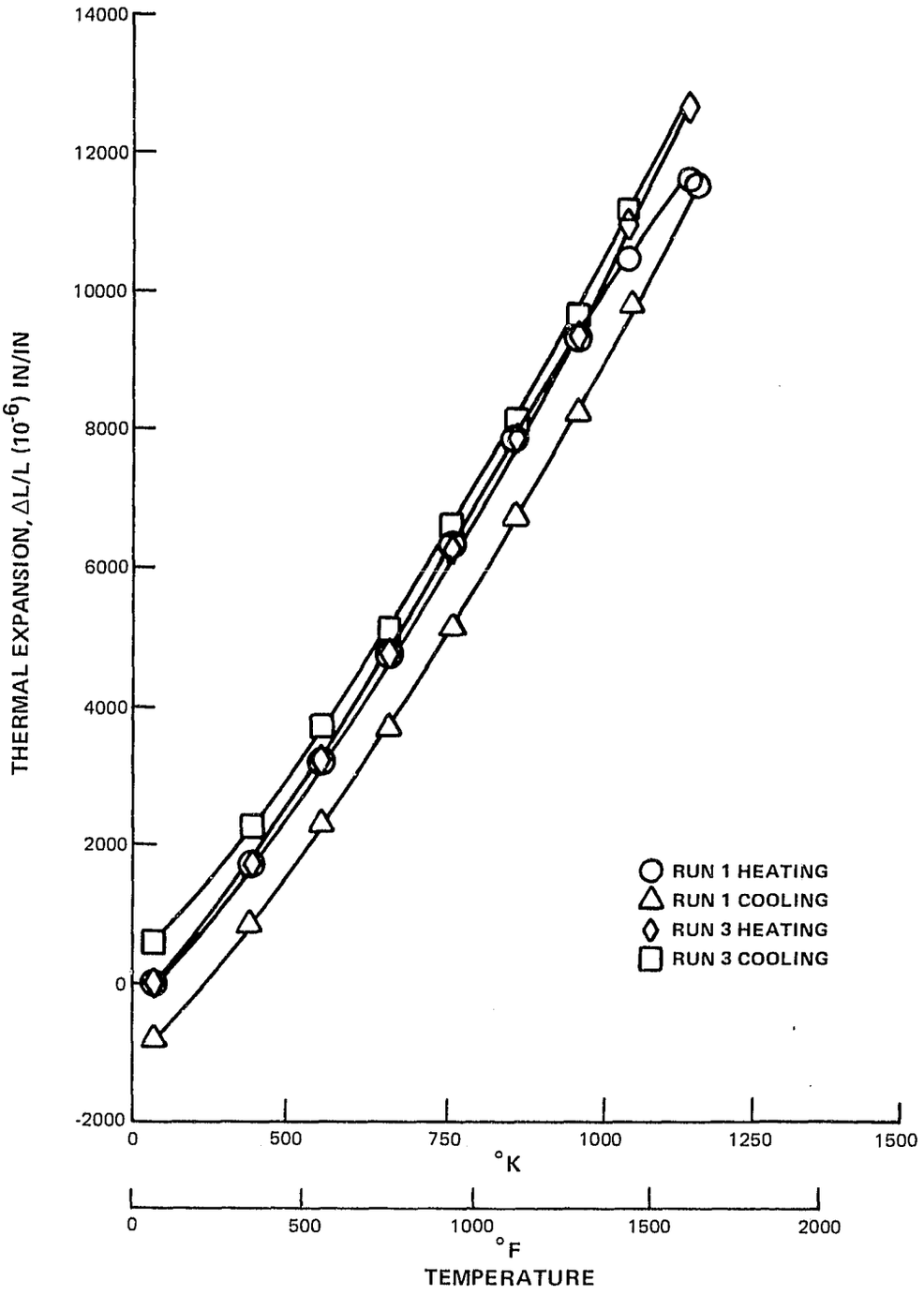

Figure 20 Thermal Expansivity Of 85/15 ZrO_2/CoCrAlY

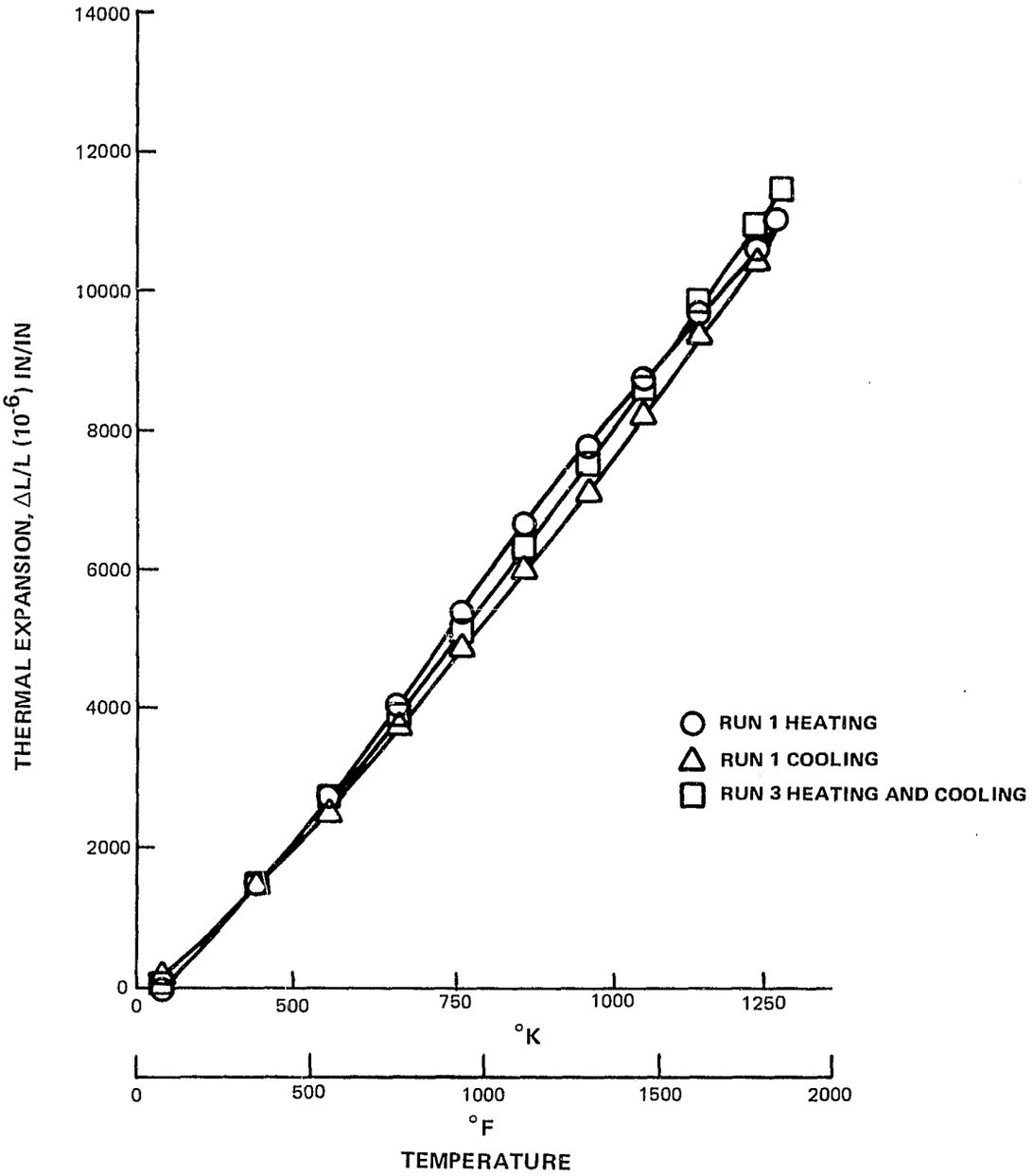

Figure 21 Thermal Expansivity of 40/60 ZrO_2/CoCrAlY

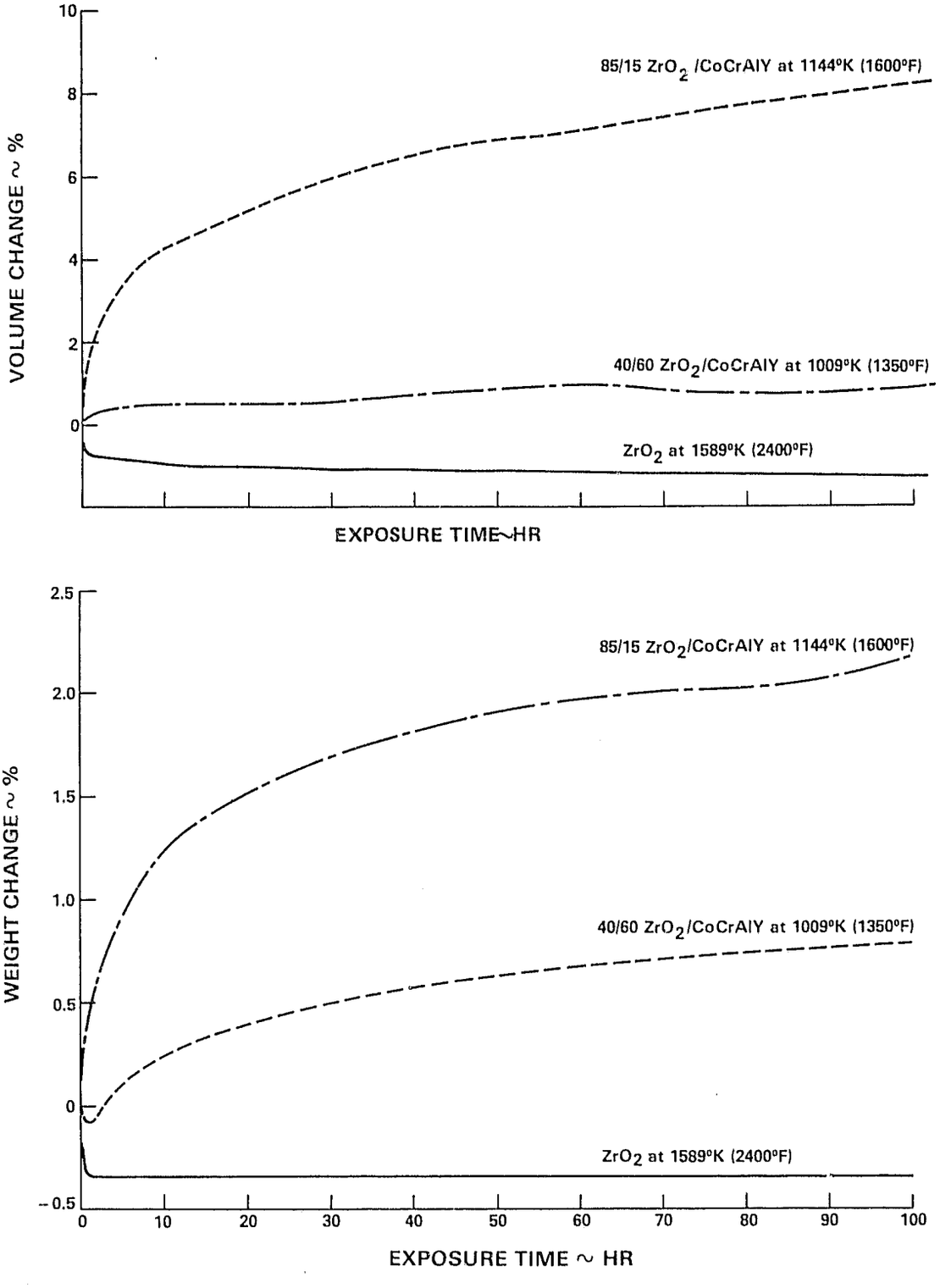

Figure 22 *Volume and Weight Change Resulting From Exposure to Temperature*

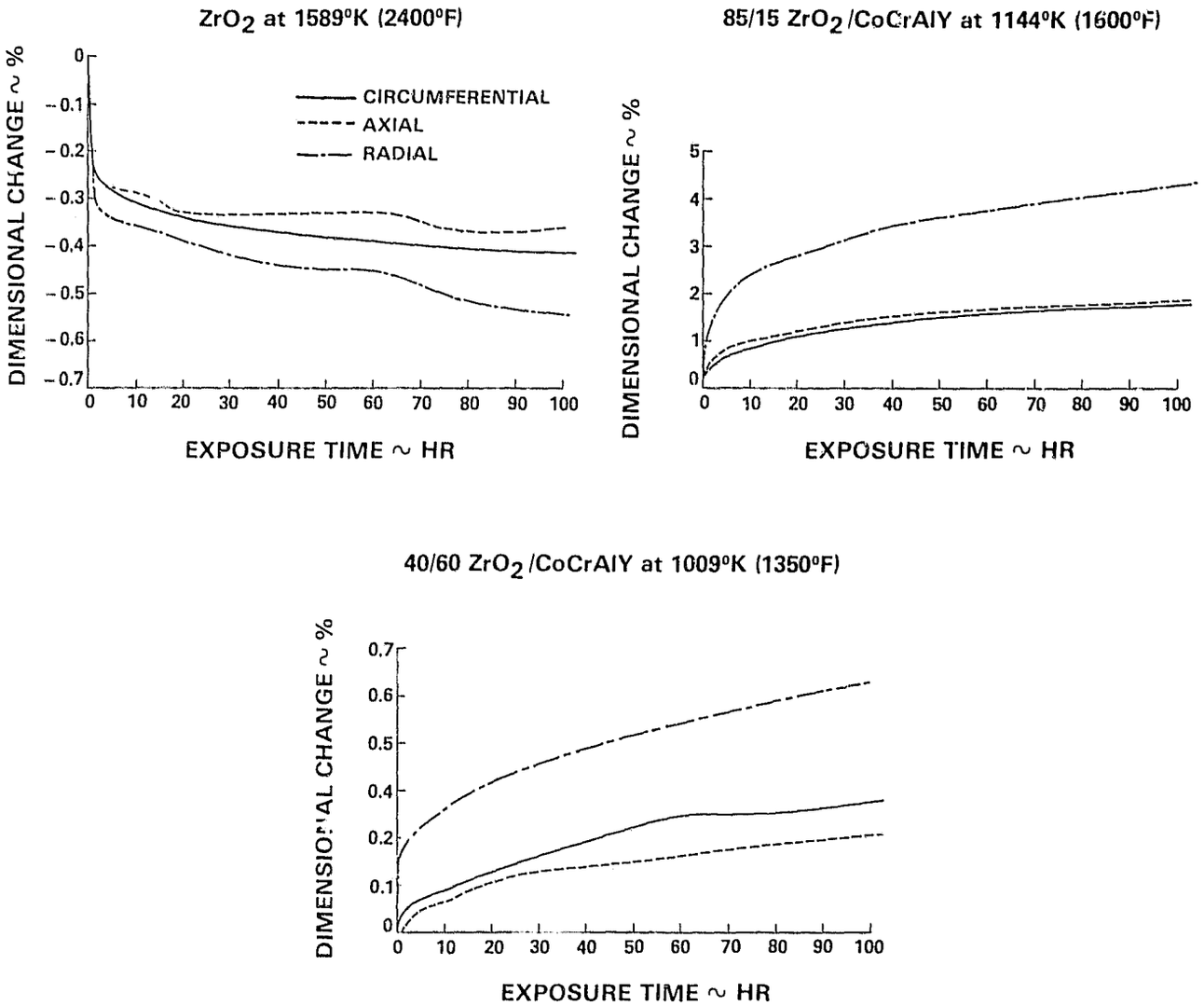

Figure 23 Dimension Change Resulting From Exposure to Temperature

Shear Strength

Laminar cracks which resulted near the layer interfaces during earlier cyclic thermal shock testing substantiated the advisability of effort to investigate the interfacial strength of the system. As a result the shear strength at the ZrO_2 layer -- 85/15 ZrO_2/CoCrAlY layer interface was measured at room temperature using the method shown in Figure 24. Most specimens fractured in a plane through both the ZrO_2 and 85/15 layers as shown in Figure 24. Since the failure plane did extend through both materials, however, the results were inconclusive.

Residual Stress

Residual strain measurements were taken on a full scale JT9D ceramic seal segment. The stress free temperature profile based on the circumferential strain is shown in Figure 25. This stress free temperature distribution was used in the analysis of the cyclic thermal shock rig test result.

3.1.4.4.2 Analytical Correlation with Cyclic Thermal Shock Test Results

The thermal stresses generated during both cyclic thermal shock tests were estimated by the two dimensional stress analyses using the latest residual stress data and the temperatures generated during the rig tests. Stresses throughout the seal system were calculated at acceleration to sea level take off, sea level take off and deceleration to idle in both the circumferential and axial planes. Results were screened to investigate stresses generated during these operational points to determine the magnitude and location of maximum principal stresses. Particular attention was directed to stresses in both the ZrO_2 and 85/15 ZrO_2/CoCrAlY layers near the interface where laminar cracking was observed as a result of the cyclic thermal shock test. Figure 26 shows the stresses at the interface for the three test conditions in the circumferential plane for both the ZrO_2 and 85/15 layer respectively. Strength of the layered material is shown for comparison purposes. Results indicate that stresses in the ZrO_2 at the center of the seal segment exceeded the strength of the ZrO_2. The direction of these principal stresses were at 0^o with the horizontal and were therefore perpendicular to the radial cracks observed in the ZrO_2. The analysis thus tends to correlate with cyclic thermal shock results which produced radial cracks at the ZrO_2 surface. Although the analytical results do show that the stresses exceeded the strength of the 85/15 layer toward the edge during the acceleration transient the angle of the principal stress was only 0.35 radians (20^o) from the horizontal at the location of the laminar cracks. The analysis therefore did not predict the occurrence of laminar cracks. A number of possible reasons for this particular lack of correlation included. 1) anisotropic properties in the sprayed materials, 2) shrinkage of the ZrO2 layer as demonstrated by thermal expansivity tests and 3) interface bond strength lower than the strength of the nearest adjacent material.

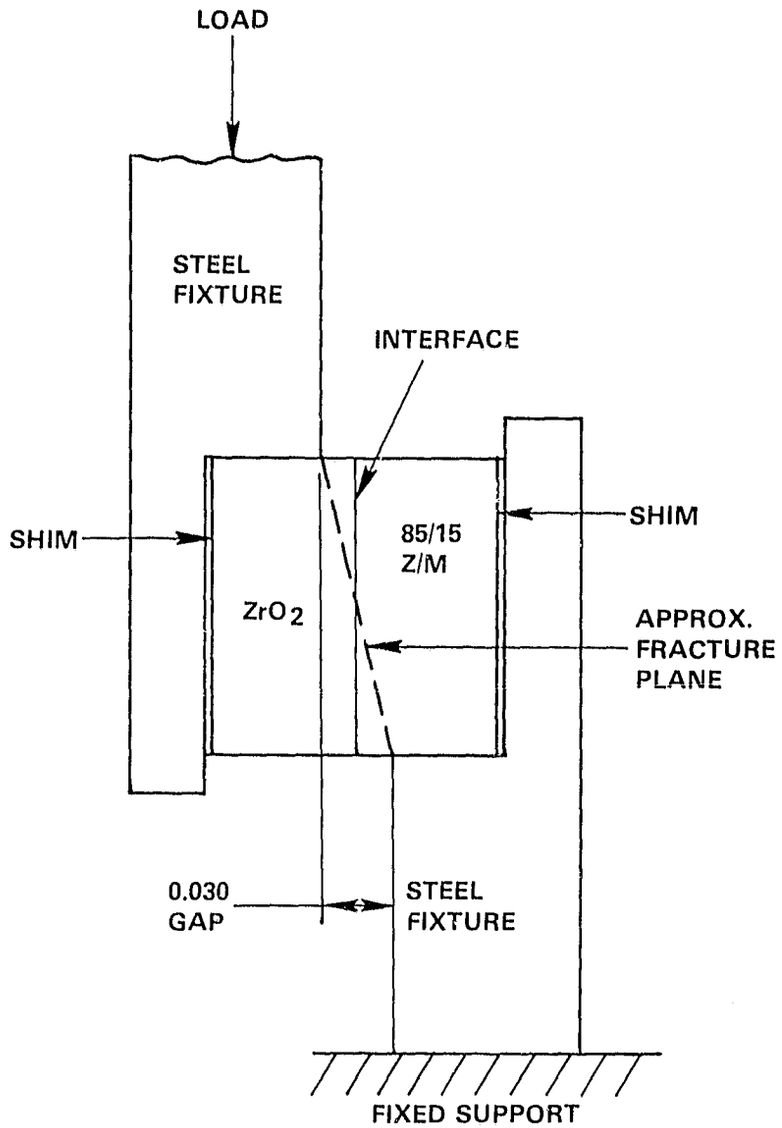

NOTE: 1. SHIMS INSTALLED WHERE SHOWN AS REQ'D TO CENTER INTERFACE IN GAP.
2. Z/M = ZrO_2/CoCrAlY

Figure 24 Interface Shear Strength Test Method

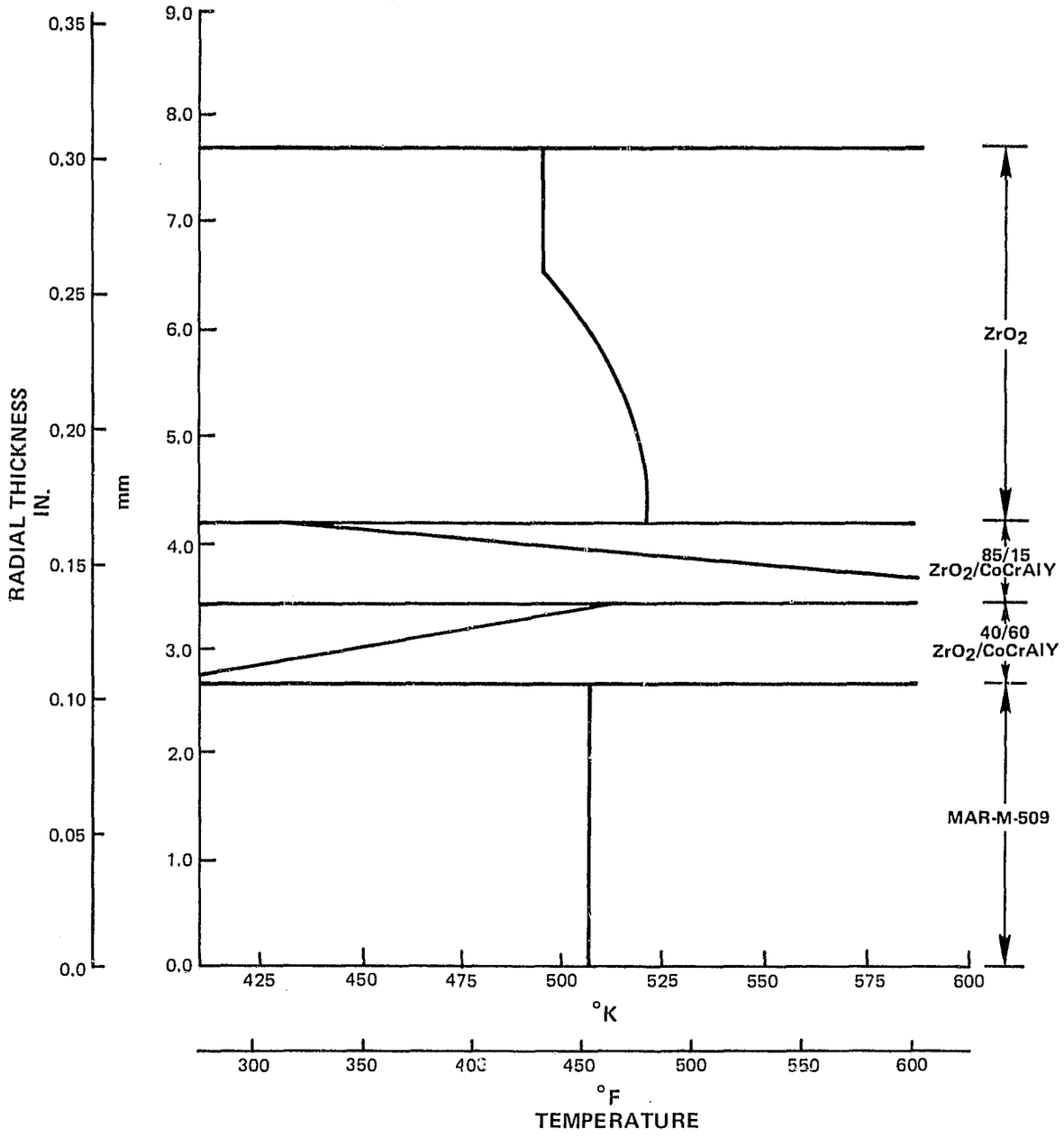

Figure 25 *Stress Free Temperature Distribution For a JT9D Ceramic Seal Segment - Initial Design*

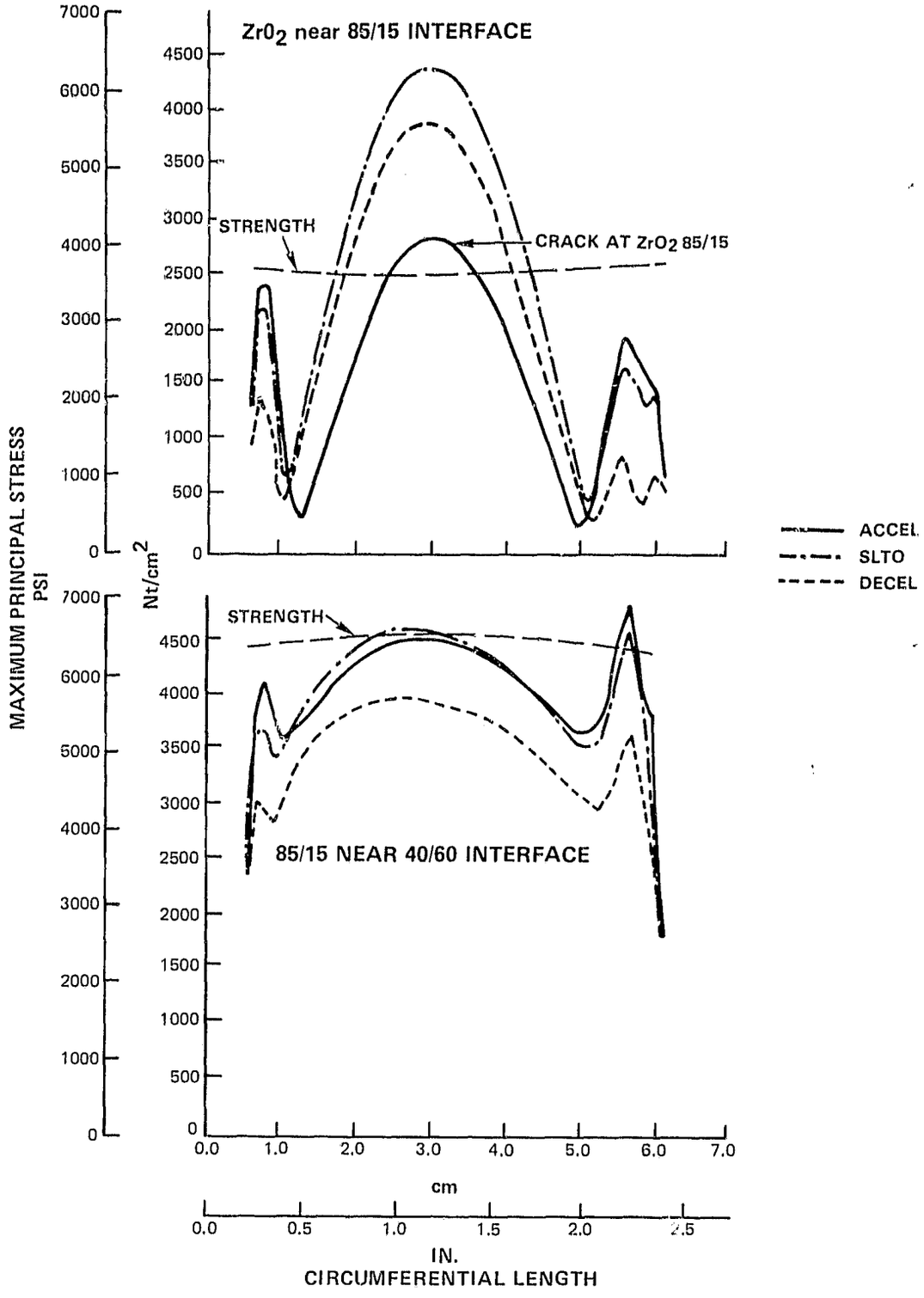

Figure 26 *Maximum Principal Stress In The Circumferential Plane During Cyclic Thermal Shock Test 2-Initial Design*

3.2 DESIGN IMPROVEMENT

Abradability and erosion resistance of the initial design were generally comparable to that of subscale parts under previous contracts which were judged to offer sufficient potential for engine test evaluation. Spalling of the ceramic did occur after 200 thermal cycles during rig testing but did not progress further with continued testing up to 1000 cycles. This test indicated that an initial crack or spalling of the ceramic would not result in secondary failure of the seal support. However, because of the basic necessity for structural stability of the ceramic system during engine thermal cycling, design modifications to inhibit crack inititation and improve thermal stability of the seal system were considered necessary. Because the occurrence and magnitude of cracks in the axial and circumferential planes during testing appeared to be related to the stiffness, an investigation of the possibility of reducing the circumferential stiffness of the seal segment was initiated. Several alternatives to reduce the circumferential stiffness of the seal by slotting the circumferential rails were evaluated. The approach of machining six 0.075 cm (0.030 in.) slots at every 0.635 cm (0.25 in.) interval was selected. The thermal stress which would have been produced during the cyclic thermal shock testing during accel, sea level take off and decel in the ZrO_2 and 85/15 ZrO_2/-CoCrAlY layers were estimated. Thermal stresses are shown in each material for each test condition in Figures 27 and 28. The benefit in terms of reduced stresses can be seen by making a comparison with the stresses generated in the initial design also shown in the figures. Maximum stress in the center and at the edges were reduced for all cases except the 85/15 layer during decel in which stresses were increased. Since the increase in stress did not exceed the strength of the material this fact was considered to be of secondary importance.

Analysis was conducted to evaluate the potential benefit of reducing the ZrO_2 layer from 0.229 cm (0.090 in.) to 0.152 cm (0.060 in.). The analysis used a simplified one dimensional temperature distribution rather than the actual temperature distribution generated during cyclic thermal shock testing. Results, shown in Figures 29 and 30 showed a very definite benefit by reducing thickness at all conditions. Further reduction in the ZrO_2 below 0.152 cm (0.060 in.) was not considered because of maximum temperature limitations of the intermediate layer.

As a result of the analytical effort to improve the design the substrate circumferential stiffness was reduced by slotting the rails. Further, a decision was made to conduct two cyclic thermal shock tests one with a seal with 0.229 cm (0.090 in.) ZrO_2 and the other with 0.152 cm (0.060 in.) ZrO_2 to evaluate experimentally the benefit of ZrO_2 thickness reduction. A drawing of the improved design is shown in Figure 31.

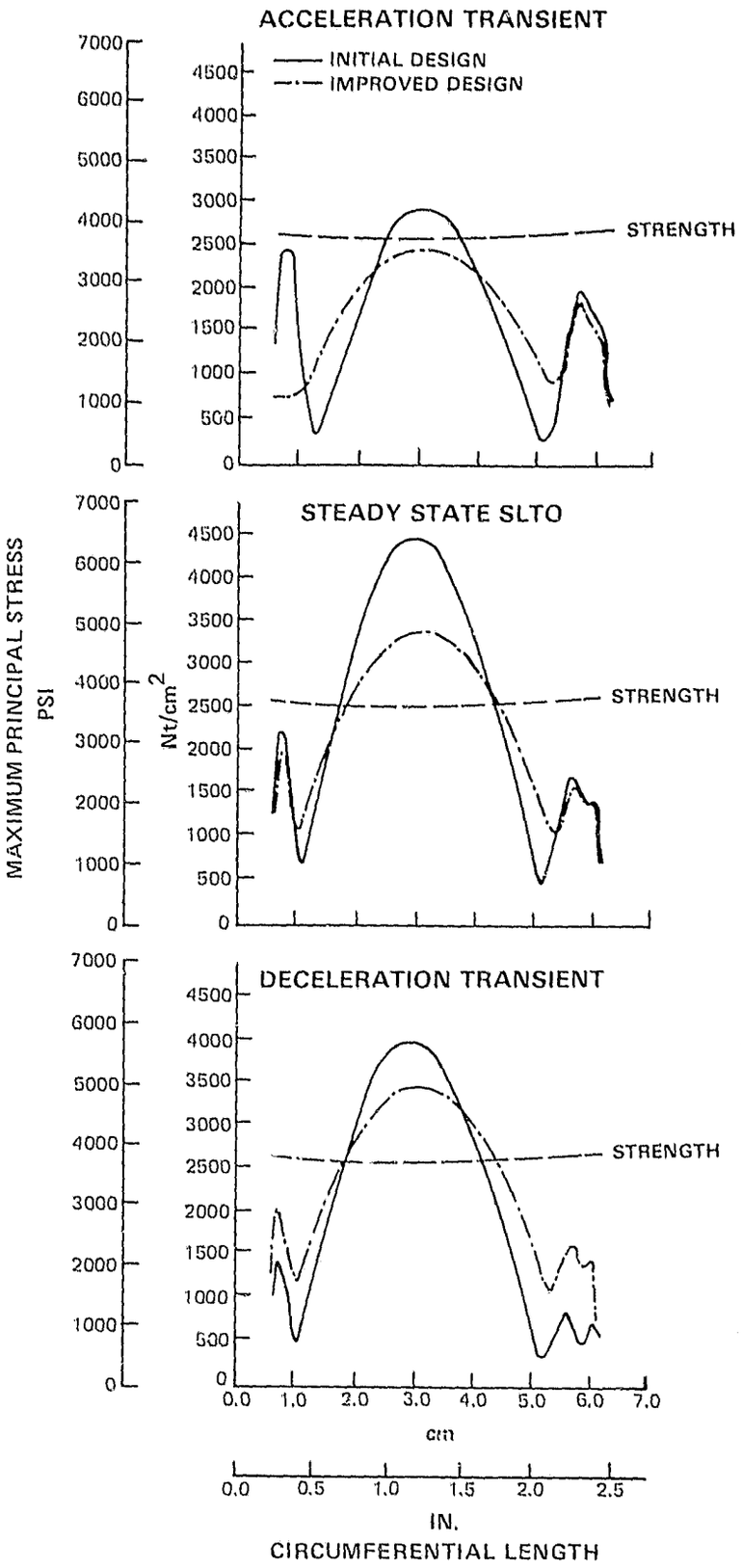

Figure 27 *Maximum Principal Stress in Circumferential Plane in ZrO_2 Near the 85/15 Interface Initial and Improved Design*

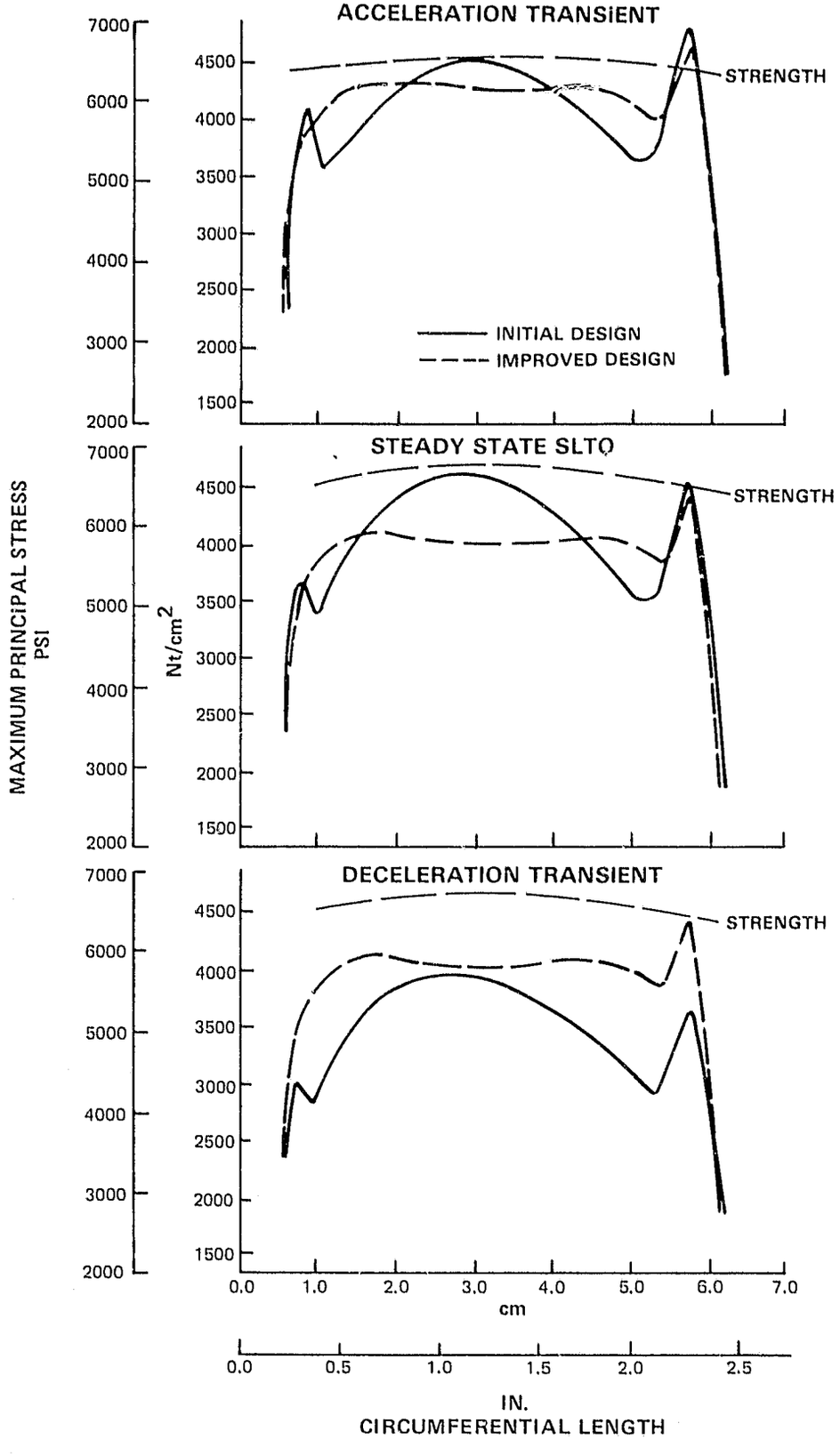

Figure 28 *Maximum Principal Stress in the Circumferential Plane in 85/15 Near the 40/60 Interface Initial and Improved Design*

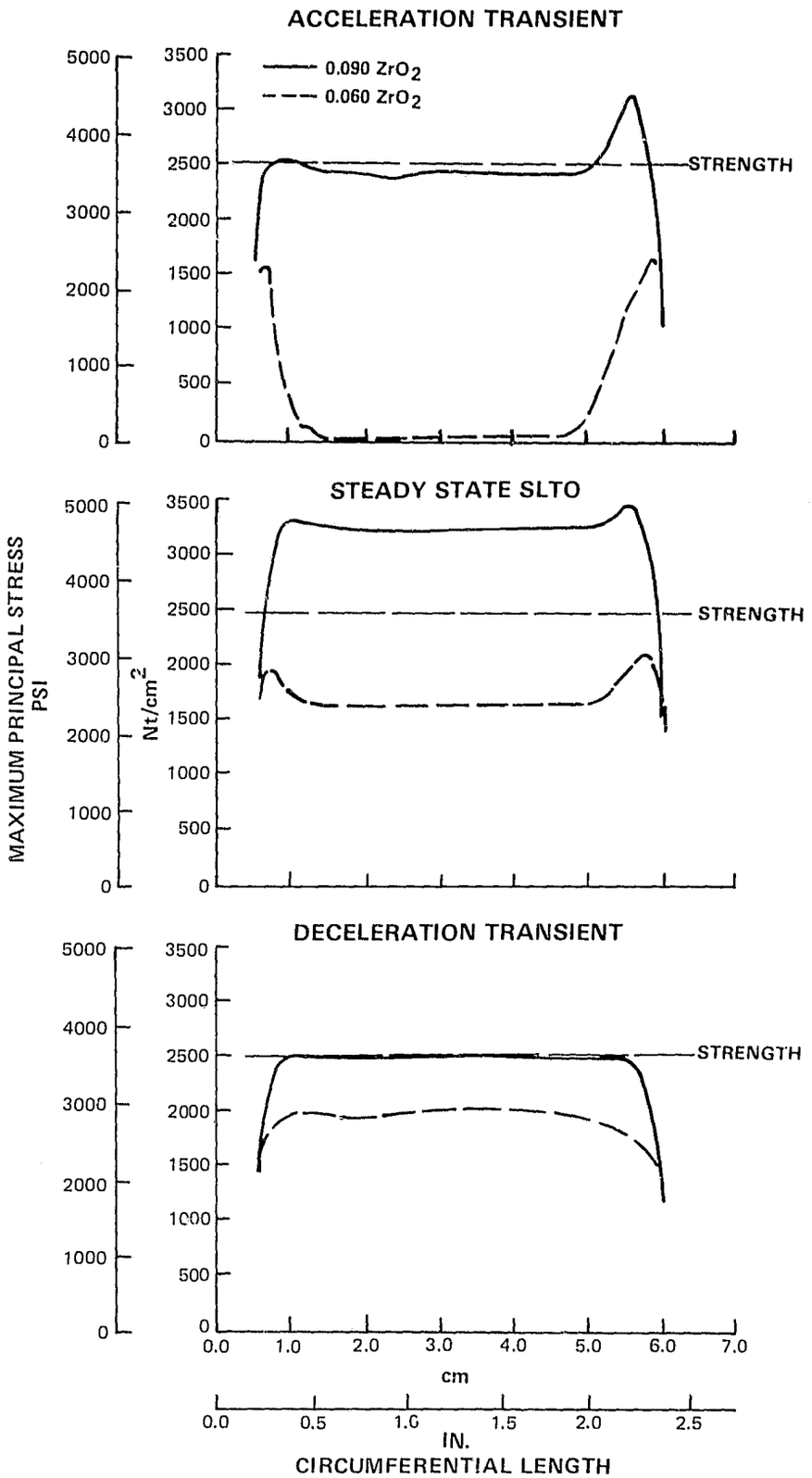

Figure 29 *Maximum Principal Stress in the Circumferential Plane in ZrO_2 Near the 85/15 Interface for Different ZrO_2 Thicknesses*

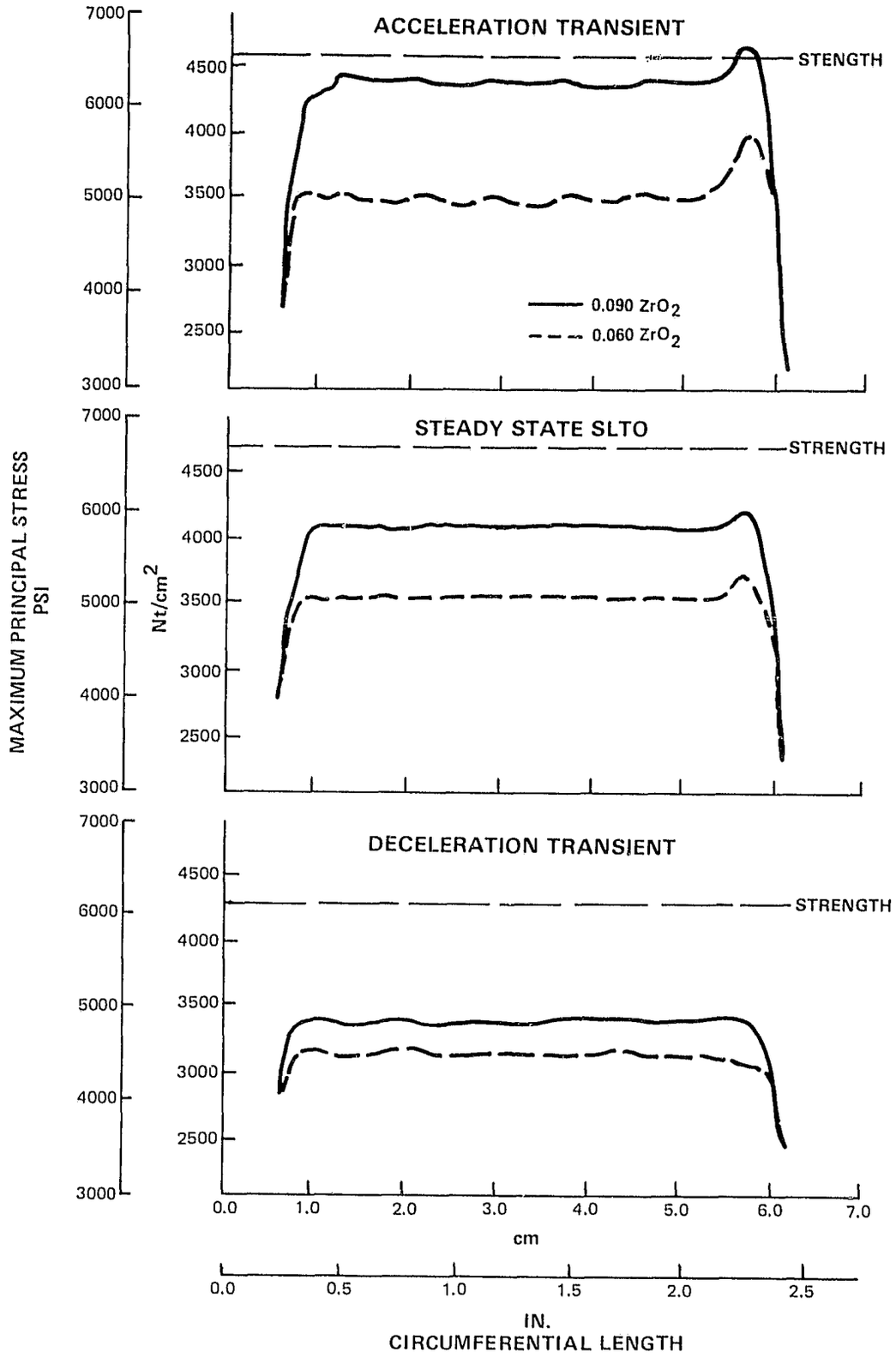

Figure 30 *Maximum Principal Stress in the Circumferential Plane in the 85/15 Near the 40/60 Interface for Different ZrO_2 Thicknesses*

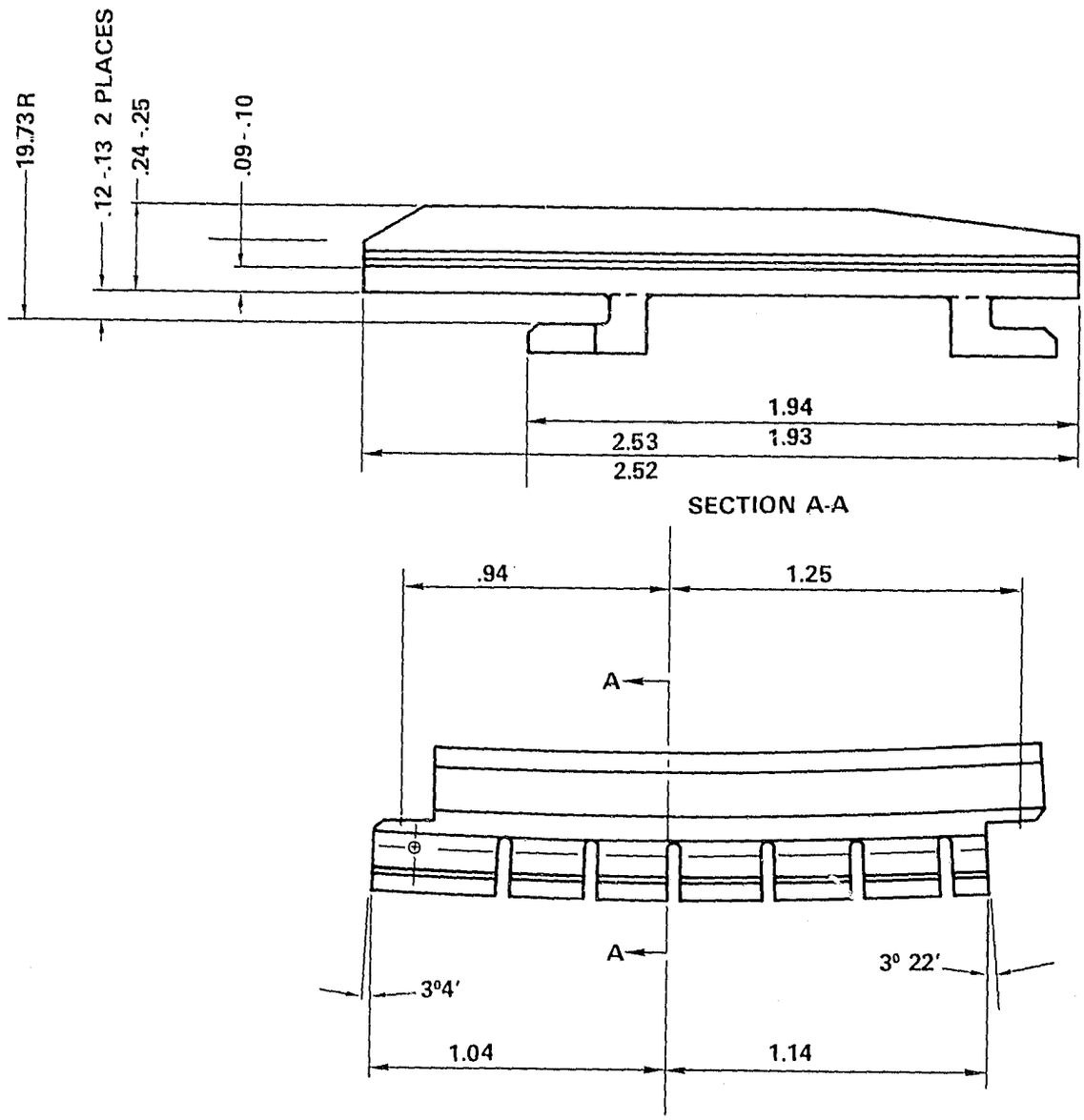

Figure 31 JT9D Ceramic Seal - Improved Design

3.3 EVALUATION OF THE IMPROVED DESIGN

Evaluation of the improved design was accomplished by 1) abradability and erosion testing at the same conditions as earlier testing, mainly to verify repeatability of performance, 2) cyclic thermal shock testing to demonstrate anticipated improved performance over the initial design and 3) engine tests to investigate the capability of the sprayed ceramic to resist the thermal environment of the engine and the blade tip rub characteristics. Residual stress was also measured and used in concert with the latest available property data in an analysis to correlate maximum principal stresses with crack initiation and progression in the cyclic thermal shock rig and engine tests of the improved design parts.

3.3.1 Rig Tests

The same rigs and procedures used to evaluate the abradability, erosion resistance and thermal shock capability of the initial design were again used to determine the benefit of the improved design. Actual engine parts were sprayed and used in both the abradability and cyclic thermal shock testing. Parts using a flat Hastelloy X substrate sprayed at the same time as engine hardware were used for erosion testing.

3.3.1.1 Abradability

Three abradability tests were conducted at the same conditions used to evaluate the initial design. Tests were conducted at 304.8 m/sec (1000 ft/sec) rate speed with incursion rates of 0.00254, 0.0254, and 0.254 mm/sec (0.0001, 0.001 and 0.010 in/sec). Results are presented in Table 3. Also shown in Table 3 for comparison purposes are the results of testing of the initial design. The data shows the same trend with the least blade wear at the nominal or 0.0254 mm/sec (0.001 in/sec) incursion rate and greater blade wear at both slower and faster incursions. A comparison of the repeatability of the magnitude of wear at the 0.0254 mm/sec (0.001 in/sec) test is difficult because of the unusual, unexplained, wear pattern of tests #4 which was discussed earlier. Abradability testing generally indicated performance repeatability of the sprayed ceramic seal system. Post test condition of the parts is pictured in Figure 32.

3.3.1.2 Erosion

Two erosion tests were conducted with a ZrO_2 surface temperature of 1589°K (2400°F) at impingement angles of 0.262 and 1.57 radians (15 and 90°). Weight loss at 5 minute intervals for both tests are shown in Figure 33. During the 1.57 radians (90°) test the specimen eroded through the ZrO_2 and 85/15 CoCrAlY layers and approximately 0.038 cm (0.015 in.) into the 40/60 ZrO_2/CoCrAlY layer. This fact probably accounts for the reduction in erosion rate from 0.32 gm/min in the 5 to 10 min internal to the 0.13 gm/min in the 15 to 20 min time period. The 0.32 gm/min is therefore considered more representative of the ZrO_2 layer erosion rate.

TABLE 3

ABRADABILITY TEST RESULTS

	Initial Design				Improved Design		
Test Conditions:	1	2	3	4	1	2	3
Seal Temp, ^{o}K (^{o}F)	1589 (2400)	1589 (2400)	1589 (2400)	1589 (2400)	1589 (2400)	1589 (2400)	1589 (2400)
Tip Speed, m/sec (ft/sec)	304.8 (1000)	304.8 (1000)	304.8 (1000)	304.8 (1000)	304.8 (1000)	304.8 (1000)	304.8 (1000)
Interaction Rate, mm/sec (in/sec)	0.0254 (0.001)	0.0254 (0.001)	0.00254 (0.0001)	0.254 (0.001)	0.0254 (0.001)	0.00254 (0.0001)	0.254 (0.01)
Interaction Depth, mm (in)	0.508 (0.020)	0.508 (0.020)	0.508 (0.020)	0.508 (0.020)	0.762 (0.030)	0.762 (0.030)	0.762 (0.030)
Number of Blades	12	6	12	12	12	12	12
Test Results:							
Seal Wear Depth, mm (in) max	0.508 (0.020)	0.381 (0.015)	0.127 (0.005)	0.381 (0.015)	0.508 (0.020)	0.508 (0.010)	0.0 (0.0)
Blade Tip Wear, mm (in) avg	0.046 (0.0018)	0.169 (0.0066)	0.335 (0.0131)	0.361 (0.0141)	0.038 (0.0015)	0.276 (0.0109)	0.524 (0.0207)
VWR = Seal Vol/Tip Vol	4.878	5.917	0.096	0.091	5.291	0.232	Undefined

TABLE 4

EROSION TEST RESULTS

	Gas Velocity	Nozzle to Specimen cm (in)	Surface Temp. ^{o}K (^{o}F)	Impingement Angle Rad (Deg)	Particulate Size	Particulate Kg/hr (lb/hr)	Particulate Flow Rate gm/mn (lb/hr)	Erosion
Improved (1) Design	0.35	3.81 (1.5)	1589 (2400)	0.262 (15°)	Al_2O_3	80 grit	2.72 (5.997)	0.075 (165.3)
Improved (2) Design	0.35	3.81 (1.5)	1589 (2400)	1.57 (90°)	Al_2O_3	80 grit	2.72 (5.997)	0.32 (705.3)
Initial (3) Design	0.35	3.81 (1.5)	1589 (2400)	2.62 (15°)	Al_2O_3	80 grit	0.544 (1.2)	0.013 (28.7)
Initial (4) Design	0.35	3.81 (1.5)	1589 (2400)	0.786 (45°)	Al_2O_3	80 grit	0.544 (1.2)	0.0247 (54.5)
Initial (5) Design	0.35	3.81 (1.5)	1589 (2400)	1.57 (90°)	Al_2O_3	80 grit	0.544 (1.2)	0.04 (88.3)

Figure 32 *Abradability Test Results of the Improved Design - Post Test Condition*

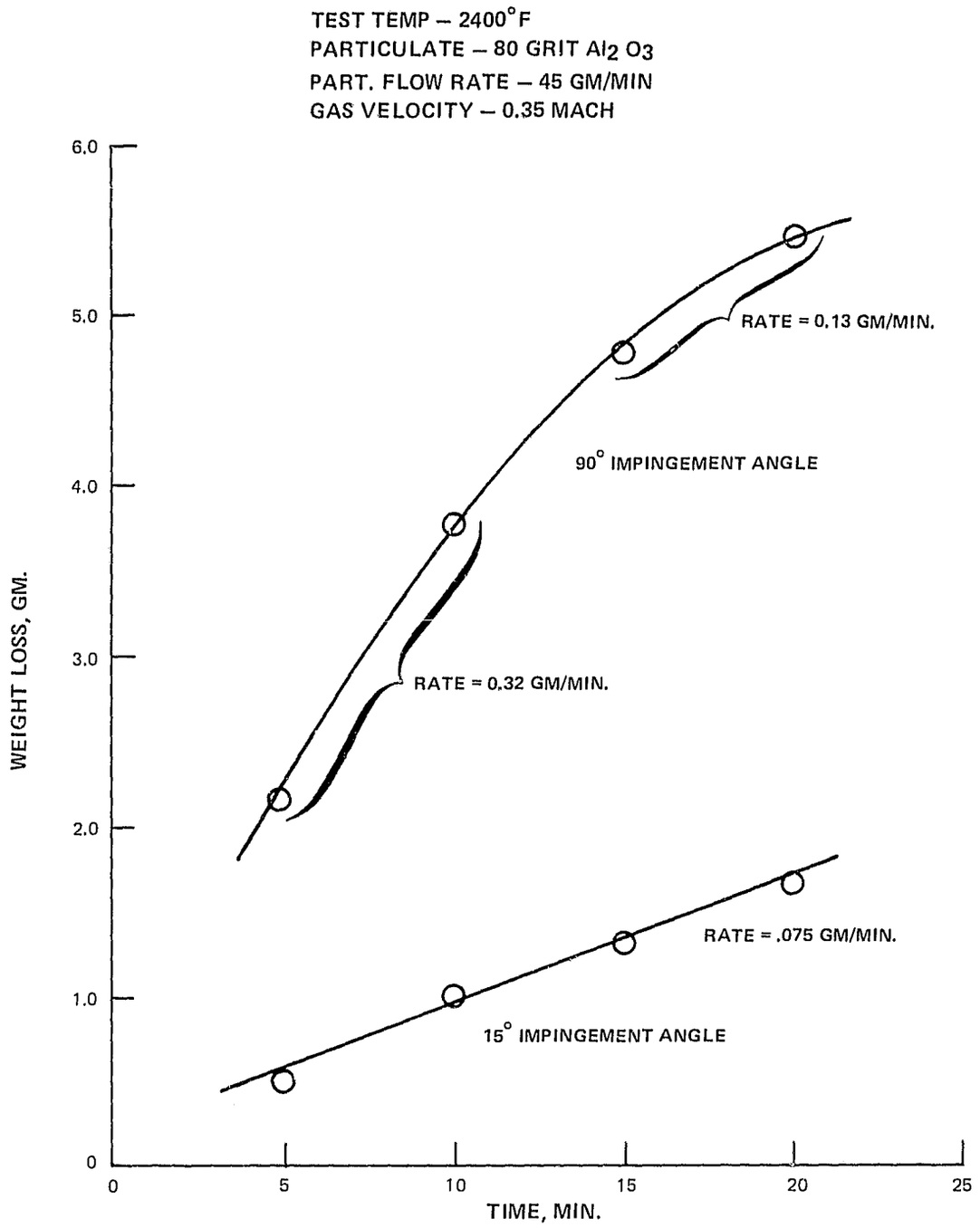

Figure 33 Erosion Test Results of the Improved Design

Results of both of these tests are shown in Table 4 along with earlier erosion testing of the intial design. The particulate flow rate in these two tests was 45 gm/min, 5 times greater than that used in earlier testing. Based on the assumption that erosion rate is directly proportional to particulate flow rate test No. 1 at a 0.262 radians (15°) angle is close to a factor of 5 greater than test No. 3 indicating good correlation. An attempt at correlating results of test No. 2 and No. 5 at 1.57 radians (90°) is compromised somewhat by 1) the erosion extending into the 85/15 and 40/60 ZrO_2/CoCrAlY layer and 2) the effect of particulate bounce back and collision with the impinging particles. Post test condition of the parts is shown in Figure 34.

Although limited, erosion data indicates similarity of the sprayed ceramic used in both the initial and improved design as would be expected.

3.3.1.3 Cyclic Thermal Shock Rig Tests

Two tests were conducted on the improved design. The first with 0.229 cm (0.090 in.) thick ZrO_2 layer completed 1000 cycles, the second with 0.152 cm (0.060 in.) ZrO_2 completed 500 cycles. These tests of the improved design produced significantly less severe cracking than previous testing of the initial design. Laminar cracks occurred primarily at the 85/15 - 40/60 ZrO_2/CoCrAlY interface.

Results of periodic inspection of the first test, 0.229 cm (0.090 in.) thick ZrO_2, are presented in Table 5 with Figure 35 for reference to part locations. A post test photograph of the tested seal is shown in Figure 36.

The second test, 0.152 cm (0.060 in.) thick ZrO_2 developed cracks comparable to that of the first test of the 0.229 cm (0.090 in.) ZrO2. However, the leading edge female shiplap joint corner, quadrant A in Figure 35 of the ZrO_2 and 85/15 ZrO_2/CoCrAlY layers did spall during removal from the fixture at the completion of the 500 cycles. The results of periodic inspection are presented in Table 6. The post test condition of the seal is shown in Figure 37.

3.3.1.3.1 Cyclic Thermal Shock Test Analysis

The thermal shock cycles generated during each of the two tests were analyzed to estimate maximum stresses and to correlate the stresses with crack initiation during testing. Typical thermal cycles from each of the tests are shown in Figure 38. These cycles were more severe in the heat-up transient than those generated during testing of the initial design as shown by comparing them with Figure 15. In spite of the more severe transient, the parts of the improved design did have less noticeable cracking than the initial design parts. The stress free temperature distribution shown in Figure 39 was used in the thermal stress analysis of the thermal shock rig test.

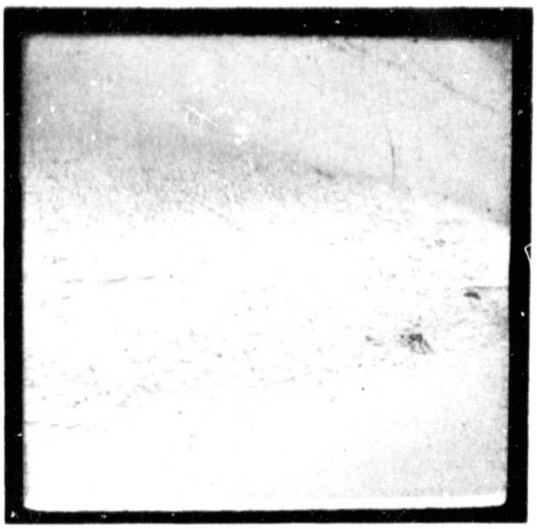

Impingment Angle = 15° (.262 radians)

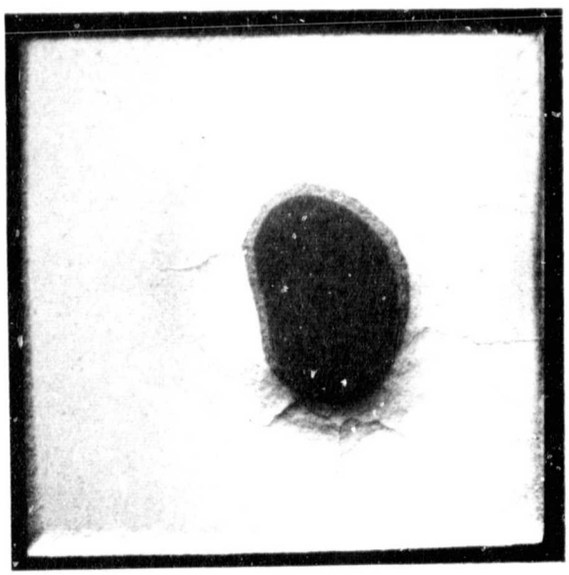

Impingment Angle = 90° (1.57 radians)

Figure 34 *Erosion Test Results of Improved Design - Post Test Condition*

TABLE 5

THERMAL SHOCK TEST INSPECTION OF IMPROVED DESIGN
(Refer to Fig. 35 for location identification)

Test No. 1

Time	Observations
Specimen No. 1	0.090" ZrO_2 Layer, Slotted Rails
After Accel Abort Cycle	1. Tight laminar crack @ interface 2 in corner A measuring approx. 3/16" axially by 1/16" circumferential.
After 1st Cycle	1. Laminar crack @ interface 2 in corner A propagated to 3/16" axial by 3/16" axial by 1/16" circumferential.
	2. Tight laminar crack @ interface 2 in corner B measuring approx. 1/16" axial by 1/16" circumferential.
After 31 cycles	1. Tight laminar crack @ interface 2 in corner A measuring approx. 5/16" axially by 5/16" circumferential.
	2. Laminar crack in corner B unchanged.
After 226 cycles	1. Laminar crack @ interface 2 in corner A propagated to 1/2" axial by 5/16" circumferential opened to approx. 1/64" max. @ corner.
	2. Unchanged otherwise.
After 600 cycles	1. Tight radial cracks noted during testing in area of hot spot in A quadrant.
After 768 cycles	1. Tight radial cracks on leading edge near corner A.
	2. Laminar crack @ interface 2 in corner A propagated to 1" axial by 0.4" circumferential, then stepped to interface 1 and extended additional 0.7" circumferential.
	3. Laminar crack @ interface 2 in corner B propagated to 0.3" circumferential by 0.2" axial, then stepped to interface 1 and extended additional 1.4" axially.
	4. Tight laminar crack @ interface 2 in corner C measuring 0.3" axial by 0.2" circumferential.
After 1000 cycles	1. Tight radial "mud-flat" cracks mostly in quadrant A roughly 0.25" diameter.
	2. Radial cracks extending inward approx. 0.25" spread roughly 0.3" apart.
	3. Laminar crack in corner A propagated additional 0.1" @ interface 1 in circumferential direction to 0.5".
	4. Laminar crack in corner B propagated additional 0.2" in axial direction @ interface 1 to 1.6".
	5. Laminar crack @ interface 2 in corner C propagated to 0.8" axial by 0.2" circumferential.

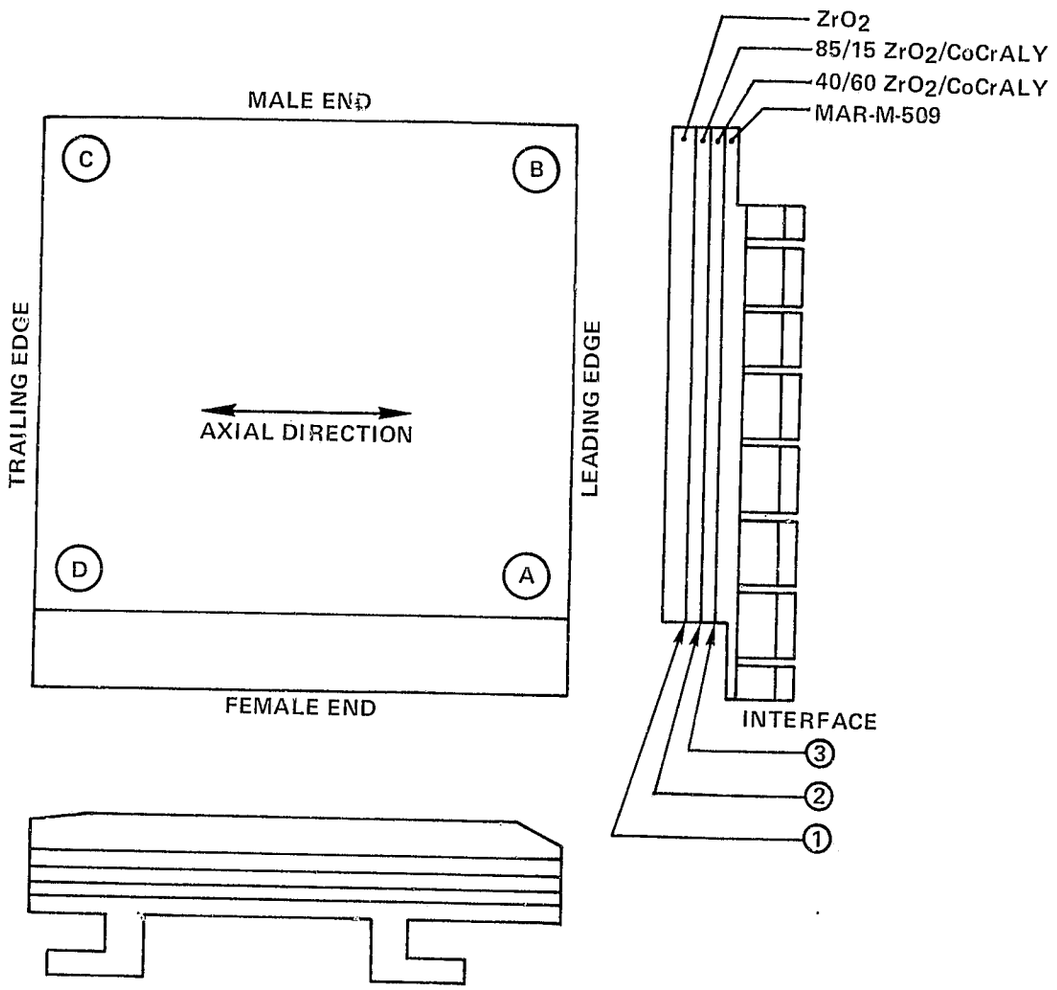

Figure 35 *Cyclic Thermal Shock Rig Crack Location and Progression Reference for use With Tables 5 and 6*

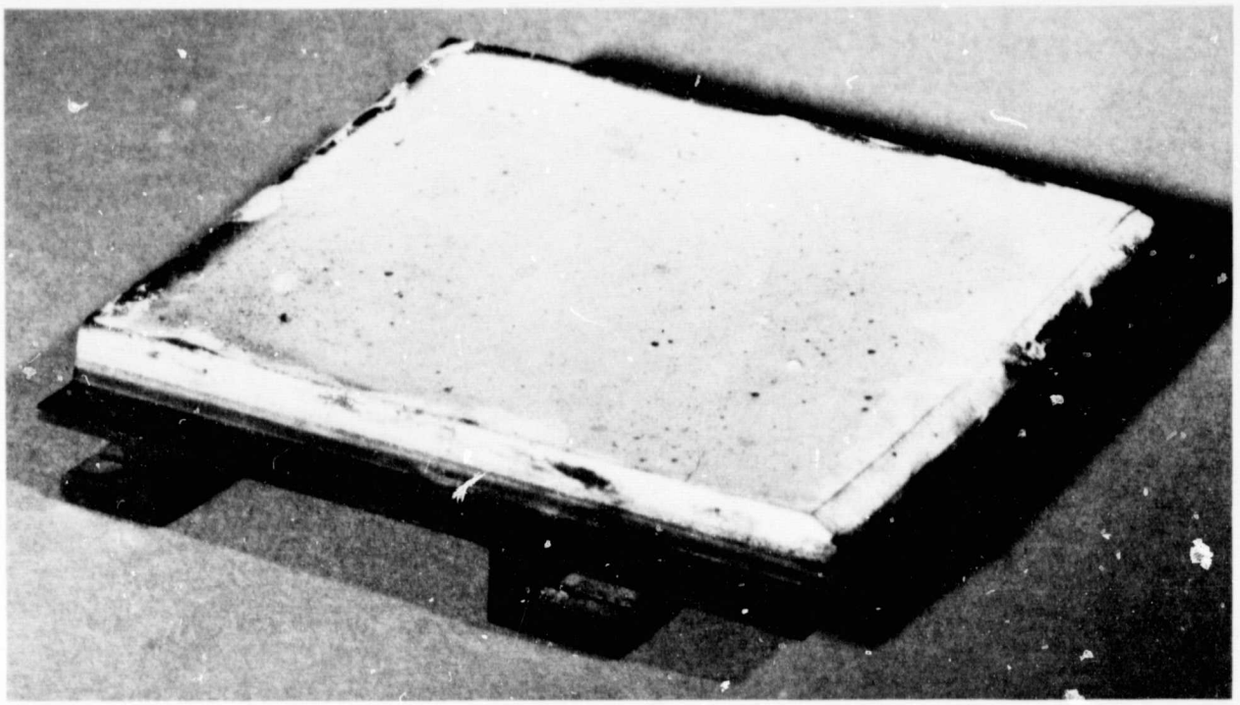

SIDE VIEW

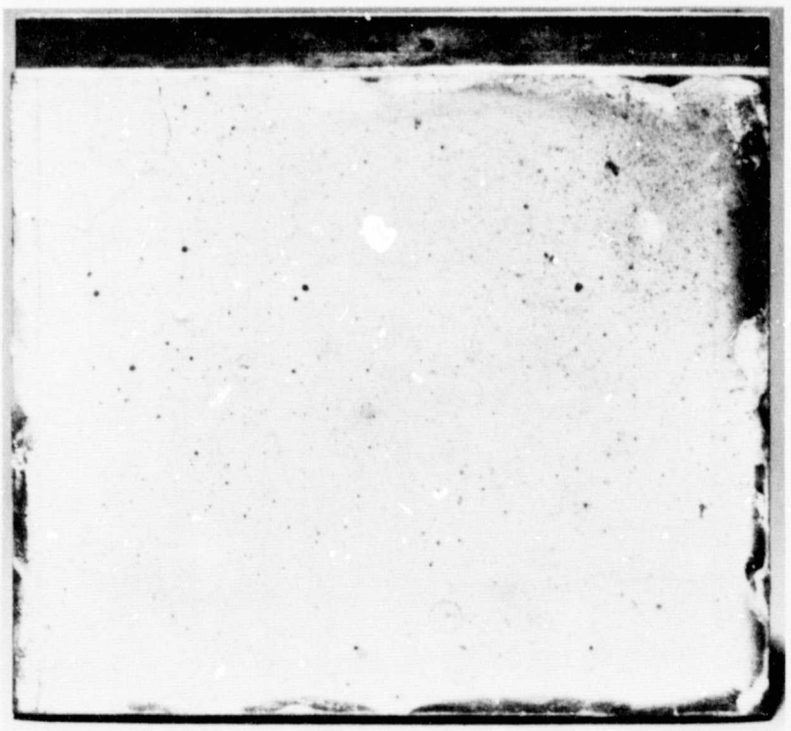

Figure 36 *Results of First Thermal Shock Test of Improved Design - 0.090in ZrO_2 - 1000 Cycles - Post Test Condition*

TABLE 6

THERMAL SHOCK TEST INSPECTION OF IMPROVED DESIGN
(Refer to Fig. 35 for location identification)

Test No. 2

After Accel Abort Cycle	1. Laminar crack @ interface 2 in corner A measuring 1/2" axial by 3/16" circumferential.
	2. Laminar crack @ interface 2 axially across male end measuring 1/16" at corner B and 3/32" at corner C in circumferential direction.
After 1st Cycle	1. Laminar crack @ interface 2 in corner A propagated to 25/32" axial by 3/16" circumferential.
	2. Laminar crack axially across male end propagated to 5/32" circumferentially in corner B @ interface 2.
After 500 cycles	1. Laminar crack in corner A propagated axially across female end @ interface 2 and circumferentially 9/16" @ interface 2, then stepped to interface 1 and extended an additional 7/16".
	2. Laminar crack across male end remained unchanged.
	3. Radial cracks spaced approx. 0.3" apart and extending inward approx. 0.25" along both ends and trailing edge.
	4. Spalled ZrO_2 layer and part of 85/15 ZrO_2/CoCrAlY layers in corner A measuring approx. 5/8" axially by 9/16" circumferentially while being removed from test fixture.

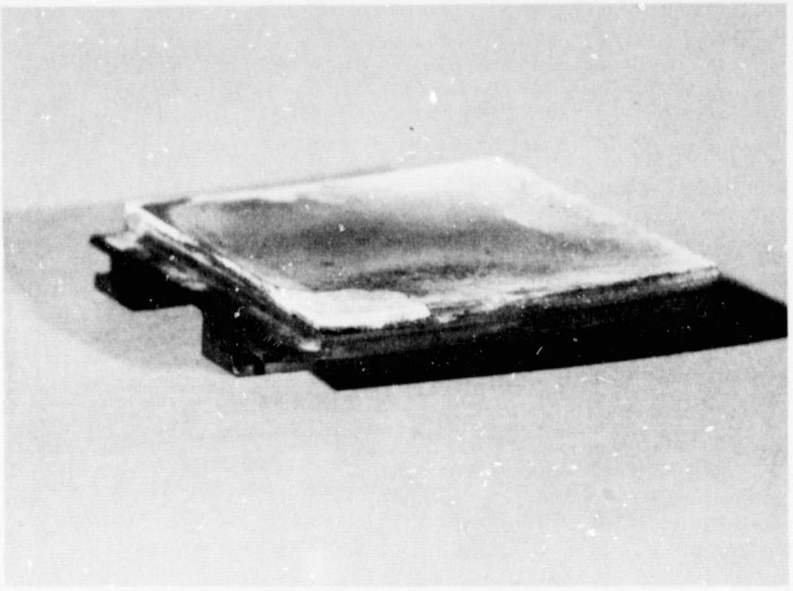

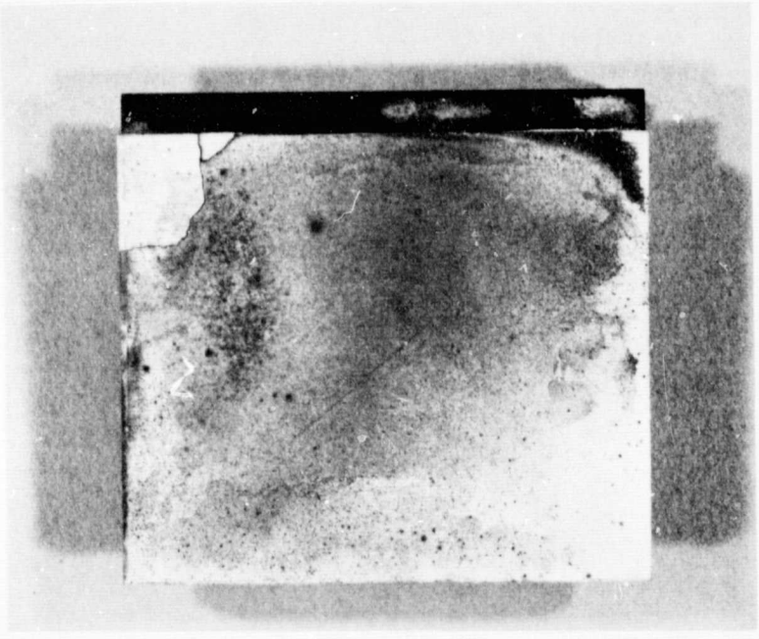

Figure 37 *Results of Second Thermal Shock Test of Improved System - .060in ZrO_2 - 500 Cycles - Post Test Condition*

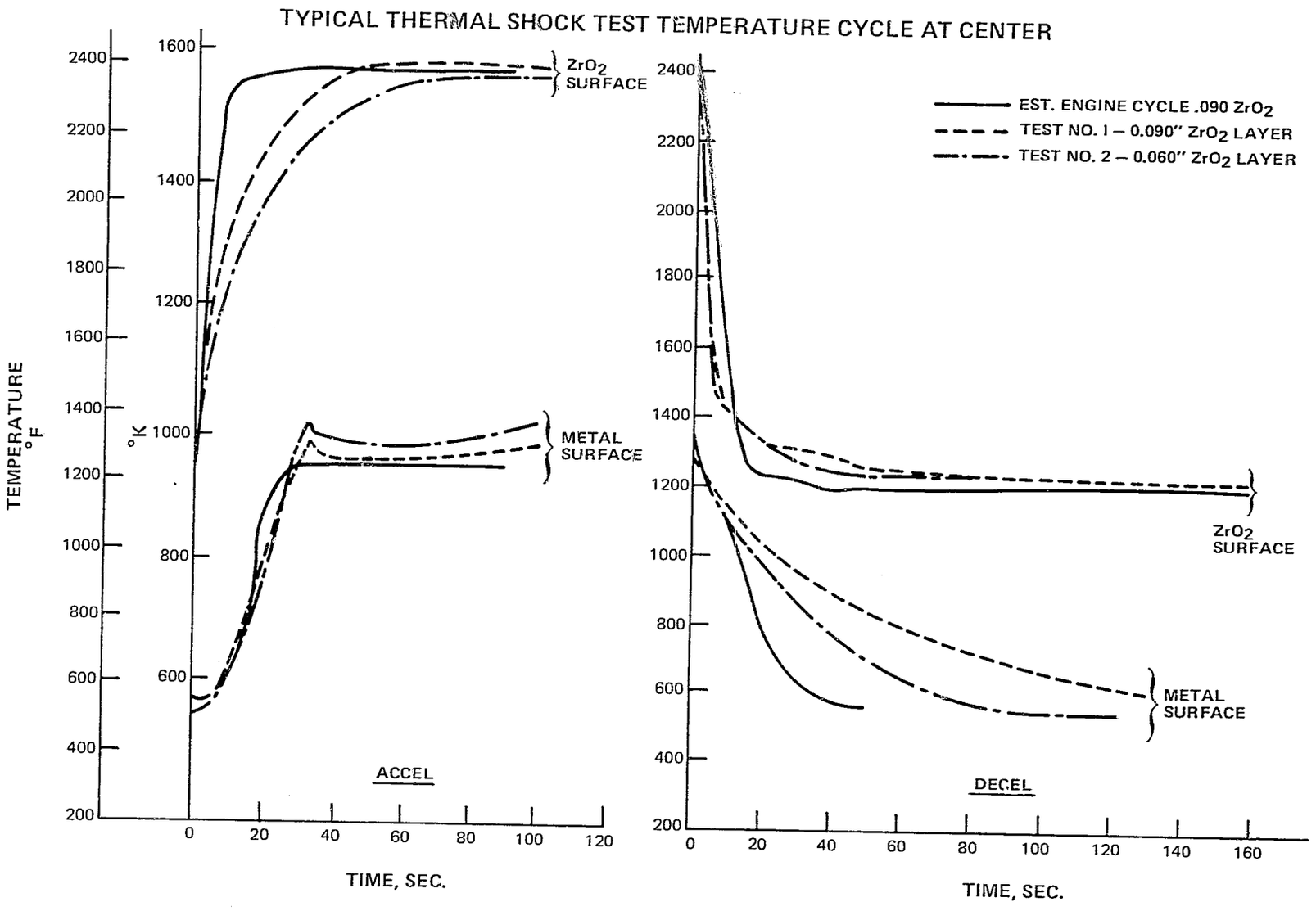

Figure 38 *Thermal Shock Test Temperature Cycle at Center of ZrO_2 and Substrate Surfaces*

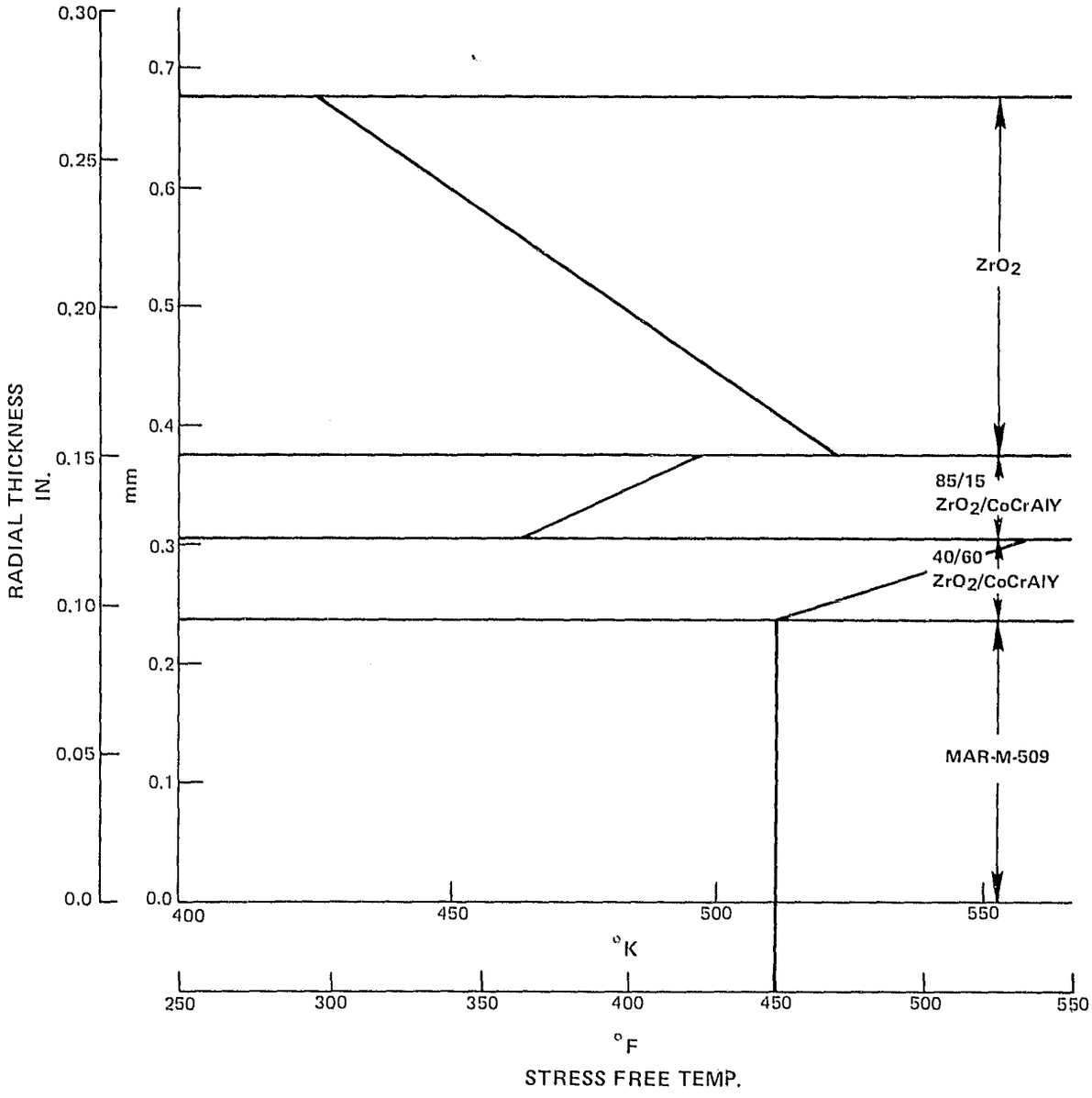

Figure 39 *Stress Free Temperature Distribution for a JT9D Ceramic Seal Segment - Improved Design*

Two dimensional stress analyses were performed in the circumferential plane through the most severe thermal profile location. A plot of the actual sea level take off circumferential temperature of the ZrO_2 surface and metal substrate measured by optical pyrometers and tc's respectively used in this analysis are shown in Figures 40 and 41. The same relative temperature distribution with reference to the temperature at the center of this seal, where the transient temperature response shown in Figure 38 was monitored, was assumed at ZrO_2 surface at the operating condition.

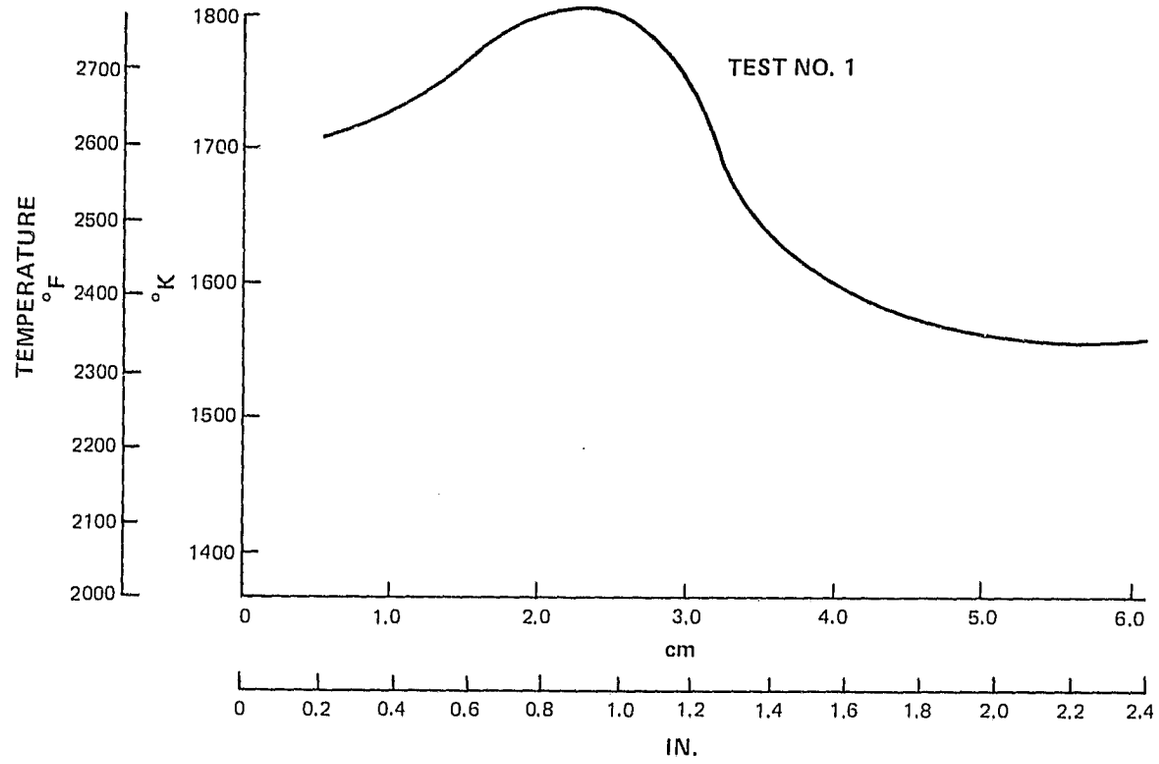

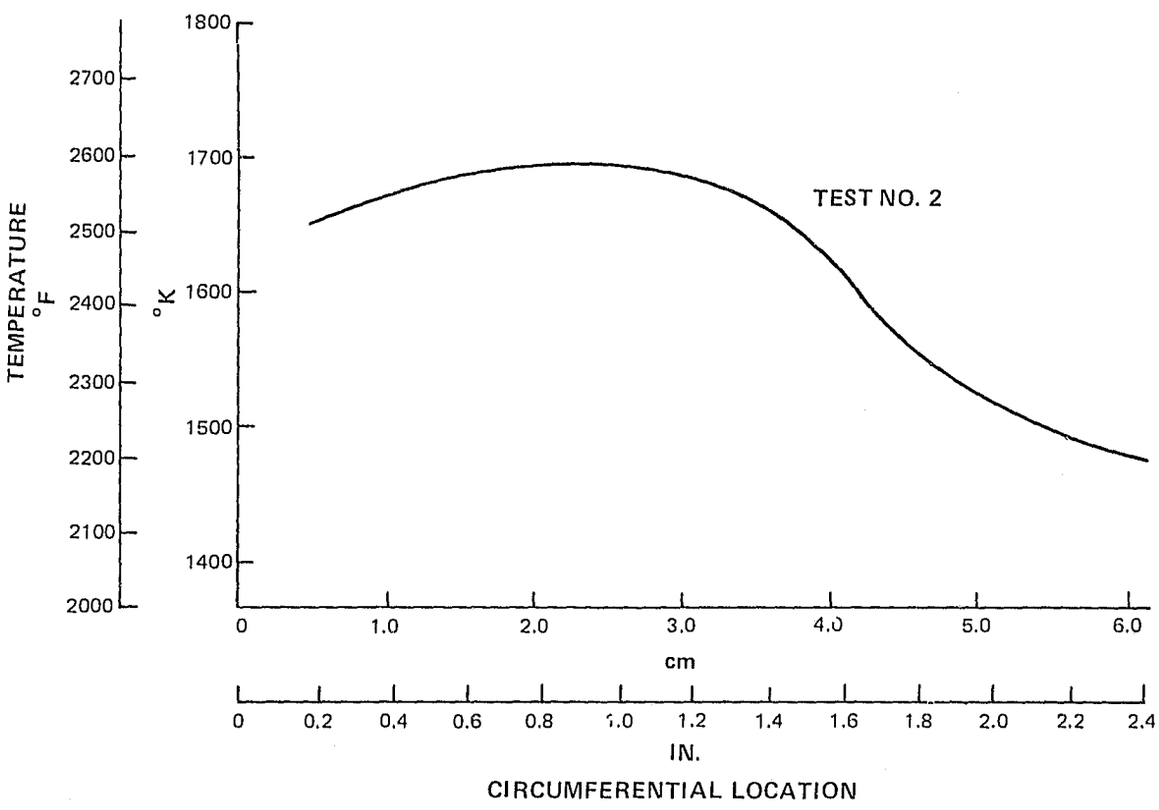

Figure 40 *Circumferential Temperature Distribution on ZrO_2 Surface During Thermal Shock Testing of Improved Design*

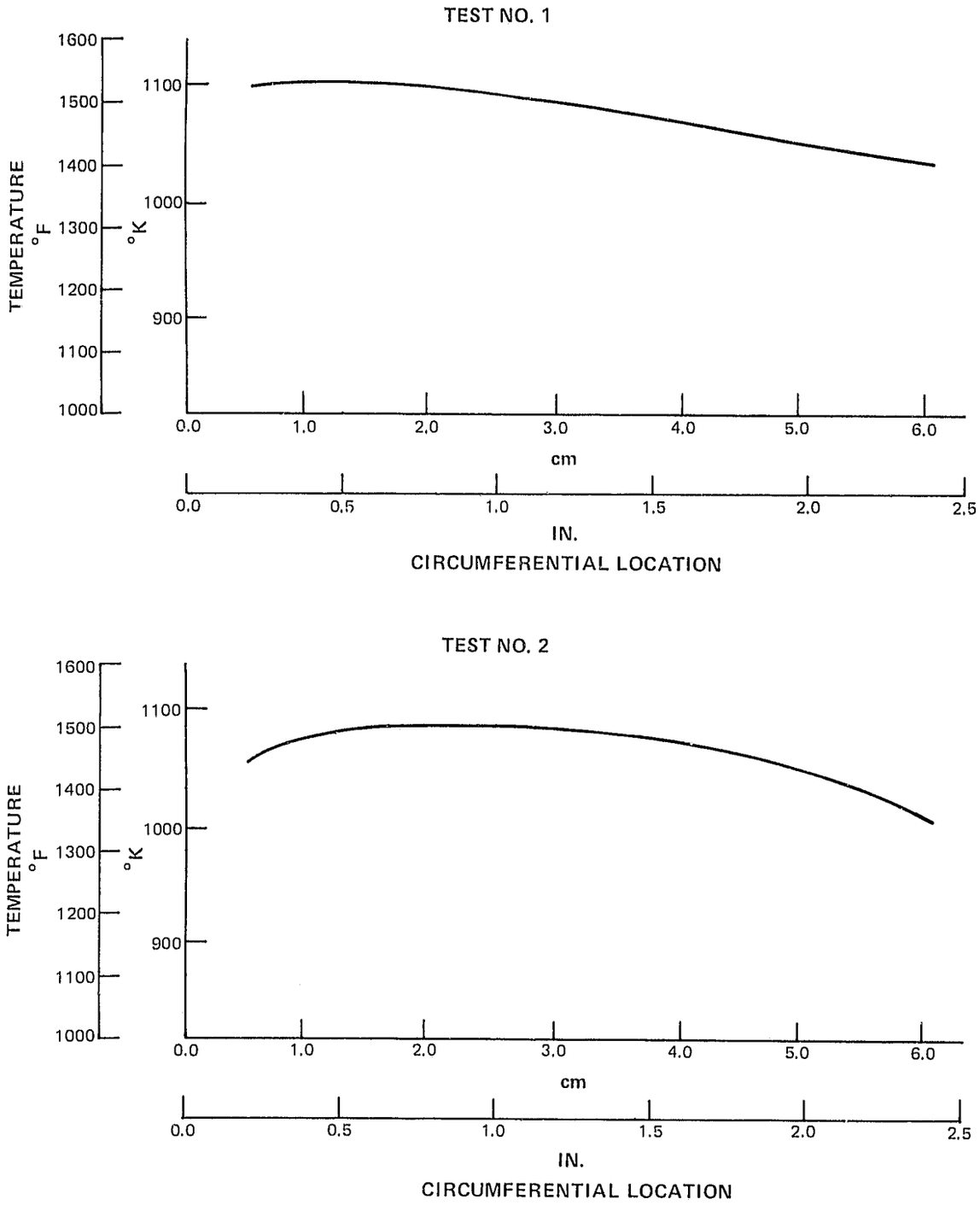

Figure 41 *Circumferential Temperature Distribution on Mar-M-509 Surface During Thermal Shock Testing of Improved Design*

The stress generated in the ZrO_2 layer near the 85/15 ZrO_2/CoCrAlY interface and in the 85/15 layer near the interface with the 40/60 layer for the two tests are noted in Figures 42 and 43. Results of this analysis indicate radial cracking in the ZrO_2, which occurred during test, would be expected. Laminar cracking in the 85/15 layer near the interface with the 40/60 would not have been predicted. The possible reasons for the lack of correlation between analyses and test results include the possibility of anisotropic properties, shrinkage of the ZrO_2 and a low interface bond strength. The expected benefit predicted analytically of reducing ZrO_2 thickness was not substantiated by the second test.

3.3.2 Engine Tests

Two JT9D engine tests were conducted to evaluate the feasibility of the sprayed ceramic seal system. The first test was conducted to evaluate the capability of the seal to withstand the thermal environment of the engine. The second engine test was conducted to evaluate the abradability characteristics of the sprayed ceramic seal when rubbed by abrasive tip blades. The second test was designed to evaluate the potential of the sprayed ceramic seal/abrasive tip blade concept to improve engine performance by allowing turbine operating clearances to be reduced because of the improved abradability.

First Engine Test - Thermal Environment

Parts fabricated with those tested in the cyclic thermal shock rig, test numbers 3 & 4, were evaluated in the engine to determine the effect on the seal of the thermal environment of the engine.

Three seal segments were fabricated. Two of these seals had a ZrO_2 top layer thickness of 0.152 cm (0.060 in) while the thickness of the ZrO_2 layer on the third seal was 0.229 cm (0.090 in). The remaining dimensions, as seen below, were the same for all three seals.

Seal Configuration	1	2	3
M-509 Substrate	0.226 cm (0.089 in.)	0.226 cm (0.089 in.)	0.226 cm (0.089 in.)
Bond Coat	0.01 cm (0.004 in.)	0.01 cm (0.004 in.)	0.01 cm (0.004 in.)
40/60 ZrO_2/CoCrAlY	0.081 cm (0.032 in.)	0.081 cm (0.032 in.)	0.081 cm (0.032 in.)
85/15 ZrO_2/CoCrAlY	0.074 cm (0.029 in.)	0.074 cm (0.029 in.)	0.074 cm (0.029 in.)
ZrO_2	0.152 cm (0.060 in.)	0.152 cm (0.060 in.)	0.229 cm (0.090 in.)

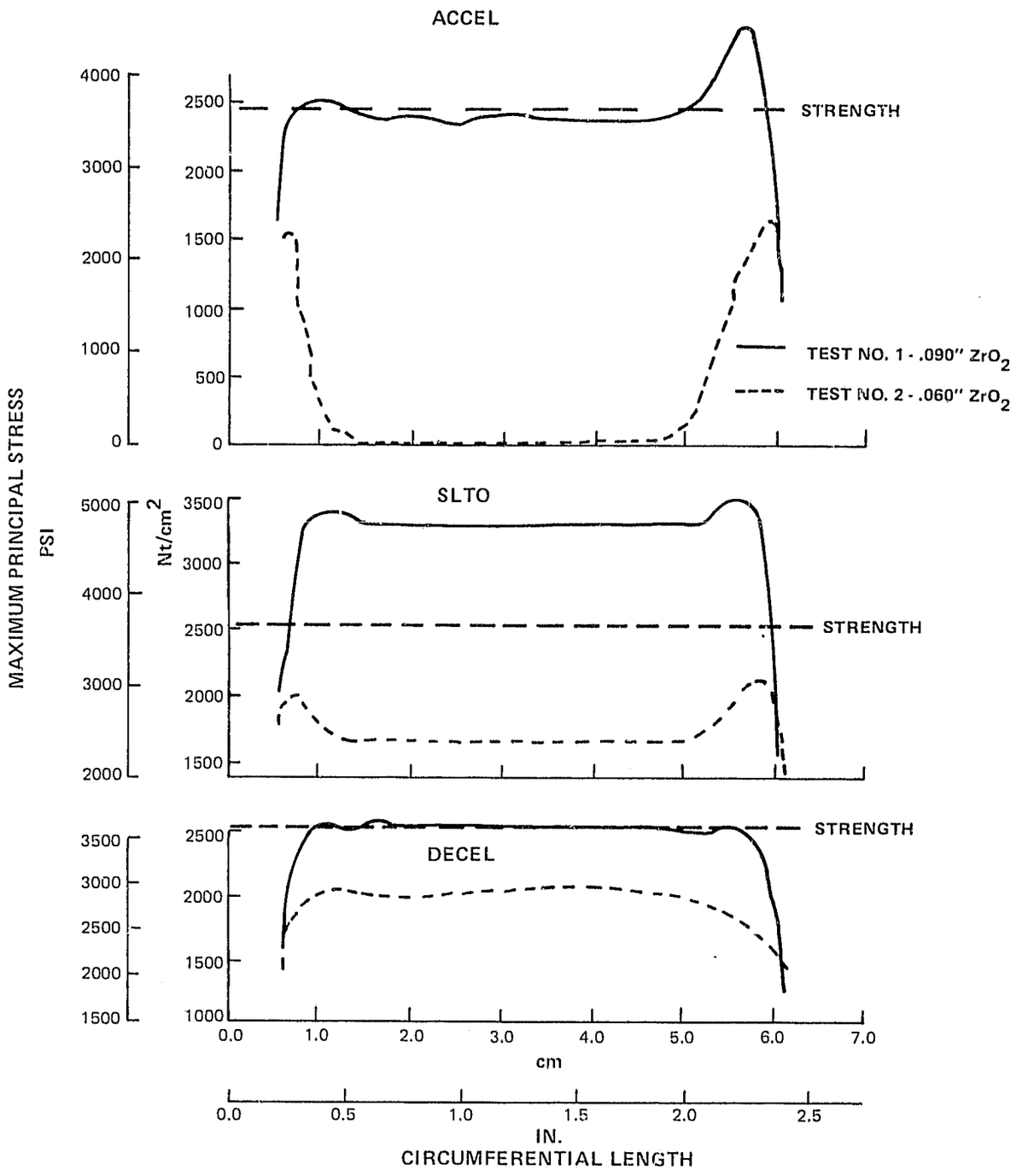

Figure 42 *Maximum Principal Stress in ZrO_2 Layer Near 85/15 Interface for Improved Design - Cyclic Thermal Shock Rig Test*

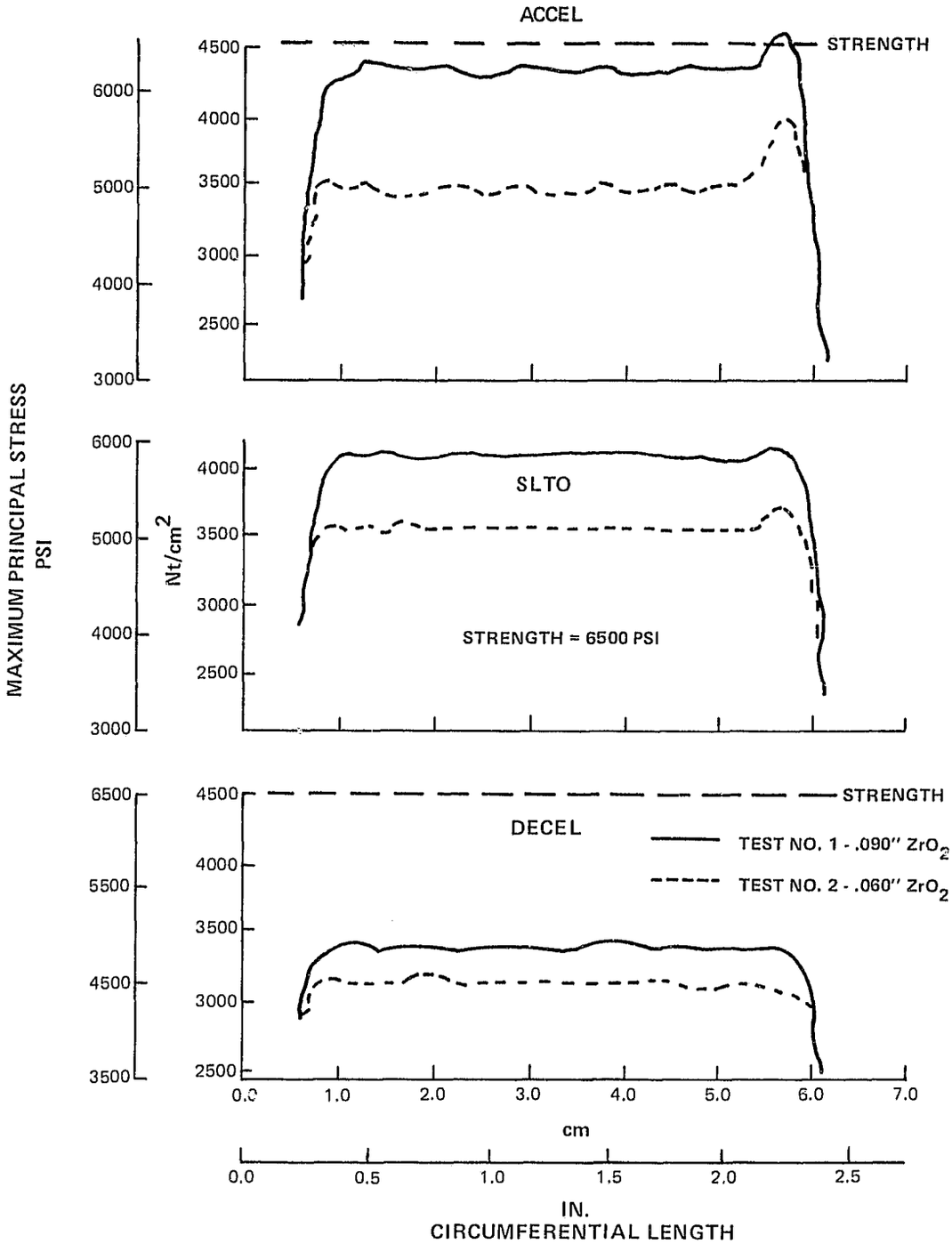

Figure 43 *Maximum Principle Stress in 85/15 Layer Near 40/60 Interface for Improved Design - Cyclic Thermal Shock Rig Test*

The ZrO_2 layer thickness was provided by overspraying the layer to a thickness of approximately 0.282 cm (0.111 in.) and grinding the required surface diameter to provide the required thickness. The two thicknesses of ZrO_2 were evaluated for the following reason. The analysis indicated that thermal stresses would be reduced with a reduction in the thickness of the ZrO_2 and the engine test could demonstrate the benefit of the ZrO_2 reduction by reduced cracking and/or spalling.

A photograph of a typical seal segment is shown in Figure 1. The three sprayed ceramic engine seal segments were ground to the required diameter and positioned in a turbine seal location to minimize the possibility of a rub interaction. Two bill-of-material metallic seals were modified at one end to accommodate the shiplap configuration of the ceramic segments and serve as transition segments. The detail of the shiplap design is shown in Figure 44. The bill-of material shiplap configuration could not be incorporated in the sprayed seal segment because of the thickness of sprayed material required.

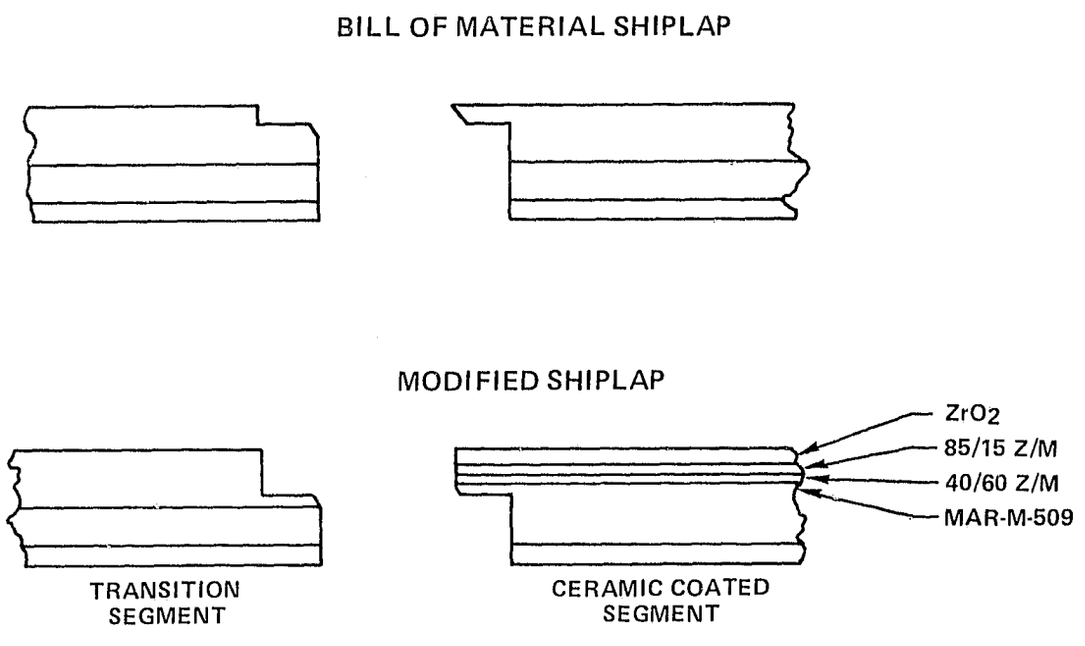

Figure 44 Shiplap Design of Transition Segment

The engine test subjected the three seal segments to two calibration cycles up to an average turbine inlet temperature of 1510°K (2260°F) and 45 start-up cycles to idle conditions for a total engine running time of 16.9 hours. All three seal segments successfully completed the test without severe cracking or any spalling.

Post test visual inspection revealed tight laminar cracks in the corners at the 85/15-40/60 ZrO_2/CoCrAlY layer interface. The cracks were similar to, but tighter and shorter than those observed, as a result of previous thermal shock rig tests of similar segments. There was no evidence of any erosion.

The location and magnitude of cracking of each of the three segments is shown in Figure 45. Figure 46 is a picture of a typical crack. The initiation of cracks, even though very tight, pointed out the need for an improved seal design.

Two alternative geometry modifications were analyzed. The two modifications each involved a further reduction in the substrate stiffness, and failed to show potential for significantly reducing thermal stresses. The two geometry modifications are shown in Figure 47 with the configurations tested in the engine for comparison purposes. The first alternative which extended the six rail slots into the substrate resulted in a slightly higher stress to strength ratio at all conditions. The second alternative, slotting the rails in thirteen locations and extending the slots 0.076 cm (0.030 in.) into the substrate produced an improvement in the deceleration portion of the operating cycle in all three layers but otherwise produced no benefit. Because modifications of the configuration indicated only marginal improvement and significant redesign was beyond the scope of the current program, a decision was made to evaluate the abradability of the sprayed ceramic seal utilizing the design evaluated in the first engine test. The cracks resulting from thermal exposure during the initial engine test were slight and at the edges and not expected to compromise the results of the engine rub test. Further, retest of the same configuration would provide an indication of the repeatability of the seal system.

Second Engine Test -- Blade Tip Rub

Six sprayed ceramic seals of the same configuration as those evaluated in the first engine test, were fabricated for engine test of abradability characteristics. The engine test evaluation of the abradability characteristics of the sprayed ceramic seal when rubbed by the other seal system component, abrasive tip blades, required special clearance control measures. Abrasive tip blade diameters and ceramic seals thickness and location were defined, based on engine operational clearance history, to insure that only the abrasive tip blades would rub only the ceramic seals.

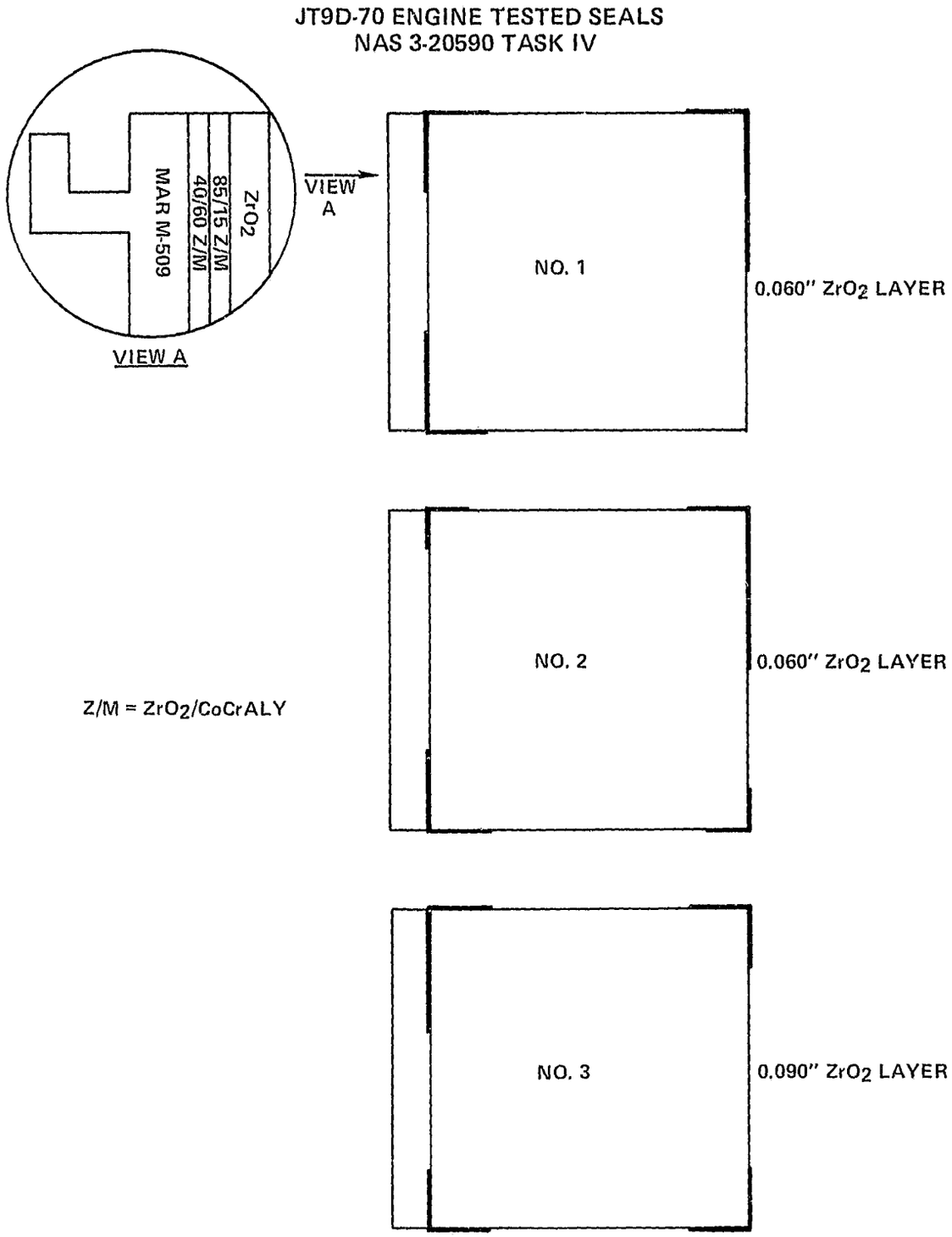

Figure 45 Crack Map of JT9D Ceramic Seal From First Engine Test

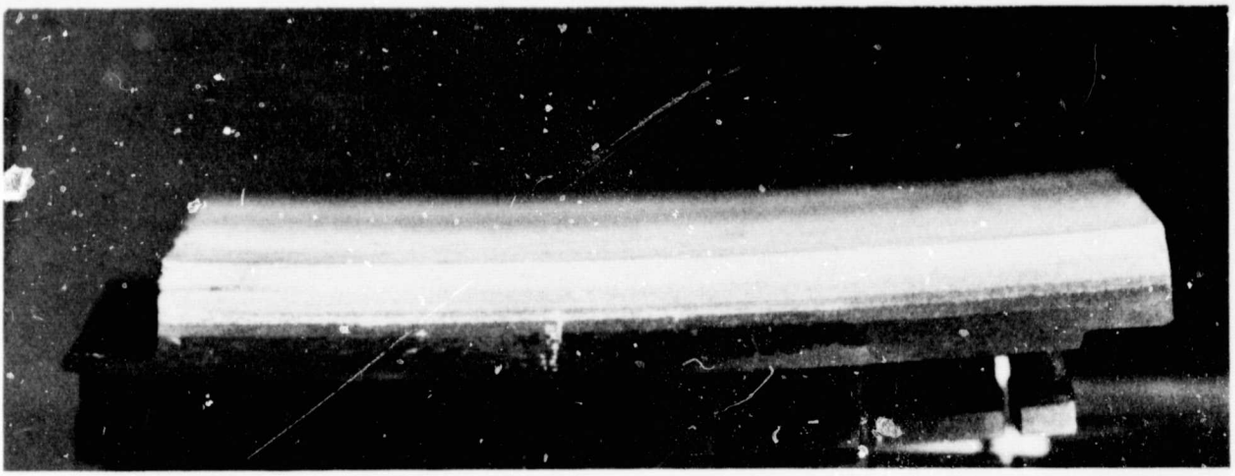

Figure 46 *Typical Crack in First JT9D Engine Test*

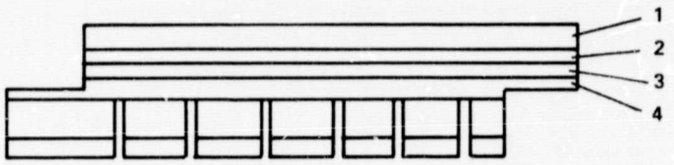

FIRST ENGINE TEST GEOMETRY

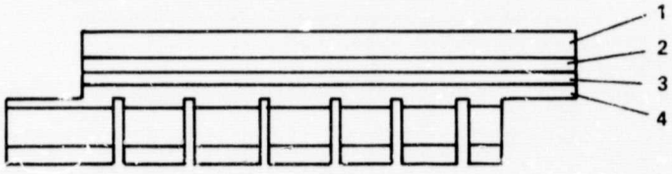

DESIGN ALTERNATIVE A

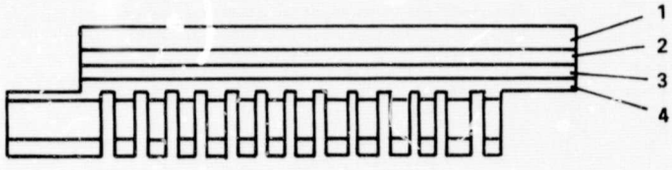

DESIGN ALTERNATIVE B

1 Z_rO_2

2 85/15 Z_rO_2/C_oC_rAlY

3 40/60 Z_rO_2/C_oC_rAlY

4 MAR-M-509

Figure 47 *Substrate Design Alternatives Shown With Reference to First Engine Test Design*

Minimum operating clearances for the test engine for the planned test program were established by means of rub buttons in 16 segments equally spaced around the circumference of the seal. Final positioning of the ceramic segments was established in part by consideration of the ZrO_2 thickness and the depth of rub desired. A maximum rub depth of 15 mils was anticipated. The sketch shown in Figure 48 illustrates the location of the ceramic seal segments. ZrO_2 thickness and pertinent configuration positions are also noted.

Fourteen abrasive tip blades with a diameter approximately 15 mils greater than bill-of-material blades were equally spaced around the rotor. Figure 49 is a picture of three typical blades prior to engine test.

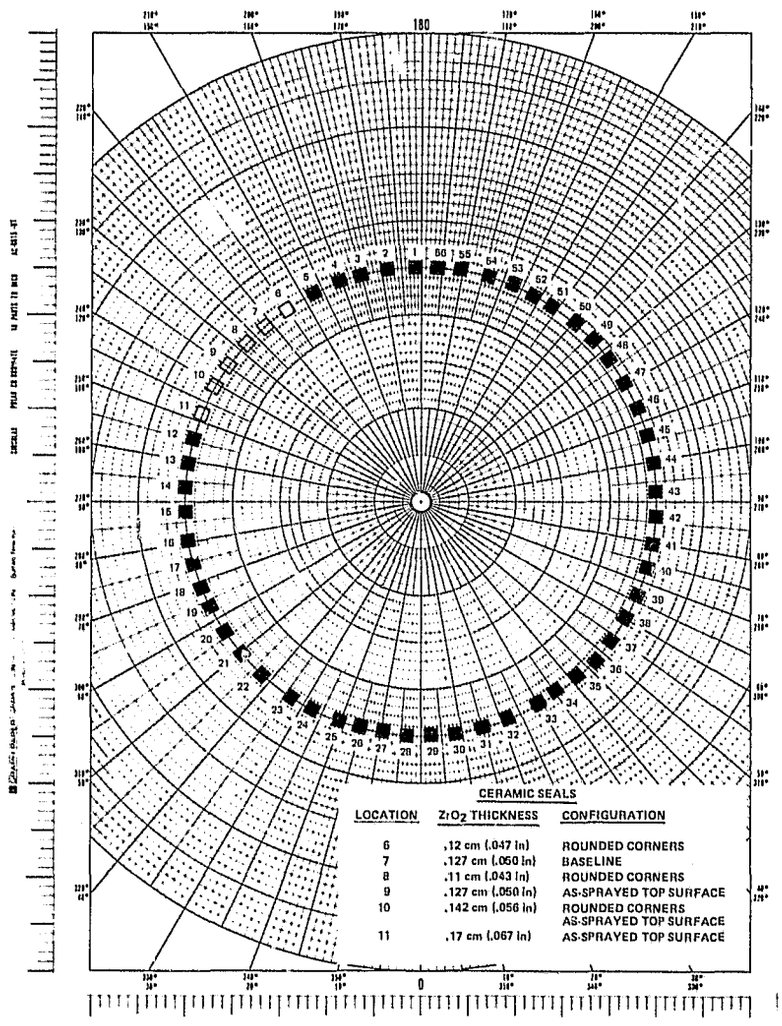

Figure 48 Location of Ceramic Seals for Rub Interaction Test

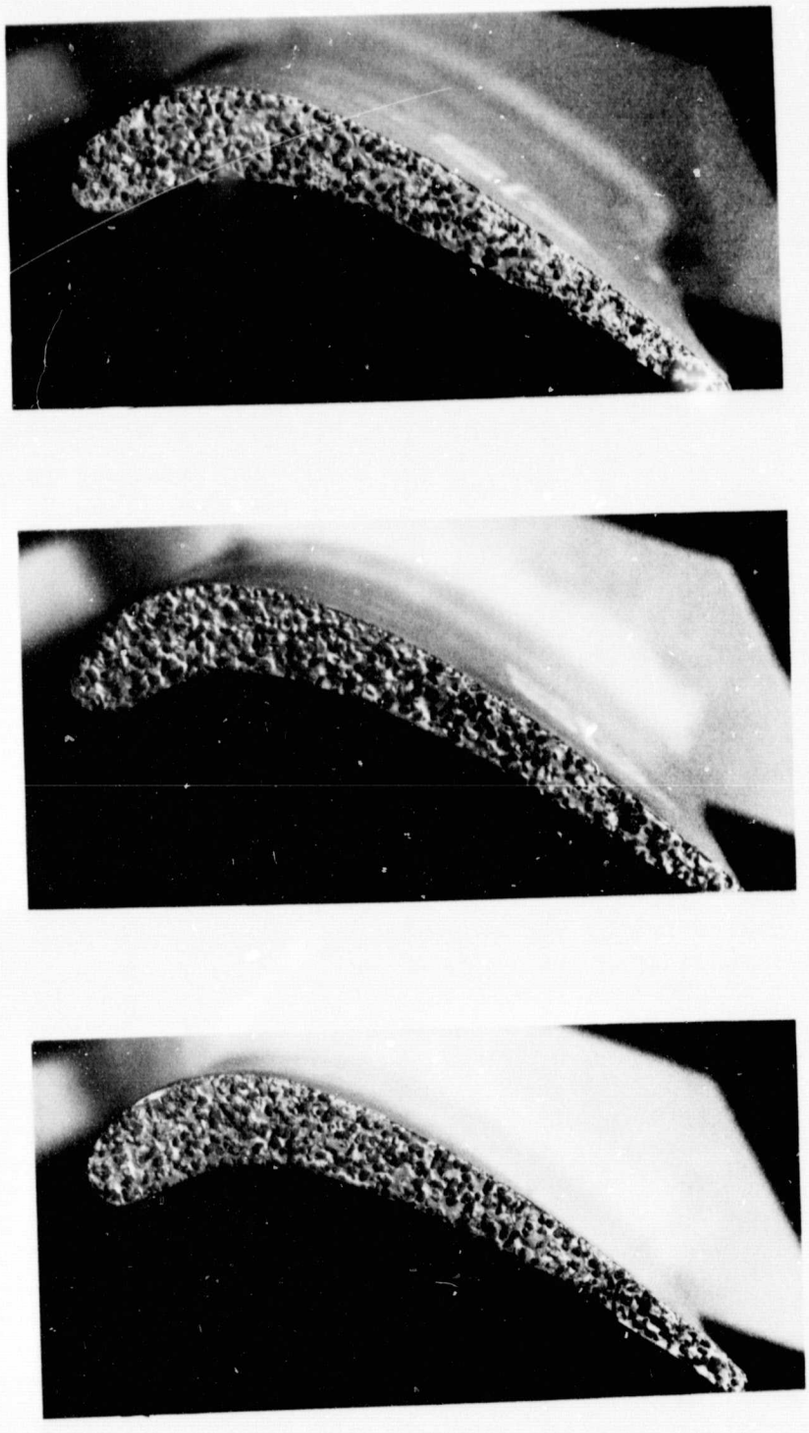

Figure 49 *Three Typical Abrasive Tip Turbine Blades - Pre Engine Test Condition*

The test was highly successful and demonstrated the capability of the sprayed ceramic seal system to abrade cleanly with minimal rotor wear and therefore offer the potential for clearance reduction and engine performance improvement. Three seal segments, those in locations 9, 10, and 11 were abraded up to a depth of 24 mils. The rub path, shown in Figure 50, was clean and generally free of blade material transfer. Inspection of the blade tips revealed that only eight of the fourteen abrasive tip blades participated in the interaction and only three blades had measurable wear up to a maximum of 5 mils. Figure 51 shows the three blades.

The engine ran a total of 8.4 total hours with 2 calibrations to maximum power. A maximum average turbine inlet temperature of 1600°K (2418°F) was attained during the test.

All six segments had corner cracks. Location and extent of the cracks for each of the segments is shown in Figure 52. Several segments were additionally machined to round the corners in an attempt to reduce stresses in these locations. Figure 52 shows, in general, that cracking was less severe but not eliminated. A comparison with the crack map of the first test Figure 46 shows the similarity between the two tests. This test, however, was some 70°K (158°F) hotter than the first.

3.3.3 Final Analysis

A thermal stress analysis of the seal segment was conducted at maximum conditions encountered during the engine tests. Engine test instrumentation during test indicated the average seal surface temperature during the maximum power conditions of that engine was 1475°K (2200°F) with a substrate outer diameter temperature of 870°K (1100°F). The analysis was conducted using the stress free temperature distribution (SFT) generated under this program as presented in Figure 39. Stesses throughout the seal were calculated and reviewed. Magnitude and location of the more significant stress to strength were determined and plotted in Figure 53 in relation to the location of cracks generated during engine test. The maximum stress to strength ratios did occur at the edge of the seal with a value of 1.6 in the ZrO_2 near the interface with the 85/15 layer and 1.1 in the 85/15 layer near the interface with the 40/60 layer. The directional angle of the corresponding principal stress at both locations was small and therefore not perpendicular to the laminar crack. Initial data presented in NASA CR 159669, however, indicated that the strength of the ZrO_2 and 85/15 layers in the radial direction was appreciably less than the circumferential strength measured by the four point bend method. It is possible that the weaker strength in the radial direction coupled with the radial component of the principal stress at the edge of the seal caused the initiation of the laminar cracks.

Figure 50 Three Rubbed JT9D Ceramic Seal Segments From Second Engine Test

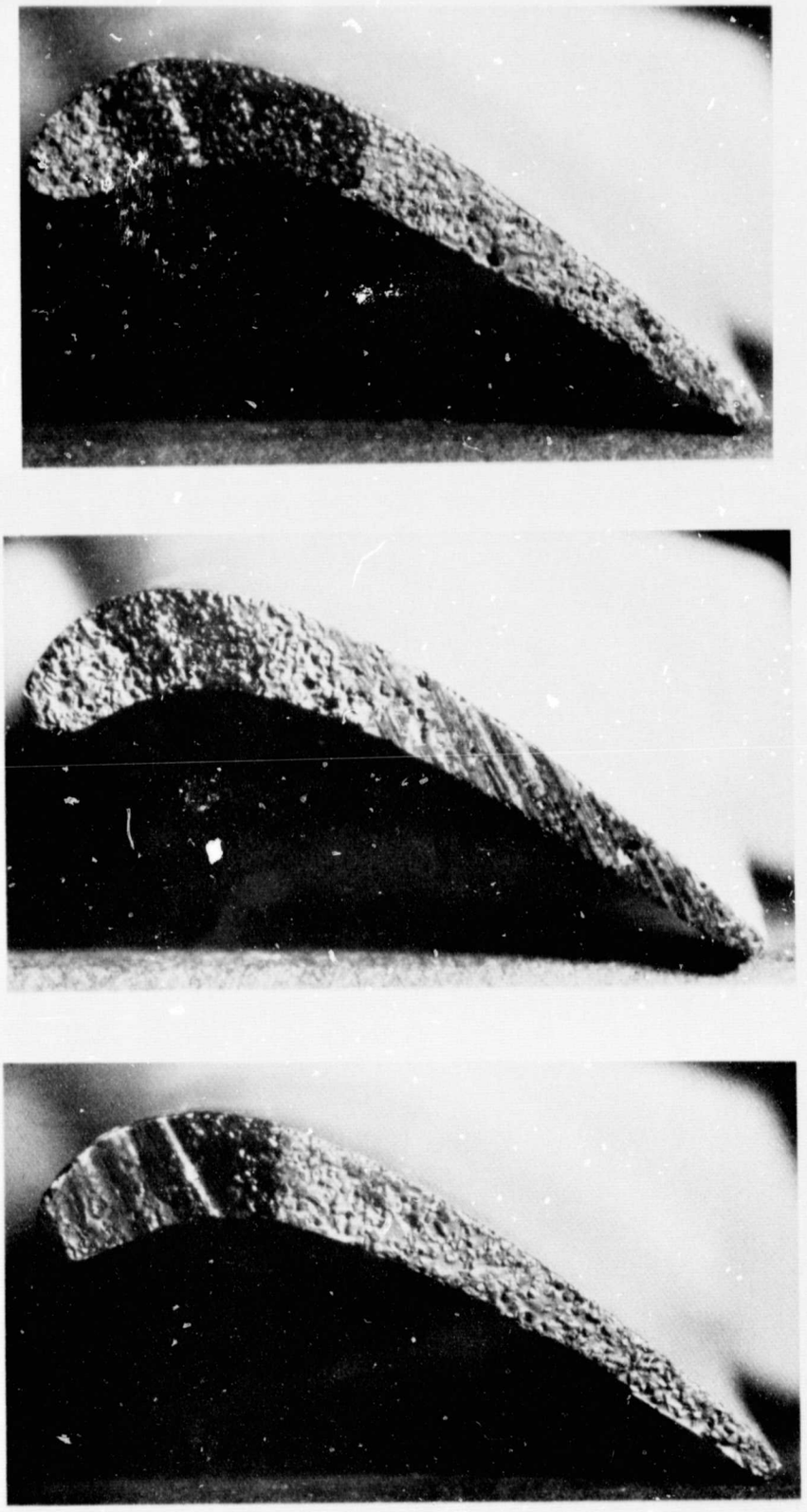

Figure 51 *Three Typical Abrasive Tip Turbine Blades - Post Engine Test Condition*

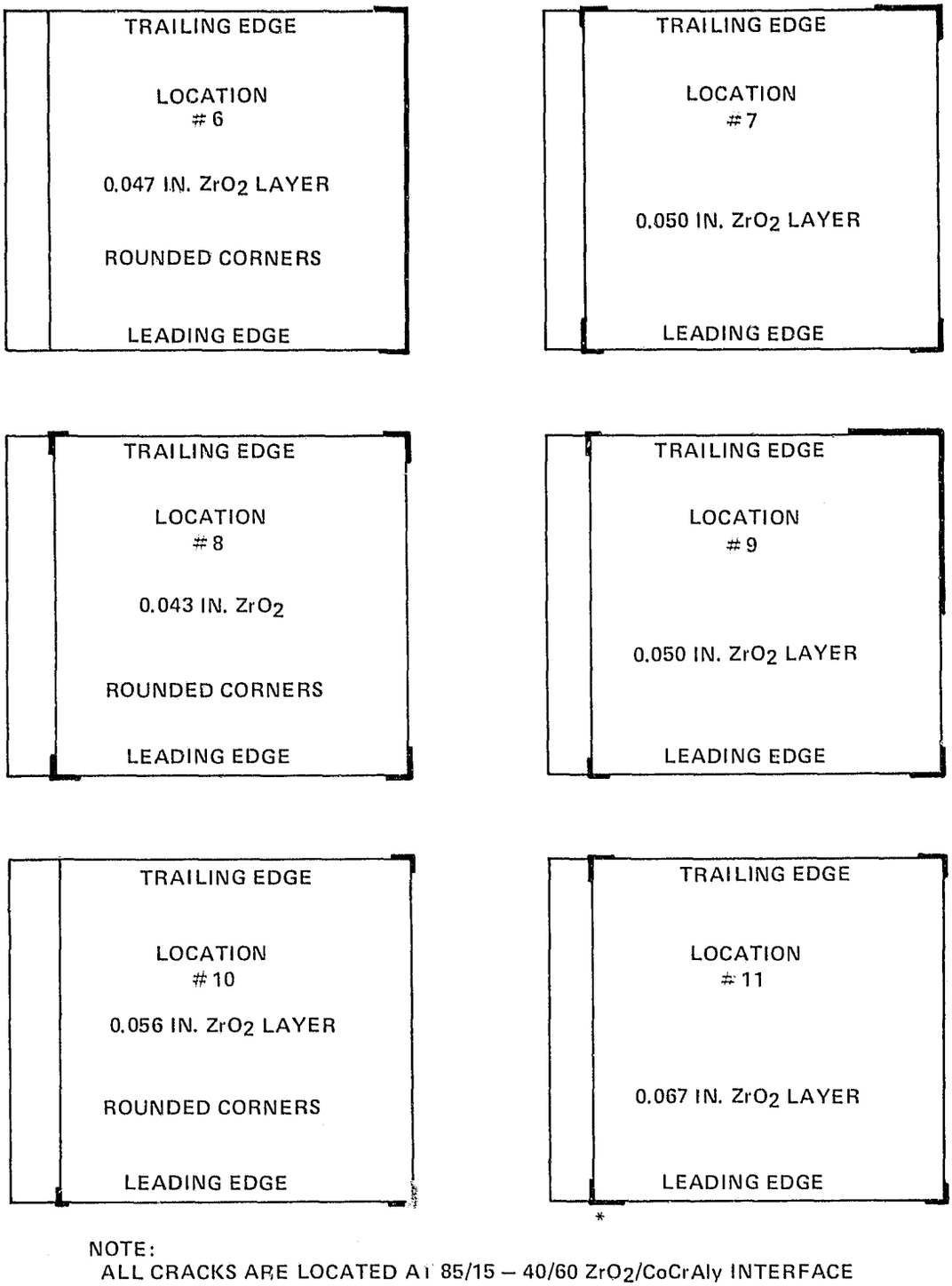

NOTE:
ALL CRACKS ARE LOCATED AT 85/15 – 40/60 ZrO_2/CoCrAlY INTERFACE
*ADDITIONAL CRACK AT ZrO_2 – 85/15 ZrO_2 /CoCrAlY INTERFACE

Figure 52 Crack Map of JT9D Ceramic Seal From Second Engine Test

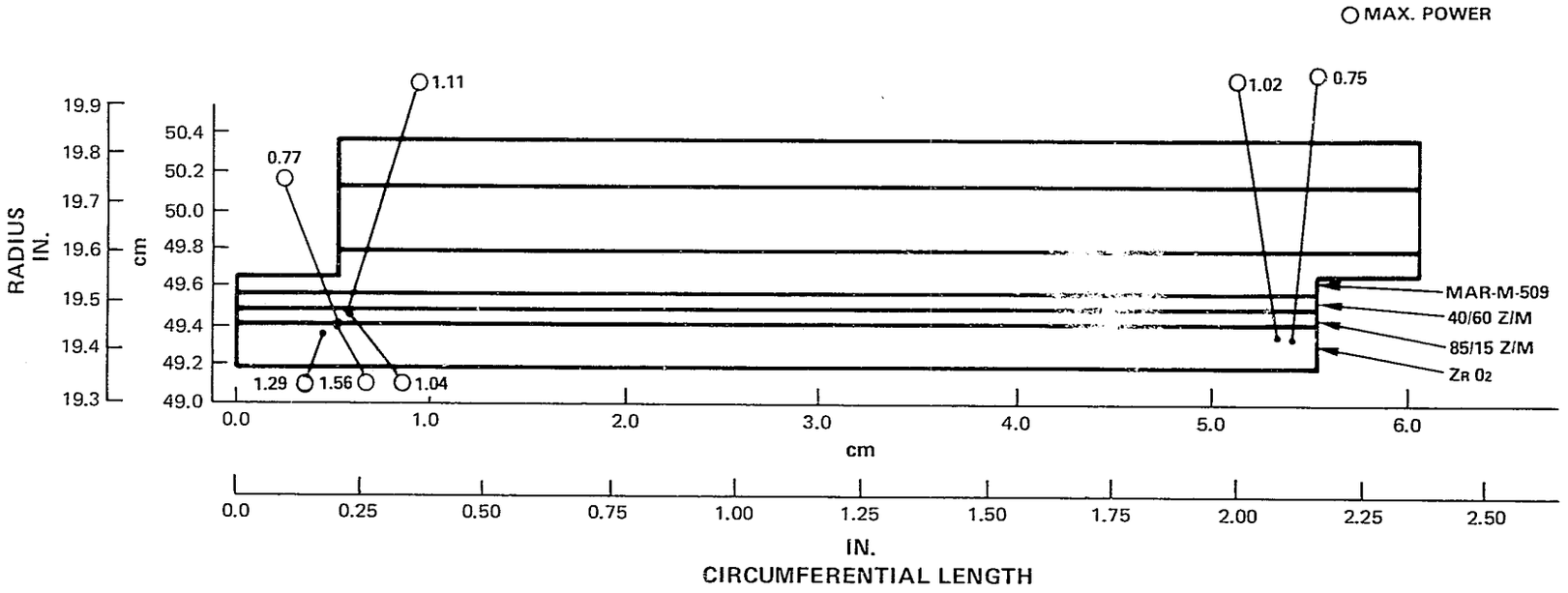

Figure 53 Stress to Strength Ratio From Second Engine Test

One of the ceramic seals which did not rub was metallographically inspected to investigate the nature of the crack. Figure 54 shows a schematic of the seal, indicating the mounted surface and a side view showing the cracks and progression of the micrographic evaluation. Material was removed during subsequent grinding to points M, N, O, and P. The crack extension within the seal was traced by photograph shown in Figure 55 which was taken at point M 0.048 cm (0.019 in.), point N 0.559 cm (0.220 in.), point O 0.635 cm (0.250 in.), and point P 0.724 cm (0.285 in.) into the seal. As seen in Figure 55, the crack was still observed, 0.137 cm (0.054 in.) in length but much tighter. Tracing the crack revealed that it existed only in the corner and did not progress in either plane beyond the length observed at the edge.

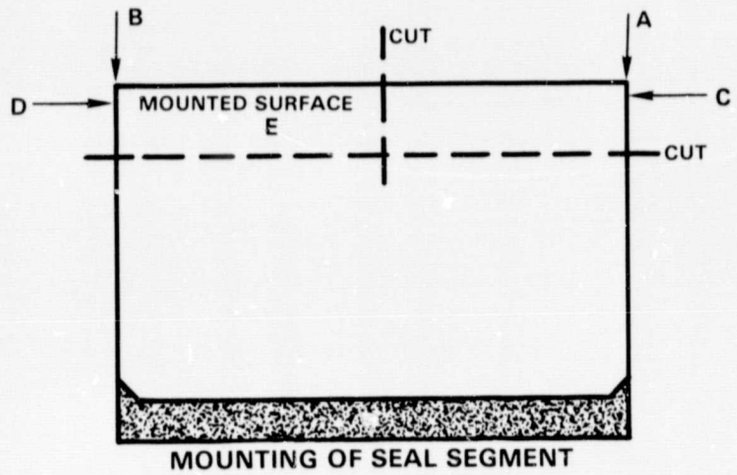

MOUNTING OF SEAL SEGMENT

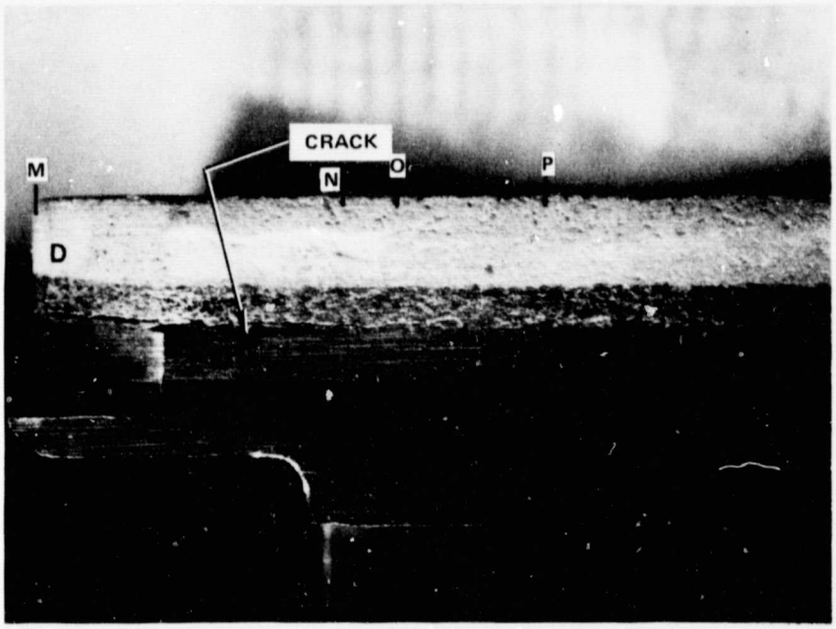

D ≈ 8X

Figure 54 *Ceramic Seal Segment From Second Engine Test With Laminar Crack*

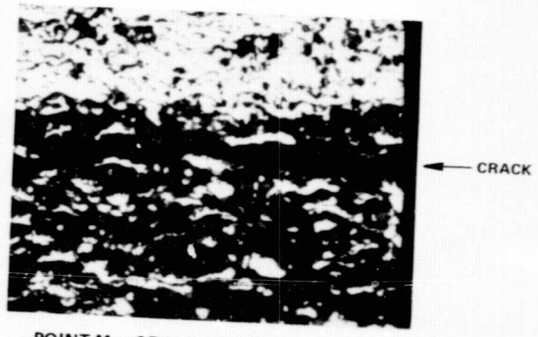

POINT M – CRACK EXTENDED 1.25 IN.

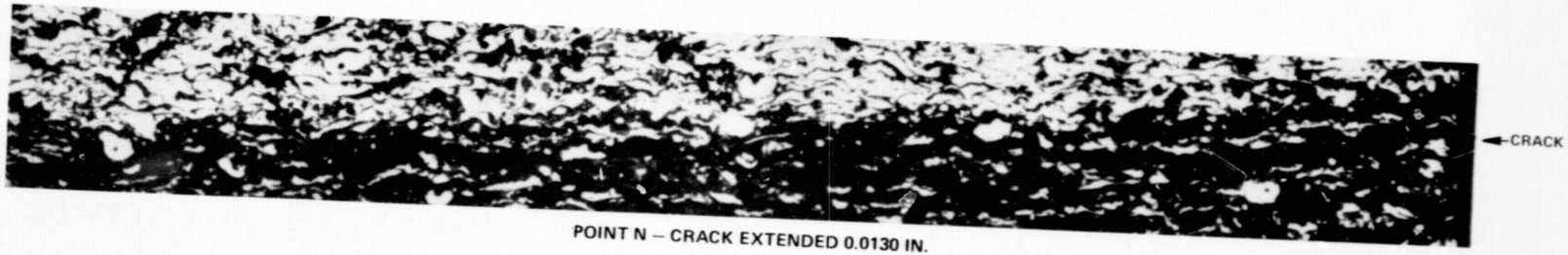

POINT N – CRACK EXTENDED 0.0130 IN.

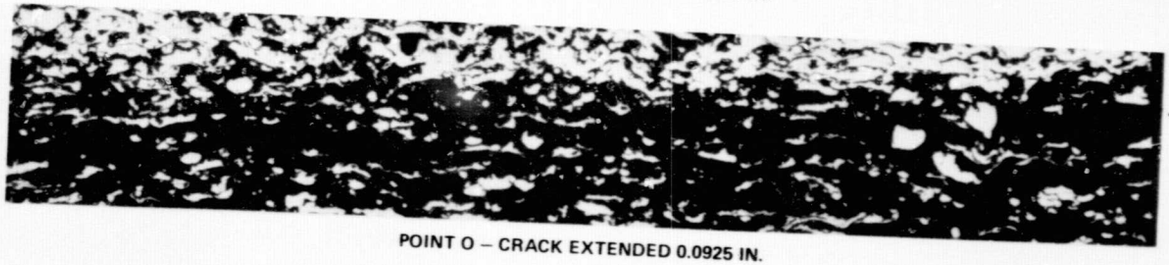

POINT O – CRACK EXTENDED 0.0925 IN.

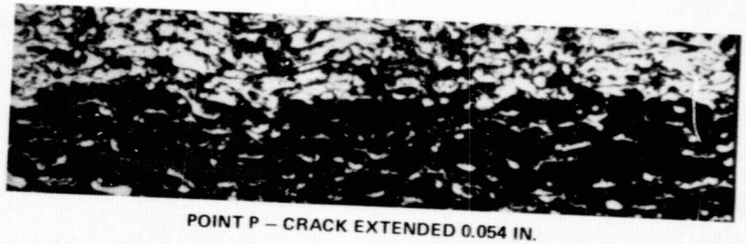

POINT P – CRACK EXTENDED 0.054 IN.

Figure 55 Micrographic Evaluation of Ceramic Seal

4.0 CONCLUSIONS AND RECOMMENDATIONS

Three main conclusions can be reached on the basis of the results of this program.

1. The sprayed graded ceramic seal system has demonstrated the ability to survive the turbine thermal environment without spalling of the ceramic.

2. Engine performance can be improved by incorporation of a sprayed ceramic turbine seal. The potential of reducing engine turbine clearances, and thereby improving engine performance, by using ceramic seals in the turbine was substantiated by results of the engine rub test. That test demonstrated that rotor interaction of up to 25 mils could be accommodated by the abrasive blade tip/ceramic seal system without rotor damage or significant blade tip wear.

3. Though the sprayed graded ceramic seal system has survived the turbine thermal environment, additional development is recommended with the aim of reducing incidence of laminar cracking and further improving structural integrity.

The JT9D engine tests conducted under this program successfully demonstrated the potential of the sprayed ceramic seal system to improve engine performance. Further effort to develop the seal system should provide 1) additional sprayed ceramic material data, 2) several iterations of design refinement, fabrication and evaluation and finally, 3) rig and performance and endurance engine tests.